

**The role of Breast Cancer Antiestrogen Resistance 3 (BCAR3) in triple-negative breast cancer growth and progression**

Janet Arras  
Chihuahua, Mexico  
El Paso, Texas

B.S., The University of Texas at Tyler, 2012  
M.S., University of Virginia School of Medicine, 2018

A Dissertation presented to the Graduate Faculty  
of the University of Virginia in Candidacy for the Degree of  
Doctor of Philosophy

Department of Microbiology, Immunology, and Cancer Biology

University of Virginia  
December, 2021

## **Abstract**

Breast cancer is the second most common cause of cancer-related deaths in women and constitutes a group of diseases that exhibit heterogeneity. Despite diagnostic and therapeutic advances, challenges remain to improve the clinical care of patients. Breast cancer subtypes have been identified based on the hormone receptor status and molecular profile of tumors. Understanding the characteristics of each subtype is important to help inform therapeutic strategies and improve patient outcomes. Triple-negative breast cancer (TNBC) is a subtype that makes up 10-20% of all breast cancer cases and has the worst 5-year survival rate. This subtype is characterized as lacking immunohistochemically detectable expression of the estrogen receptor (ER), progesterone receptor (PR), and human epidermal growth factor receptor 2 (HER2). TNBC typically presents with aggressive, high-grade lesions and is more prevalent among black women of African descent. Previous work from our group and others showed that the adaptor molecule Breast Cancer Antiestrogen Resistance 3 (BCAR3) together with Cas and Src, promotes breast cancer cell migration and invasion. The work presented in this thesis focuses on identifying the role of BCAR3 in TNBC growth and progression. Using *in vivo* and *in vitro* approaches, the data presented in this thesis demonstrate that BCAR3 promotes TNBC tumor growth, proliferation, and migration. Our studies show that BCAR3 protein expression is elevated in patient-derived breast cancer tumor samples and in TNBC cell lines, and elevated BCAR3 mRNA levels are associated with poor outcomes in patients with TNBC. This work is the first to report that BCAR3 regulates TNBC tumor growth in mouse orthotopic

xenograft models. Our data also show that BCAR3 is a regulator of MET signaling and that BCAR3-MET coupling has a functional role in TNBC.

As a follow up to these findings, studies were undertaken to understand the role of BCAR3-MET coupling in basal-like TNBC. Using biochemical approaches, preliminary data are presented showing that basal-like TNBC cells with reduced BCAR3 expression exhibit elevated levels of MET receptor expression and phosphorylation. Conversely, when BCAR3 was over-expressed in a basal-like cell line with low endogenous levels of BCAR3, MET receptor levels and phosphorylation were reduced. These changes were not observed in claudin-low TNBC cells, suggesting that BCAR3 may regulate MET signaling differently based on the genetic background of TNBC. Future studies are needed to determine the functional significance of these findings.

Finally, preliminary studies are presented using computational approaches to investigate the transcriptional landscape regulated by BCAR3 in TNBC cells. Differential gene expression analysis on cells cultured on plastic, matrigel, and in mouse mammary epithelial cell organoids showed that BCAR3 regulates a broad set of genes and pathways. While the expression of 33 genes was impacted by loss of BCAR3 under all three conditions, a subset of the pathways regulated by BCAR3 in TNBC cells cultured on plastic was distinct from those in cells cultured in 3D matrigel. Validation as well as functional studies are needed to make conclusions about the transcriptional networks regulated by BCAR3.

The data presented in this thesis indicate that BCAR3 is an important promoter of TNBC growth and may serve as a valuable biomarker and/or

therapeutic target to improve the clinical care of patients with TNBC in this age of precision medicine. Future studies are required to explore how BCAR3 serves to integrate signals that promote aggressive tumor phenotypes to maximize targeting of functional BCAR3 signaling nodes.

## **Table of Contents**

Abstract .....	i
Table of Contents .....	iv
List of Figures .....	xi
List of Tables .....	xiv
List of Abbreviations .....	xv
Acknowledgments .....	xix
Chapter 1: Introduction .....	1
1.1 Breast cancer overview .....	1
1.1.1 Incidence and survival statistics .....	1
1.1.2 Breast cancer pathology .....	2
1.1.3 Hormone receptor and human epidermal growth factor receptor 2 (HER2) status .....	3
1.1.4 Molecular profiling of breast cancer .....	5
1.1.5 Mechanisms of breast cancer initiation .....	9
1.1.6 Mechanisms of breast cancer progression .....	10
1.1.7 Therapeutic strategies .....	16
1.2 Targeted therapy for breast cancer .....	18
1.2.1 Targeted therapies for hormone receptor-positive and HER2- positive breast cancer .....	18
1.2.2 Targeted therapies for BRCA-mutated breast cancer .....	20
1.3 Triple-negative breast cancer (TNBC) .....	21
1.3.1 Incidence and molecular profile of TNBC .....	21

1.3.2	TNBC mechanisms of growth and progression .....	24
1.3.3	Therapeutic strategies and challenges for TNBC.....	25
1.4	Role of growth factor receptor signaling in TNBC .....	26
1.4.1	EGFR family members .....	26
1.4.2	Fibroblast growth factor receptors (FGFRs).....	28
1.4.3	MET receptor signaling.....	29
1.5	BCAR3/CAS/Src signaling in TNBC .....	31
1.5.1	Breast Cancer Antiestrogen Resistance 3 (BCAR3) .....	31
1.5.2	Cas .....	35
1.5.3	Src .....	38
1.6	Autocrine/paracrine signaling in TNBC.....	40
1.6.1	HGF/MET signaling .....	40
1.6.2	TGF $\beta$ signaling .....	41
1.7	Significance and overview .....	43

Chapter 2: Breast Cancer Antiestrogen Resistance 3 (BCAR3) promotes tumor growth and progression in triple-negative breast cancer.....	46
2.1 Abstract.....	46
2.2 Introduction .....	48
2.3 Materials and methods.....	50
2.3.1 Histological staining and microarray analysis .....	50
2.3.2 Patient survival analysis .....	50
2.3.3 Cell culture .....	50

2.3.4	Ectopic expression and knockdown of BCAR3.....	50
2.3.5	Tumor xenografts.....	53
2.3.6	Immunoblotting .....	54
2.3.7	Organoid cultures .....	54
2.3.8	Cell proliferation and colony growth.....	54
2.3.9	Survival assay.....	57
2.3.10	Gene set variation analysis (GSVA) .....	57
2.3.11	Transwell migration assay .....	57
2.3.12	Drug inhibitor assays .....	58
2.3.13	Quantitative real-time PCR.....	58
2.3.14	Statistical analysis .....	59
2.4	Results .....	61
2.4.1	BCAR3 is upregulated in breast cancer tumor samples and TNBC cell lines.....	61
2.4.2	BCAR3 promotes TNBC tumor growth <i>in vivo</i> .....	64
2.4.3	BCAR3 promotes TNBC cell proliferation.....	67
2.4.4	BCAR3 is required for budding of mouse mammary epithelial organoids in response to growth factors.....	70
2.4.5	BCAR3-MET coupling regulates TNBC cell proliferation and migration.....	73
2.4.6	HGF promotes colony growth in Hs578T cells .....	85
2.5	Discussion.....	90
2.5.1	BCAR3 is a regulator of MET signaling .....	90

2.5.2 Targeting BCAR3 signaling pathways for the treatment of TNBC ....	
.....	94
Chapter 3: BCAR3-MET coupling in triple-negative breast cancer .....	97
3.1 Abstract.....	97
3.2 Introduction .....	98
3.3 Materials and methods.....	100
3.3.1 Cell culture .....	100
3.3.2 Principal component analysis (PCA) .....	101
3.3.3 Small-interfering RNA transfection .....	101
3.3.4 Immunoblotting .....	102
3.3.5 Growth factor and inhibitor assays .....	102
3.3.6 Quantitative real-time PCR analysis .....	102
3.3.7 Ectopic expression of BCAR3.....	103
3.3.8 Statistical analysis .....	103
3.4 Results .....	104
3.4.1 MET signaling gene sets differentially align with the Basal A and Basal B TNBC subtypes .....	104
3.4.2 BCAR3 regulates MET protein levels and phosphorylation in basal- like TNBC cells .....	104
3.4.3 “Gain of function” approach supports reciprocal co-regulation of BCAR3-MET expression .....	118

3.4.4	MET expression does not exhibit BCAR3-dependent regulation in claudin-low TNBC cells.....	121
3.4.5	Src reduces MET upregulation in HCC1937 cells .....	126
3.5	Discussion.....	129
Chapter 4: Exploring the transcriptional landscape regulated by BCAR3 .....		135
4.1	Abstract.....	135
4.2	Introduction .....	137
4.3	Materials and methods.....	138
4.3.1	Cell culture .....	138
4.3.2	Stable knockdown of BCAR3.....	138
4.3.3	3D matrigel cell culture .....	139
4.3.4	Organoid cultures .....	139
4.3.5	RNA sequencing and differential gene expression analysis.....	139
4.3.6	Quantitative real-time PCR .....	140
4.3.7	Identification of differentially expressed genes and pathway enrichment analysis.....	141
4.3.8	Statistical analysis .....	141
4.4	Results .....	144
4.4.1	Identification of differentially expressed genes in MDA-MB-231 cells as a function of BCAR3 expression .....	144
4.4.2	Pathway enrichment in MDA-MB-231 cells reveals novel BCAR3-regulated pathways .....	150

4.4.3	BCAR3 regulates genes involved in cell adhesion .....	153
4.4.4	Identification of differentially expressed genes as a function of BCAR3 in mouse mammary organoids .....	157
4.4.5	BCAR3-regulated pathways in mouse mammary organoids may drive cell growth.....	165
4.5	Discussion.....	168
Chapter 5: Perspectives .....		171
5.1	BCAR3-MET dependent regulation of aggressive phenotypes in TNBC..... .....	172
5.1.1	How does BCAR3 regulate MET signaling in claudin-low TNBC? ... .....	172
5.1.2	How does BCAR3 regulate MET expression in basal-like TNBC?... .....	174
5.1.3	Does BCAR3-MET coupling serve as a molecular switch of aggressive phenotypes in basal-like TNBC? .....	175
5.1.4	What are the implications of changes in MET phosphorylation? .....	176
5.2	Molecular functions of BCAR3 in regulating the transition to invasive breast cancer .....	178
5.2.1	What is the role of BCAR3 in early-stage breast cancer? .....	178
5.2.2	Can BCAR3 serve as a prognostic tool? .....	180

- 5.3 Role of BCAR3 as an integrator of mechanical signals from the tumor microenvironment ..... 182
  - 5.3.1 Can BCAR3 contribute to the cellular responses to mechanosensory stimuli present in the tumor microenvironment? .. ..... 182
  - 5.3.2 Is BCAR3 a functional regulator of the mammary circadian clock?.. ..... 183
- 5.4 Potential role of BCAR3 as a biomarker for targeted therapy and/or a therapeutic target in breast cancer ..... 184
  - 5.4.1 Can BCAR3 serve as a biomarker to identify breast cancer patients for targeted therapy? ..... 185
  - 5.4.2 Can BCAR3 serve as a therapeutic target?..... 186
- 5.5 Final conclusions ..... 189
- 5.6 References..... 190

**List of Figures**

Figure 1-1	“Intrinsic” breast cancer molecular subtypes .....	6
Figure 1-2	Models of breast cancer initiation .....	11
Figure 1-3	Epithelial-to-mesenchymal transition .....	14
Figure 1-4	Triple-negative breast cancer molecular subtypes .....	22
Figure 1-5	Schematic diagram of BCAR3 .....	32
Figure 1-6	Schematic diagram of a potential BCAR3-Cas-Src complex..... .....	36
Figure 2-1	BCAR3 is upregulated in breast cancer samples and TNBC tumor cell lines.....	62
Figure 2-2	BCAR3 promotes tumor growth in orthotopic MDA-MB-231 mouse xenograft models .....	65
Figure 2-3	BCAR3 promotes TNBC cell proliferation.....	68
Figure 2-4	BCAR3 knockdown does not impact cell viability at 24 or 72 hours.....	71
Figure 2-5	BCAR3 promotes budding of mammary organoids under conditions of FGF2 and TGF $\alpha$ treatment.....	74
Figure 2-6	BCAR3 and MET function in the same proliferation and migration pathways.....	77
Figure 2-7	Foretinib inhibits MET receptor activation but does not impact viability at 50nM .....	80
Figure 2-8	BCAR3 regulates MET receptor activation in cells cultured long- term.....	83

Figure 2-9	HGF treatment differentially impacts colony size distribution of Hs578T cells as a function of BCAR3.....	87
Figure 2-10	BCAR3-MET coupling in TNBC cells.....	91
Figure 3-1	TNBC cell lines cluster based on their molecular profile when MET pathway genes are analyzed .....	105
Figure 3-2	BCAR3 regulates MET receptor protein expression in HCC1937 cells.....	108
Figure 3-3	HCC1937 cells exhibit elevated levels of MET phosphorylation following acute HGF stimulation .....	110
Figure 3-4	BCAR3 expression is elevated in HCC1937 cells following prolonged HGF treatment.....	113
Figure 3-5	MDA-MB-468 cells exhibit sustained MET and AKT phosphorylation following prolonged HGF treatment.....	116
Figure 3-6	MET receptor expression and phosphorylation is reduced in HCC1937 cells with BCAR3 overexpression .....	119
Figure 3-7	MET receptor expression and phosphorylation are not altered in claudin-low TNBC cells following prolonged HGF treatment.....	122
Figure 3-8	MET receptor expression and phosphorylation are not altered in claudin-low TNBC cells following short-term HGF stimulation.....	124
Figure 3-9	BCAR3 overexpression does not alter MET receptor expression and phosphorylation in claudin-low MDA-MB-436 cells.....	127

Figure 3-10	Src inhibition reduces MET receptor elevation in HCC1937 cells with BCAR3 knockdown .....	130
Figure 4-1	Identification of differentially expressed genes in TNBC cells cultured on plastic and in matrigel as a function of BCAR3 expression .....	145
Figure 4-2	BCAR3-dependent differentially expressed genes that were common to both plastic and matrigel culture conditions are altered in similar directions .....	148
Figure 4-3	Pathway enrichment in MDA-MB-231 cells with reduced BCAR3 expression .....	151
Figure 4-4	Pathway enrichment of genes altered as a function of BCAR3 expression that are unique to each culture condition .....	154
Figure 4-5	BCAR3-dependent differentially expressed genes that overlap between MDA-MB-231 cells cultured on plastic or matrigel map to the focal adhesion pathway .....	158
Figure 4-6	BCAR3-dependent differentially expressed genes that overlap between MDA-MB-231 cells cultured on plastic or matrigel map to molecules involved in cell adhesion.....	160
Figure 4-7	Identification of differentially expressed genes in mouse mammary organoids as a function of BCAR3 expression .....	163
Figure 4-8	Pathway enrichment in mouse mammary organoids with BCAR3 knockout .....	166

**List of Tables**

Table 2-1	Cell lines used in this study .....	51
Table 2-2	Antibodies used in this study .....	55
Table 2-3	Primer sequences for qRT-PCR .....	60
Table 4-1	Human primer sequences for qRT-PCR.....	142
Table 4-2	Mouse primer sequences for qRT-PCR.....	143

**List of Abbreviations**

ADC = Antibody-drug conjugate

ADCC = Antibody-dependent cellular cytotoxicity

ADH = Atypical ductal hyperplasia

ALH = Atypical lobular hyperplasia

ANOVA = Analysis of variance

B3KO = BCAR3 knockout

BCAR3 = Breast Cancer Antiestrogen Resistance 3

BL1 = Basal-like 1

BL2 = Basal-like 2

BTRF = Biorepository and Tissue Research Facility

BSA = Bovine serum albumin

CAF = Cancer-associated fibroblasts

Cas = p130<sup>Cas</sup>

CASS4 = Cas scaffolding protein family member 4

CCLC = Cancer cell line encyclopedia

CDH3 = P-cadherin

CDK = Cyclin-dependent kinase

CRL5 = Cullin5/RBX2 ligase

CSC = Cancer stem-like cell

DCIS = Ductal carcinoma *in situ*

DMEM = Dulbecco's modified Eagle's medium

Dox = Doxycycline

ECM = Extracellular matrix

EFS = Embryonal Fyn-associated substrate

EGF = Epidermal growth factor

EGFR = Epidermal growth factor receptor

EMT = Epithelial-to-mesenchymal transition

ER = Estrogen receptor

ER $\alpha$  = Estrogen receptor-alpha

ER $\beta$  = Estrogen receptor-beta

FAK = Focal adhesion kinase

FBS = Fetal bovine serum

FEA = Flat epithelial atypia

FFPE = Formalin-fixed, paraffin-embedded

FGFR = Fibroblast growth factor receptor

GATA3 = GATA binding protein 3

Gab1 = Grb2 associated binding protein 1

GEF = Guanine nucleotide exchange factor

GSVA = Gene set variation analysis

H&E = Hematoxylin and eosin

HER2 = Human epidermal growth factor receptor 2

HER3 = Human epidermal growth factor receptor 3

HEY1 = Hairy/enhancer-of-split related with YRPW motif protein 1

HGF = Hepatocyte growth factor

HR = Hormone receptor

Ig = Immunoglobulin

IHC = Immunohistochemistry

IM = Immunomodulatory

IP = Intraperitoneal

IPT = Immunoglobulin-like regions in plexins and transcription factors

K14 = Cytokeratin 14

KEGG = Kyoto Encyclopedia of Genes and Genomes

LAR = Luminal androgen receptor

LCIS = Lobular carcinoma *in situ*

LLGL2 = LLGL scribble cell polarity complex component 2

M = Mesenchymal

MAME = Mammary architecture and microenvironment engineering

MMP = Matrix metalloproteinase

MSL = Mesenchymal stem-like

NEDD9 = Neural precursor cell expressed developmentally down-regulated 9

NSP = Novel SH2-containing protein

PAM = Prediction analysis of microarray

PARP = Poly (ADP-ribose) polymerase

PCA = Principal component analysis

RT-PCR = Real-time polymerase chain reaction

PDGF = Platelet-derived growth factor

PID = Pathway Interaction Database

PR = Progesterone receptor

PSI = Plexin-semaphorin-integrin  
PTP1B = Protein tyrosine phosphatase 1B  
PTP $\alpha$  = Protein tyrosine phosphatase  $\alpha$   
RIPA = Radioimmunoprecipitation assay  
RPMI = Roswell Park Memorial Institute  
SEM = Standard error of the mean  
Sema = Semaphorin  
SF = Scatter factor  
SH = Src homology  
Shc2 = SHC adaptor molecule 2  
shRNA = Short hairpin RNA  
siRNA = Small interfering RNA  
SNAI2 = Snail family transcriptional repressor 2  
Src = c-Src  
TCPTP = T-cell protein tyrosine phosphatase  
TGF $\alpha$  = Transforming growth factor alpha  
TGF- $\beta$  = Transforming growth factor beta  
TNBC = Triple-negative breast cancer  
TNM = Tumor, nodes, metastases  
Trop-2 = Trophoblast cell surface antigen 2  
TRP63 = Transformation-related protein 63  
WT = Wildtype

## **Acknowledgments**

I dedicate this thesis to my family, my parents Jose Luis Arras and Isabel Arras, and my sister Brenda Arras. Thank you for your endless support. Your hard work, perseverance, and determination have inspired me throughout my life. Thank you for always encouraging me through this journey, listening to my thoughts, giving me advice, and always brightening my day. I could not have done any of this without you.

I would like to thank my mentor Dr. Amy Bouton for the support, mentorship, patience, training, guidance, and feedback she provided throughout my graduate school career. Amy pushed me to think outside my comfort zone, trained me to think critically, focused on rigor and reproducibility, and shaped me to become a well-rounded scientist. I have learned so much during these last few years and I am very grateful to have had the opportunity to be a member of this lab. I will always remember the lab lunches, meetings, conversations, and laughs we shared. I would also like to thank Keena Thomas for her constant support, help, and advice. I could not have completed my graduate training without her help. I hope to one day be as organized and efficient as Keena.

I would also like to give my sincerest thank you to my committee members Dr. Andrew Dudley, Dr. Janet Cross, Dr. Kevin Janes, Dr. David Brautigan, and Dr. Hui Zong for their encouragement, insightful comments, suggestions, and guidance through this project. In addition, I would like to give a special thank you to Dr. Matthew Lazzara and Paul Myers for their collaboration in this project. Paul Myers provided important computation analyses for this project and our

discussions helped me gain a better understanding of computational approaches that can be used for data analysis.

Finally, I would like to thank past members of the lab who significantly contributed to the work in this thesis, Dr. Allison Cross, Mira Sridharan, Amare Osei, Garvey Cummings, Ryan Chipman, and Gabriel Vazquez, as well as all the friends that helped me and provided encouragement during my training.

## **Chapter 1: Introduction**

### **1.1 Breast cancer overview**

#### **1.1.1 Incidence and survival statistics**

Breast cancer accounts for 30% of new cancer cases and 15% of cancer-related deaths in females [1]. The lifetime likelihood of a woman developing invasive breast cancer is about 13% (1 in 8). The incidence rates of breast cancer in women continue to rise by 0.5% per year, this rise in cases has been associated with risk factors such as increased body mass index and decreased fertility rates seen in recent years [1,2]. Breast cancer is associated with non-modifiable and modifiable risk factors. Non-modifiable risk factors include age, sex, BRCA1/BRCA2 gene mutations (involved in DNA damage repair), family history, age of menarche, age of menopause, high breast density, and history of breast disease among others [3–5]. Hereditary breast cancers are most frequently associated with BRCA1 or BRCA2 mutations, which together have been associated with a cumulative breast cancer risk of about 84% by the age of 70 [6]. Modifiable risk factors include, obesity, physical inactivity, alcohol consumption, tobacco use recent and long-term, use of menopausal hormone therapy, and hormonal contraceptive use [5]. Breast cancer survival rates vary by molecular subtype, with estrogen receptor positive (ER+), progesterone receptor positive (PR+) and human epidermal growth factor receptor 2 negative (HER2-) breast cancer having a 5-year survival rate of 92.5%, followed by ER+/PR+/HER2+ breast

cancer (90.3%), ER-/PR-/HER2+ breast (82.7%), and triple-negative ER-/PR-/HER2- breast cancer having the worst survival rate at 77% [7]. The stages of breast cancer include the local stage where a tumor is confined to the site of origin, the regional stage where a tumor has extended beyond the site of origin and has infiltrated surrounding tissues and regional lymph nodes, and the distant stage where tumor cells have spread to distant sites [8]. The stage at which breast cancer is diagnosed influences patient survival rates, with breast cancer diagnosed at the local stage having a 5-year survival rate of 99%, regional (86%), and distant (28%). Racial and ethnic disparities, socioeconomic status, and late-stage breast cancer at diagnosis are all factors that also influence breast cancer survival rates [9,10].

### **1.1.2 Breast cancer pathology**

Progression of breast cancer is generally thought to occur through a series of processes beginning with hyperplastic lesions in the breast, subsequent development of *in situ* carcinoma, and finally invasive carcinoma [11]. Several models of breast cancer progression have been proposed. One such model describes flat epithelial atypia (FEA), atypical ductal hyperplasia (ADH), and ductal carcinoma *in situ* (DCIS) as non-obligate precursors to invasive ductal carcinoma [12]. For invasive lobular carcinoma a proposed model includes atypical lobular hyperplasia (ALH) and lobular carcinoma *in situ* (LCIS) as non-obligate precursor lesions.

Breast cancer encompasses a group of diseases typically assessed by lymph node status, tumor size, metastasis, and molecular biomarkers [13].

Histological grade is also used to characterize breast tumors and is divided into 3 grades [14]. Grade 1 tumors are characterized as being well-differentiated with high resemblance to the normal breast tissue, >75% tubule formation (formation of small ducts), a mild degree of nuclear irregularity, and low mitotic count. Grade 2 tumors are characterized as moderately differentiated tumors and grade 3 tumors as poorly differentiated with high irregularity of cell shape and size, high mitotic count, and no tubule formation. The two most common types of invasive breast cancers are ductal and lobular breast carcinomas, which constitute about 73% and 15% of invasive breast tumors [15]. Less frequent histological types of breast cancers include mucinous, comedo, tubular, and medullary carcinomas, each of which accounts for less than 2% of all breast cancer cases.

### **1.1.3 Hormone receptor and human epidermal growth factor receptor 2 (HER2) status**

Identifying the hormone and human epidermal growth receptor status of a breast cancer tumor is an important way to assess prognosis as well as clinical management of the patient. Hormone receptor status indicates the presence/expression of the estrogen receptor (ER) and progesterone receptor (PR) in breast tumor samples. These receptors are of interest because estrogen and progesterone, both circulating steroid hormones, have been found to bind to their respective receptors and elicit activation of signaling networks that influence a broad range of cellular behaviors including cell proliferation. High levels of circulating progesterone and estrogen together have been found to increase the

risk of breast cancer [16]. Estrogen most commonly functions by binding to nuclear ER, which in turn promotes occupancy of estrogen response elements present in DNA, causing changes in gene transcription [17]. Estrogen can bind to two forms of the ER, estrogen receptor-alpha ( $ER\alpha$ ) and estrogen receptor-beta ( $ER\beta$ ) both of which have a high degree of homology in their ligand binding domains and interact with identical DNA response elements [18]. Studies have shown that  $ER\alpha$  and  $ER\beta$  expression differs, with normal areas of breast tissue exhibiting low expression of  $ER\alpha$  and high expression of  $ER\beta$  and areas of DCIS exhibiting elevated levels of  $ER\alpha$  expression and reduced expression of  $ER\beta$  [19]. Elevated levels of  $ER\alpha$  have been found in early invasive ductal carcinoma and in advanced invasive lobular carcinoma. Mechanistically,  $ER\alpha$  and  $ER\beta$  seem to exhibit antagonizing effects in breast cancer cell lines, with  $ER\alpha$  promoting cell proliferation by driving transcription of genes involved in cell growth and  $ER\beta$  inhibiting cell growth [20].

Progesterone is a steroid hormone that can bind to the PR and together this interaction is important for mammary gland development [21]. Studies have found that  $PR\alpha$  and  $PR\beta$  are differentially localized within the developing mammary gland, with  $PR\beta$  being essential for normal mammary gland development while  $PR\alpha$  is essential for uterine development [22–24].

About 20-30% of breast cancers are positive for HER2 as measured by copy number changes (HER2 overexpression) or fluorescence in-situ hybridization (HER2 amplification) [25,26]. HER2 belongs to the epidermal growth factor

receptor (EGFR) family, does not have any specific ligand, and functions by dimerizing with other EGFR family members, driving signaling mechanisms involved in tumor growth and metastasis [27–29]. Together, screening for ER, PR, and HER2 expression in breast tumors has emerged as a valuable prognostic tool. Due to their contribution to tumor growth and progression, these receptors have also become important therapeutic targets.

#### **1.1.4 Molecular profiling of breast cancer**

Advancements in gene expression profiling of breast tumors has enabled the distinction of different subtypes of breast cancer. Studies by Perou *et al.* aimed to improve the molecular classification of breast cancer by using gene expression analysis [30]. Their findings identified subsets classified as ER+/luminal-like, basal-like, HER2+, and normal breast. Subsequent analysis of these breast cancer subgroups further classified them into more discrete “intrinsic subtypes” termed, luminal subtype A, luminal subtype B, luminal subtype C, normal breast-like, basal-like, and HER2+ (Figure 1-1) [31]. These subgroups were subsequently analyzed to identify potential differences in overall patient survival and relapse-free survival. Basal-like and HER2 enriched subtypes of breast cancer were found to have the shortest survival times and shortest relapse-free survival times. The luminal C subtype was associated with worst patient outcomes compared to luminal A and luminal B subtypes and was also identified as having similar gene expression patterns to ER- basal-like and HER2+ subtypes.

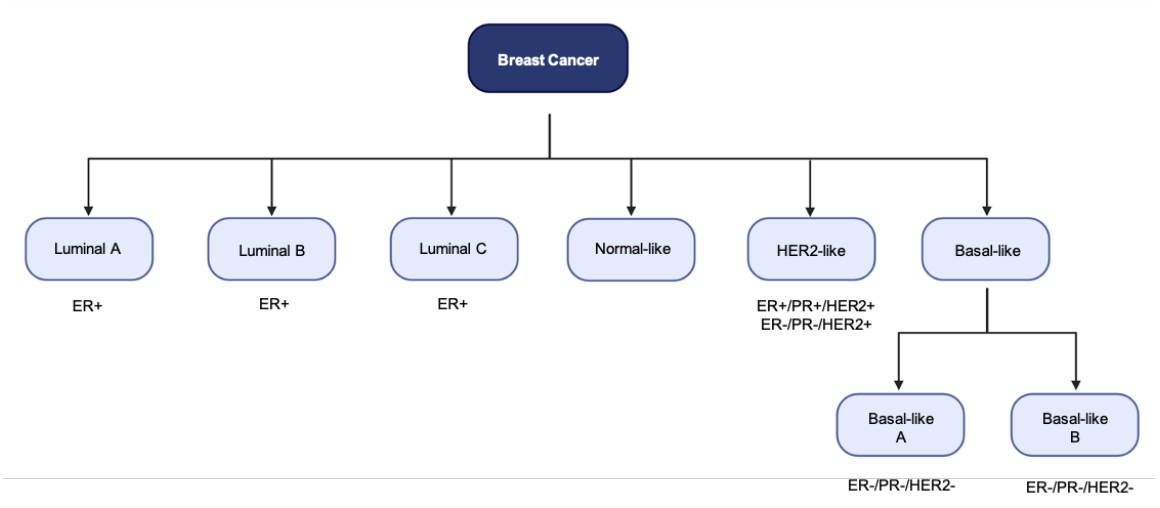


**Figure 1-1. “Intrinsic” breast cancer molecular subtypes.** The flow-chart diagram shows “intrinsic” breast cancer molecular subtypes identified using cDNA microarrays and hierarchical clustering. Figure created with BioRender.com.

To further assess the prognostic value of the “intrinsic” subtypes previously identified (luminal A, luminal B, HER2-enriched, basal-like, and normal-like), a 50 gene set was compared for reproducibility in identifying the molecular subtypes using a form of machine learning that utilizes mean-based clustering called “Prediction Analysis of Microarray (PAM)” [32]. This 50 gene-set, now referred to as the “PAM50,” was then used for the molecular classification of patient-derived tumor samples and prediction of clinical outcomes such as relapse-free survival and response to neoadjuvant (pre-surgery) chemotherapeutic drug treatment. Overall, the PAM50 gene set was found to be a valuable tool in the identification of intrinsic molecular subtypes and modeling risk prediction.

Studies using the PAM50 gene set further identified an additional subtype of breast cancer labeled as claudin-low [33]. This subtype of breast cancer was found to have enrichment of genes involved in the epithelial-to-mesenchymal transition (EMT; a process that promotes migration and invasion) such as SNAIL and TWIST, immune system responses, and stem-cell features. Like the basal-like subgroup, most tumors classified as claudin-low exhibited ER-/PR-/HER2- status and showed a lower pathological complete response after chemotherapy.

In parallel to efforts aimed at detecting deregulated genes in breast cancer subsets, other studies aimed at identifying the functional contributions of identified gene sets. Studies by R. Neve *et al.* used transcriptional profiles along with hierarchical clustering to identify molecular signatures present in breast cancer cell lines [34]. These studies further identified two groups within the basal cluster labeled basal A and basal B (Figure 1-1). The basal A cluster exhibited

characteristics more similar to the basal-like group of the “intrinsic subtypes” originally found in the studies by Perou *et al.* The cells in this cluster expressed basal markers and exhibited either luminal-like or basal-like morphologies. On the other hand, the basal B cluster expressed stem-cell related genes, appeared less differentiated with mesenchymal morphologies, and had increased invasion.

Together, molecular subtyping of breast tumors together with TNM staging (tumor size, lymph node status, and metastasis), histology, hormone receptor status, and HER2 status have improved the prognosis and clinical management of patients with breast cancer [32].

### **1.1.5 Mechanisms of breast cancer initiation**

As described above, development of breast cancer occurs through multiple steps involving hyperplasia of breast tissue, carcinoma *in situ*, and invasive carcinoma [11,12,35]. Processes that are important for normal mammary gland development have also been reported to be involved in cancer progression when de-regulated [36,37]. Postnatal mammary gland development is a dynamic process that involves mammary branching morphogenesis and formation of terminal end buds, tubule formation, and differentiation into distinct luminal or myoepithelial cells [38]. Lineage tracing studies have shown that the mammary gland develops from embryonic cytochrome 14 positive (K14+) progenitors that give rise to long-lived lineage restricted stem cells that differentiate into either myoepithelial cells or luminal cells [39].

The presence of long-lived stem cells in mammary glands and the identification of breast cancer stem cells has led to several theories about how breast cancer initiates [39,40]. The main theories are 1) the cell of origin theory and 2) the stochastic theory [35,41]. The cell of origin/cancer stem cell theory postulates that each tumor subtype is initiated by the same stem cell or progenitor cell (Figure 1-2A). The stochastic theory postulates that any epithelial cell type (stem cell, progenitor, or differentiated cell) can be the target of an initiating event that gives rise to different tumor subtypes (Figure 1-2B). Recent studies have demonstrated that BRCA1-mutated breast cancer originates from luminal stem cell progenitors despite having basal-like characteristics [42]. Despite this evidence, more studies are needed to understand how stem or progenitor cells as well as tumor initiating events play a role in driving breast cancer development.

### **1.1.6 Mechanisms of breast cancer progression**

As previously stated, various key molecules have been identified as drivers of oncogenic signaling that promote breast cancer growth, such as ER, PR, and HER2. The ability of breast cancers to grow and eventually invade/colonize distant sites (metastasize) is the predominant cause of breast cancer-related mortality. The 5-year survival of breast cancer patients who present with distant (metastatic) disease is about 28% [8]. Understanding the mechanisms that drive breast cancer invasion is important in order to improve patient prognosis. The EMT is an important process that occurs during development wherein epithelial cells gain mesenchymal characteristics and exhibit increased migration and invasion [43]. In

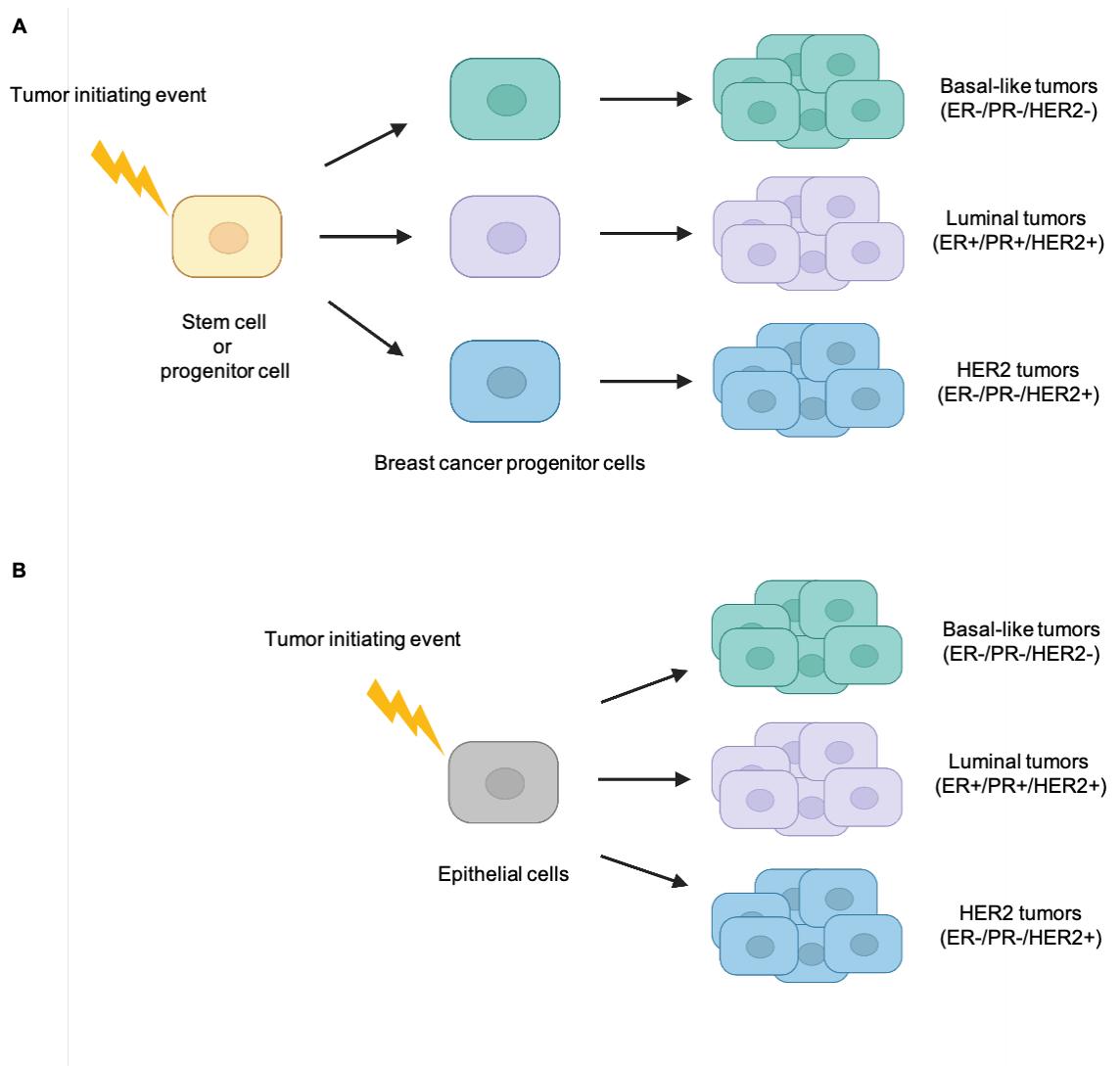


**Figure 1-2. Models of breast cancer initiation.** (A) The cell of origin/cancer stem cell theory postulates that each tumor subtype is initiated by the same stem cell or progenitor cell, which in turn gives rise to breast cancer progenitor cells (breast cancer stem cells) from which different subtypes of breast cancer arise. (B) The stochastic theory postulates that any epithelial cell type (stem cell, progenitor, or differentiated cell) can be the target of an initiating event that gives rise to different tumor subtypes. Figure created with BioRender.com.

the context of cancer, EMT enables cancer cells to gain increased migratory and invasive capabilities as well as chemotherapeutic resistance [43,44]. During cancer progression, cancer cells integrate signals from the surrounding microenvironment that enable EMT (Figure 1-3). These signals promote intracellular signaling in response to growth factors present in the tumor microenvironment such as hepatocyte growth factor (HGF), epidermal growth factor (EGF), platelet-derived growth factor (PDGF), and transforming growth factor  $\beta$  (TGF- $\beta$ ), leading to changes in transcription factors like SNAIL, SLUG, TWIST, and ZEB1 that promote EMT [43]. Cancer cells undergoing EMT typically exhibit loss of E-cadherin protein expression and increased expression of markers such as vimentin. EMT is a process that enhances the metastatic potential of cancer cells by increasing cell migration and invasion capabilities.

Migration and invasion are processes highly influenced by the extracellular microenvironment. In order to migrate, cells can form various types of protrusions, mainly through sequential activation of the Rho family GTPases Cdc42, Rac1, and Rho [45]. Specialized structures termed invadopodia are involved in breast cancer cell migration and invasion [46]. Interaction with the extracellular matrix (ECM) is stabilized by engaging integrins, which engage other regulatory linker molecules like paxilin to form cell adhesions [47,48]. Following stabilization of adhesions, actomyosin contractions together with adhesion disassembly enable cells to move forward. Other mechanisms thought to enable migration and invasion include the process of collective cell migration and macrophage-tumor cell interactions [49]. Collective cell migration is a means by which groups of cells invade into the

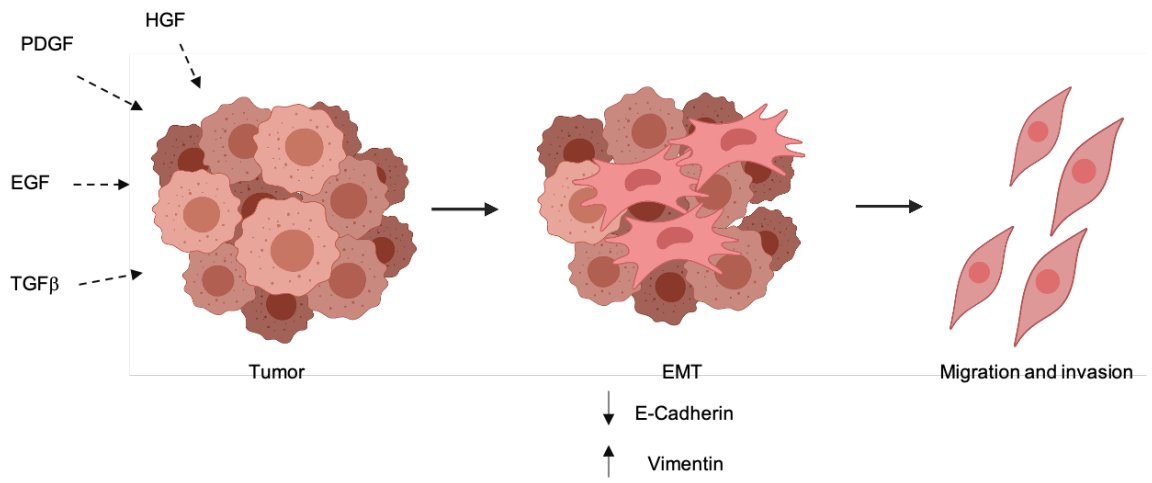


**Figure 1-3. Epithelial-to-mesenchymal transition.** Schematic representation of tumor responses to signals from the extracellular microenvironment. Cellular responses to factors such as HGF, TGF $\beta$ , EGF, or PDGF elicit downstream signaling events that lead to the activation of transcription factors that enable the downregulation of E-cadherin and upregulation of Vimentin, causing cells to acquire migratory properties. After undergoing EMT, tumor cells can migrate and invade distant sites. Figure created with BioRender.com

surrounding tissue and can involve fibroblast “leader” cells that serve to remodel the ECM, generating tracks that enable tumor cells to infiltrate the stroma. This process can also involve tumor “leader” cells, which are cells with a greater intrinsic invasion potential that have the ability to create tracks that other tumor cells can use for invasion. Further, macrophages have been reported to 1) secrete factors that enable tumor cell invasion and 2) facilitate tumor cell infiltration into blood vessels. Together, EMT and mechanisms that enable migration and invasion are essential components of the metastatic process.

### **1.1.7 Therapeutic strategies**

Tumor staging based on size, lymph node infiltration, and metastasis (TNM) along with hormone receptor/HER2 status are currently the main tools used to determine therapeutic strategies for patients with breast cancer. Lobular carcinoma *in situ* has low risk of progression to invasive disease so no advanced treatment is typically recommended other than increased routine screening [50]. Ductal carcinoma *in situ* is usually treated with breast-conserving surgery focused on removal of the lesion followed by radiation therapy to reduce the risk of recurrence in the same breast. Depending on the size of the DCIS lesion, mastectomy may be recommended followed by systemic endocrine therapy if the lesion is hormone receptor positive [51]. For early-stage breast cancer (Stage I-III), tumor size and hormone receptor status determine patient treatment, which may include breast-conserving surgery to remove the tumor or full mastectomy followed by radiation therapy. If there is suspicion that there is lymph node

infiltration, then neoadjuvant endocrine therapy may be recommended in patients with early-stage breast cancer depending on hormone receptor and HER2 status. Post-surgical treatment for patients with early-stage breast cancer includes endocrine therapy or HER2-targeted therapy. If advanced disease is detected, then chemotherapy may be recommended. For patients with late-stage (Stage IV) metastatic breast cancer, hormone therapy, chemotherapy, targeted drug therapy, or a combination of these treatments may be used.

Common therapeutic approaches for ER+ breast cancers involve targeting estrogen or the ER with 1) aromatase inhibitors that prevent production of estrogen by blocking the enzyme aromatase, 2) tamoxifen, which functions by blocking the ER, or 3) fulvestrant, which among other activities inhibits ER dimerization [52–54]. HER2-targeted therapy for HER2+ breast cancers involves the use of trastuzumab, which is a humanized monoclonal antibody that binds to HER2 and triggers antibody-dependent cellular cytotoxicity (ADCC) [55]. Studies have shown that trastuzumab binds to HER2-overexpressing cells, which triggers natural killer cells to initiate ADCC [56]. Trastuzumab is also thought to trigger internalization of HER2, leading to its degradation via activation of the ubiquitin ligase c-Cbl [57]. Together, these therapeutic options have increased patient survival rates to 91% for patients diagnosed with early-stage hormone receptor positive or HER2+ breast cancer [58].

## **1.2 Targeted therapy for breast cancer**

### **1.2.1 Targeted therapies for hormone receptor-positive and HER2-positive breast cancer**

In addition to the therapies described above, there are currently various clinically approved targeted therapies available for patients with hormone receptor positive (ER+/PR+) and HER2-positive breast cancers. Among the targeted therapies available for ER+/PR+ breast cancer are CDK4/6 inhibitors like palbociclib, ribociclib, and abemaciclib. CDK4 and CDK6 are cyclin-dependent kinases activated by cyclin D molecules that enable entry into the DNA synthesis (S) phase of the cell cycle. Inhibition of these molecules triggers apoptosis [59]. CDK4/6 became targets of interest in breast carcinomas when it became clear that cyclin D1 was overexpressed in breast cancers [60]. Further rationale for targeting CDK4 and CDK6 comes from preclinical studies showing that CDK4 is overexpressed in breast cancer and the interaction between cyclin D1 and CDK4 is important for tumor growth and progression [61]. Clinical approval of these agents was based on clinical trials demonstrating that CDK4/6 inhibitors, in addition to standard endocrine therapy, improved progression-free survival compared to endocrine therapy alone [62]. Consistent with targeting molecules that promote proliferation, mTOR inhibitors have also been recognized as valuable therapeutic agents. Clinical trials showed that patients with advanced hormone receptor positive breast cancer treated with the mTOR inhibitor, everolimus, in combination with the aromatase inhibitor, exemestane, exhibited increased progression-free survival compared to patients treated with aromatase inhibitor

alone [63]. PI3KCA, another important molecule that drives cell growth, has been reported to be mutated in 20-35% of all breast cancers and 40% of hormone receptor (HR)+/HER2- breast cancer. Mutations of PI3KCA are associated with tumorigenic potential, providing further rationale for targeting this molecule [64–66]. In clinical trials, patients with PI3KCA-mutated breast cancer treated with the PI3K inhibitor, alpelisib, in combination with the ER antagonist, fulvestrant, demonstrated increased progression-free survival compared to those treated with fulvestrant alone [66]. As stated above, HER2 is a receptor tyrosine kinase that elicits pro-survival signaling and promotes breast cancer growth. Clinical trials using targeted agents aimed at inhibiting HER2 kinase activity with the small molecule inhibitor lapatinib demonstrated that patients treated with lapatinib in combination with chemotherapy had prolonged time-to-progression and increased overall survival compared to those treated with chemotherapy alone [67]. Other clinically approved agents that target HER2 kinase activity include tucatinib and neratinib, both of which have shown clinical success in patients with HER2+ breast cancer [68,69]. Additionally, trastuzumab, an antibody targeting HER2, can be linked to chemotherapy for targeted drug delivery. Clinically approved antibody drug conjugates such as ado-trastuzumab emtansine or fam-trastuzumab deruxtecan demonstrated clinical efficacy in early stage HER2+ breast cancer and in metastatic breast cancer respectively [70,71]. Ongoing clinical trials are aimed at targeting additional molecules known to elicit pro-growth signaling such as histone deacetylases, new generations of PI3KCA inhibitors, immunotherapy, or different combinations of the targeted therapies stated above.

### **1.2.2 Targeted therapies for BRCA-mutated breast cancer**

Hereditary breast cancers are most frequently associated with BRCA1 or BRCA2 mutations, which together have been associated with a cumulative breast cancer risk of about 84% by the age of 70. BRCA1 is involved in maintaining genome integrity by functioning in DNA damage repair, where it is recruited to double stranded DNA breaks, becomes part of a complex that promotes 5'-end resection of double stranded breaks, and also helps recruit molecules such as the recombinase RAD51 [72]. BRCA1 is also involved in non-homologous end joining, single strand annealing, and in G1/S, S-phase, and G2/M checkpoints. On the other hand, the main function of BRCA2 is in homologous recombination repair of DNA, where it functions to recruit RAD51. Given that BRCA1 and BRCA2 mutations heavily impact DNA damage repair, breast cancer therapy for tumors with these mutations has focused on targeting additional DNA damage repair agents like poly (ADP-ribose) polymerase (PARP) for a combined effect to induce synthetic lethality [73]. The PARP inhibitor, olaparib, is approved for clinical use based on trials showing that breast cancer patients harboring germline BRCA mutations treated with olaparib had longer progression-free survival compared to patients receiving standard therapy alone [74]. Ongoing clinical trials for patients with BRCA mutations include early breast cancer detection trials (aimed at detecting circulating microRNAs), risk reduction trials, and trials targeting other agents involved in DNA damage repair like ATR and WEE1.

### 1.3 Triple-negative breast cancer (TNBC)

#### 1.3.1 Incidence and molecular profile of TNBC

Triple-negative breast cancer (TNBC) constitutes 10-20% of all breast cancer cases and is characterized as lacking immunohistochemically detectable expression of ER, PR, and amplified HER2 [75]. TNBC tumors typically affect younger patients and are more prevalent among black women of African descent [76,77]. TNBC tumors are identified as having a basal-like molecular subtype [78]. On pathology, these tumors present as high-grade at diagnosis, with features of basal-like tumors including elevated mitotic rate, geographic tumor necrosis, and pushing margins of invasion [77,78].

Gene expression and ontology analysis of TNBC patient tumor samples by Lehman *et al.* revealed six subtypes of TNBC, including two types of basal-like TNBC (BL1 and BL2), an immunomodulatory (IM), a mesenchymal (M), a mesenchymal stem-like (MSL), and a luminal androgen receptor (LAR) subtype (Figure 1-4) [75]. Gene expression analysis of TNBC tumor samples found that the majority of the previously identified basal A cell lines (described above) belonged to the BL1 and BL2 subtypes, whereas most basal B cell lines belonged to the M and MSL subtypes. These analyses also showed that BL1 and BL2 subtypes were enriched in pathways involved in cell cycle progression as seen by expression of genes such as AURKA, MYC, and NRAS as well as genes involved in the DNA damage response such as ATR/BRCA, CHEK1, and RAD51 among others. Drug sensitivity assays revealed that these subtypes of TNBC were more sensitive to DNA damaging agents like cisplatin. Furthermore, enrichment analysis showed

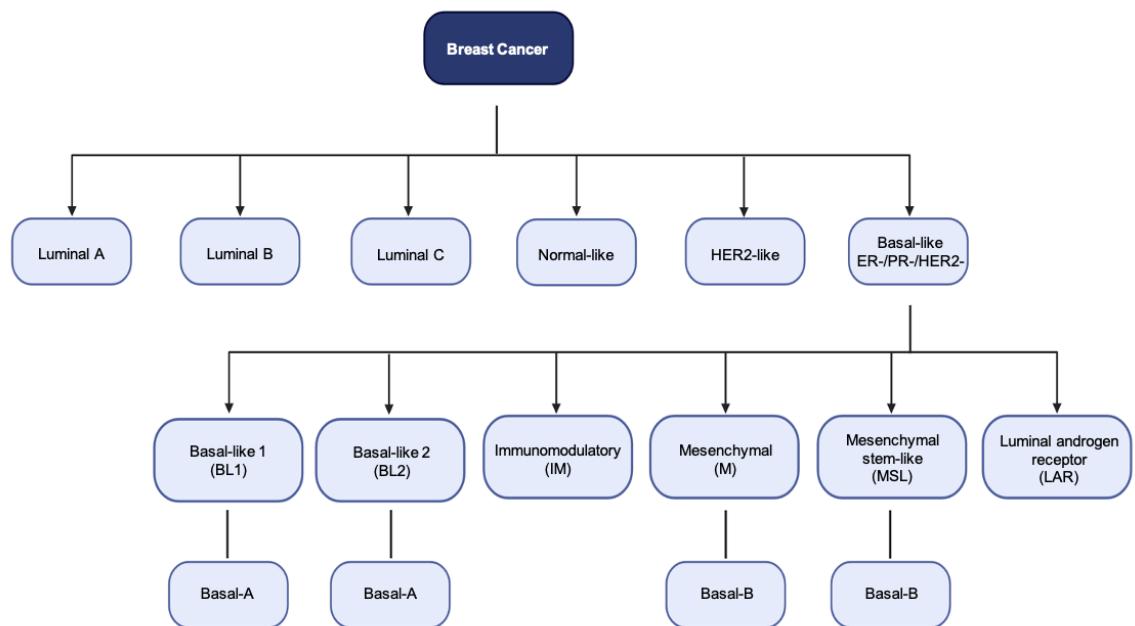


**Figure 1-4. Triple-negative breast cancer molecular subtypes.** The flow-chart diagram shows triple-negative breast cancer molecular subtypes identified using gene enrichment and pathway enrichment analyses. Figure created with BioRender.com.

that, while the BL1 subtype had enrichment of cell cycle and cell division components and pathways, the BL2 subtype had elevated enrichment in growth factor receptor gene expression such as EGFR, MET receptor, and ephrin type-A receptor 2 (EPHA2). The findings in this study further support previous histological observations that most triple negative breast cancers classify to the basal-like molecular subtype.

The immunomodulatory (IM) subtype of TNBC displayed enrichment of pathways involved in immune processes such as the TH1/TH2 pathway, NK cell pathway, and B cell receptor signaling among others. Mesenchymal (M) and mesenchymal stem-like (MSL) subtypes exhibited enrichment of EMT and growth factor gene expression and demonstrated increased sensitivity to a PI3K/mTOR inhibitor and to the Src inhibitor, dasatinib. Mesenchymal stem-like (MSL) subtypes were also found to have reduced expression of claudins 3, 4 consistent with the claudin-low subtype of breast cancer. Lastly, the LAR subtype exhibited gene enrichment of androgen receptor (AR) signaling and had increased sensitivity to the AR antagonist, bicalutamide. Together, this evidence shows that TNBC tumors have heterogeneity of mechanisms that enable growth, many of which could be targeted therapeutically.

### **1.3.2 TNBC mechanisms of growth and progression**

TNBCs are highly associated with the BRCA1 germline as well as somatic mutations. In addition, 81% of TNBCs have a mutation in TP53, 21% have a MUC16 mutation, and 20% having a PI3KCA mutation [75,79]. The BL1 subtype

of TNBC has been identified as having the highest rate of TP53 mutations. As stated above, TNBC tumors exhibit heterogeneity in the mechanisms that drive growth and progression. Further analysis by Bareche *et al.* of the TNBC subtypes stated above revealed that BL1 tumors had high levels of genomic instability as seen by high copy number losses of TP53, RB1, and BRCA1/2 and high copy numbers of PPAR1. Elevated mRNA levels of KRAS, NRAS, BRAF, PI3KCA, AKT2, and AKT3 genes were also observed in BL1 tumors. LAR subtype tumors had elevated mRNA expression of AKT1 and mesenchymal stem-like (MSL) subtype tumors had elevated levels of angiogenesis markers like PDGFR and VEGFR. Mesenchymal (M) subtype tumors were found to have elevated mRNA levels of EGFR, NOTCH1, and NOTCH3. Tumors identified as immunomodulatory (IM) subtype had elevated levels of immune checkpoint inhibitor genes such as PD1, PD-L1, and CTLA4 [79]. Together, these analyses demonstrate the wide array of signaling mechanisms involved in driving TNBC cell growth and progression and highlight the importance of identifying the molecular characteristics of each subtype for a targeted therapy approach.

### **1.3.3 Therapeutic strategies and challenges for TNBC**

The lack of immunochemically detectable levels of ER, PR and HER2, make TNBC a challenging disease to treat. The current standard-of-care for patients with TNBC is chemotherapy; however, novel therapeutic strategies have recently been approved for clinical use. Recent advances in immunotherapy have shown that patients with advanced stage TNBC achieve a significantly higher pathologic

complete response when they receive neoadjuvant treatment with the PD-1 receptor blocker, pembrolizumab, in combination with chemotherapy compared to chemotherapy alone [80]. Additionally, advances in antibody-drug conjugates (ADCs) have generated the ADC sacituzumab govitecan, which utilizes the glycoprotein trophoblast cell surface antigen 2 (Trop-2) that is frequently overexpressed in TNBC for targeted delivery of the topoisomerase I inhibitor, irinotecan [81,82]. The clinical approval of sacituzumab govitecan stems from clinical trials showing that patients with advanced TNBC who had previously received chemotherapy achieved a partial response or complete response to sacituzumab govitecan, with a high percentage of patients reporting reduced tumor burden [83]. Currently, there are ongoing clinical trials involving the use of inhibitors targeting PARP alone or in combination with chemotherapy [84]. Other ongoing trials target cyclin-dependent kinases (CDKs), DNA repair molecules (CHK1 and WEE1), growth factors and promoters of angiogenesis (EGFR, HER2, VEGF, VEGFR2, VEGFR/FGFR), AR, the PI3K/AKT/MTOR pathway, Src, and WNT signaling pathways.

## **1.4 Role of growth factor receptor signaling in TNBC**

### **1.4.1 EGFR family members**

EGFR family members are receptor tyrosine kinases implicated in driving many different types of cancer and consist of EGFR (ErbB1, HER1), HER2 (ErbB2, neu in rodents), HER3 (ErbB3), and HER4 (ErbB4) [85]. The structure of these receptors consists of a ligand-binding extracellular domain, a hydrophobic

transmembrane region, a catalytic intracellular kinase domain, and a carboxy-terminal region with tyrosine autophosphorylation sites [86,87]. The reported ligands for EGFR consist of epidermal growth factor (EGF), transforming growth factor alpha (TGF $\alpha$ ), and amphiregulin [85]. Unlike the other receptors, HER2 does not have a reported ligand capable of binding with high affinity [86]. Reported ligands for HER3 include neuregulin 1 and 2, and ligands for HER4 include betacellulin, epigen, epiregulin, and HER3-activating ligands [85]. Upon ligand binding, these receptors activate downstream signaling by forming homodimers or heterodimers between other EGFR family members. EGFR activation creates docking sites for adaptor molecules like Grb2, SHC adaptor molecule 2 (Shc2), and Grb2 associated binding protein 1 (Gab1), which then elicit activation of Ras/Raf/MET, PI3K/AKT, PLC $\gamma$ /PKC, and STAT signaling. EGFR activation has been reported to activate molecules such as c-Src (Src) which then in turn enhance EGFR signal activity [88,89]. Following activation, signal attenuation can be achieved through phosphatase-mediated dephosphorylation such as that of protein tyrosine phosphatase 1B (PTP1B), or through receptor internalization followed by ubiquitination and degradation mediated by the E3-ubiquitin ligase Cbl [85].

This EGFR family of receptors has been implicated in driving breast cancer growth and progression, with HER2 being expressed in about 20-30% of all breast cancers and EGFR being detected in about 56% of TNBC tumors [25,26,75]. Despite the high expression of EGFR in TNBC tumors, EGFR-targeted therapy has not been successful [90]. This underscores the need to further understand the

molecular mechanisms that drive different subsets of TNBC to identify susceptible tumors as well as potential therapeutic combinations.

#### **1.4.2 Fibroblast growth factor receptors (FGFRs)**

The fibroblast growth factor receptor (FGFR) family are receptor tyrosine kinases that include FGFR1, FGFR2, FGFR3, and FGFR4. They are important in a wide range of functions, including development, metabolism, tissue homeostasis, and cancer progression. The general structure of this receptor family consists of an extracellular domain, a transmembrane domain, and an intracellular domain. The extracellular domain contains a signal peptide, three immunoglobulin (Ig)-like domains (I, II, and III), an acidic box, a heparin binding motif, heparin cofactors, and any additional partner proteins [91]. The intracellular domain contains a juxtamembrane region that is involved in receptor dimerization and a split kinase domain that is involved in activation of downstream signaling. The reported ligands for FGFR are members of the large family of fibroblast growth factors (FGFs). Like EGFR, ligand binding induces homodimers or heterodimers of FGFR family members, recruiting Grb2 and activating similar downstream signaling cascades as stated above. FGFR has been reported to interact with cell adhesion molecules and integrins, as well as with other receptor tyrosine kinases [91,92]. Together these interactions play significant roles in cell growth and migration. In breast cancer, genes encoding FGF receptors have been implicated in approximately 12% of breast cancers, particularly FGFR1 amplification, which has been detected in 16%-27% of luminal B-type breast cancers [93,94].

Additionally, studies have shown that TNBC patients with tumors that have elevated FGFR1 expression have reduced overall survival and that TNBC cell lines with reduced FGFR1 expression have reduced migration capabilities [95]. Further, TNBC cell lines with reduced FGFR3 expression exhibit reduced viability [96]. These studies suggest that targeting members of the FGFR family may be a valuable approach with the caveat that different FGFR family members may serve distinct roles in cell proliferation, migration, and invasion that have not been explored.

#### **1.4.3 MET receptor signaling**

The MET receptor is a receptor tyrosine kinase that is expressed in epithelial cells of many organs including liver, pancreas, prostate, kidney, muscle, and bone marrow. It is responsible for the cell scattering phenotype [97,98]. The MET proto-oncogene is located on chromosome 7q21-31 and encodes a protein that must undergo proteolytic processing to become a single-pass heterodimer, linked by disulphide bonds between the extracellular  $\alpha$  chain and the transmembrane  $\beta$  chain [97,99]. The extracellular component of MET consists of a SEMA (sema homology region) domain, a PSI (plexin-semaphorin-integrin) domain, and four IPTs (immunoglobulin-like regions in plexins and transcription factors) [99]. The intracellular component of MET consists of a juxtamembrane domain, a tyrosine kinase domain, and a C-terminal multifunctional docking site. The most studied ligand of MET is hepatocyte growth factor (HGF), also known as scatter factor (SF), which was first identified as a powerful mitogen in rat

hepatocytes and later identified as a secretory product of fibroblasts that increases migration and invasiveness of epithelial cells [100–102]. HGF binds to the SEMA domain of MET and elicits autophosphorylation of the phospho-tyrosine sites Tyr1234 and Ty1235 in the C-terminal domain. This then induces conformational changes that expose the multifunctional docking site [99]. Exposure of the docking site facilitates recruitment of adaptors like Grb2, Gab1, and Shc2, which then activate pro-growth and motility signaling like Ras/Raf/MAPK, STAT3, FAK, JNK, and AKT [97]. Studies show that recruitment of the adaptor molecule Gab1 to the docking site of MET creates binding sites for more downstream adaptor molecules and is important for the induction of cellular responses seen after MET activation [103]. In fact, overexpression of Gab1 in kidney cells alone was sufficient to induce ligand-independent cell scattering and branching morphogenesis. These data indicate that adaptor molecules like Gab1 may have, as of yet, undefined roles in receptor tyrosine kinase signaling.

MET regulates cell migration of breast epithelial cells through interactions with focal adhesion kinase (FAK), a process that is regulated by Src kinase [104]. MET has also been reported to crosstalk with other receptors like semaphorin receptors, EGFR, HER2, and HER3 [97]. Additionally, reports show that the semaphorin 4D (Sema 4D) can bind to plexin B1 and induce plexin B1 coupling with the MET receptor to promote invasive growth [105].

Like EGFR, MET activation is regulated by receptor internalization followed by Cbl-mediated ubiquitination and degradation or by protein phosphatases such as PTP1B [106,107]. In addition, MET activation is antagonized by binding of the

ligand Decorin, which has been reported to induce ectodomain shedding, receptor internalization, and degradation [108].

MET receptor protein expression has been reported to be elevated in 15-20% of breast cancer cases and is associated with poor outcomes among different subtypes of breast cancer, including TNBC [109–112]. Studies in mouse models have shown that genetically engineered mice with MET overexpression develop diverse mammary tumors with basal-like characteristics [113]. Together, this evidence suggests that the MET receptor may be a valuable therapeutic target. Clinical trials have focused on MET inhibitors such as the tyrosine kinase inhibitors tivantinib, cabozantinib, and foretinib, and the anti-MET antibody onartuzumab [114].

## **1.5 BCAR3/Cas/Src signaling in TNBC**

### **1.5.1 Breast Cancer Antiestrogen Resistance 3 (BCAR3)**

Breast cancer antiestrogen resistance 3 (BCAR3) is a cytoplasmic adaptor molecule that was first identified during a screen of genes implicated in driving resistance to antiestrogen therapy in ER+ breast cancers [115]. BCAR3 is a member of the novel SH2-containing protein (NSP) family of adaptor molecules that includes NSP-1 and NSP-3 (SHEP1) [116]. The structure of BCAR3 contains a Src homology 2 (SH2) protein domain that is involved in binding tyrosine-phosphorylated proteins and a C-terminal domain that shows homology to the guanine nucleotide exchange factor (GEF) domain of the Cdc25 protein family (Figure 1-5) [115,117]. Despite the C-terminal domain of BCAR3 having sequence

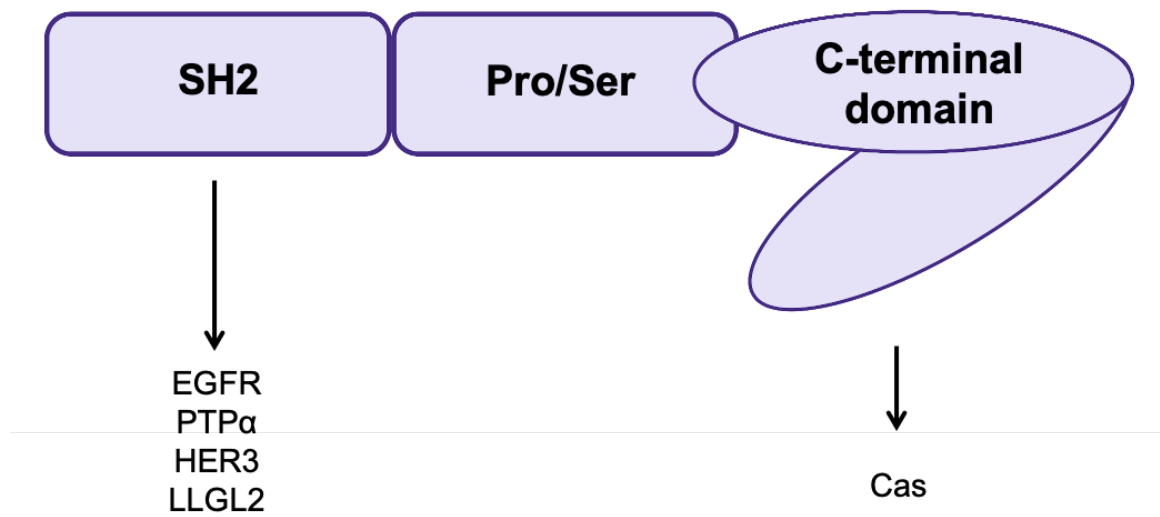


**Figure 1-5. Schematic diagram of BCAR3.** The schematic diagram of the structure of BCAR3 shows the SH2 domain, the proline/serine domain, and the C-terminal domain adopting a closed conformation. The reported SH2 domain and C-terminal domain binding partners are stated. Figure created with BioRender.com.

homology to the GEF domain, a structural study revealed that the C-terminus employs a closed conformation when bound to p130<sup>Cas</sup> (Cas), rendering BCAR3 incapable of any enzymatic activity [118]. Although BCAR3 does not have any enzymatic activity, various studies have described roles of BCAR3 in mouse development and as a driver of breast cancer cell growth, migration, and invasion. Studies in mice found that BCAR3 gene mutations resulted in truncated proteins and mice developed cataracts due to lens extrusion [119]. Lens defects have also been observed in other studies using mice with BCAR3 global knockout, where lens rupture was detected one month after birth [120]. BCAR3 has been reported to bind tyrosine phosphorylated residues in EGFR and PTP $\alpha$  (protein tyrosine phosphatase  $\alpha$ ) through its SH2 binding domain (Figure 1-5) [121,122]. Other molecules that have been reported to bind to the SH2 domain include HER3 and LLGL2 (LLGL Scribble Cell Polarity Complex Component 2) [123]. Binding of BCAR3 to EGFR was found to mediate EGF-induced DNA synthesis in breast cancer cell lines [121]. Overexpression of BCAR3 has been reported to lead to activation of the Rho family GTPases Cdc42 and Rac, both of which are important regulators of cell migration [124]. In addition, BCAR3 overexpression was found to induce PAK1 activation and activation of cyclin D1. Numerous studies have implicated BCAR3 as an important driver of migration and invasion. Binding of BCAR3 to PTP $\alpha$  was found to recruit BCAR3 and Cas to cell adhesions, where together they promoted integrin-induced migration [122]. Studies have demonstrated that BCAR3 and Cas form a complex that regulates cell adhesion dynamics, promoting TNBC cell migration and invasion [125,126]. The BCAR3-

Cas complex has also been shown to enhance Src kinase activity resulting in enhanced cell migration (Figure 1-6) [127]. Recent studies have uncovered a new phospho-tyrosine site (phospho-Tyr117) in BCAR3 that was found to be involved in the regulation of BCAR3 protein stability by the E3 ubiquitin ligase Cullin5/RBX2 (CRL5), impacting cell migration and invasion [128]. This phospho-site together with the SH2 domain of BCAR3 were found to be important contributors to Cas and Src activation. While BCAR3 has been shown to be involved in regulating aggressive phenotypes, the signaling mechanism by which it does so are not well understood. Further studies are needed to uncover the signaling networks regulated by BCAR3.

### 1.5.2 Cas

Crk-associated substrate (Cas) also known as p130<sup>Cas</sup>, belongs to the Cas family of adaptor molecules that includes neural precursor cell expressed developmentally down-regulated 9 (NEDD9), embryonal Fyn-associated substrate (EFS), and Cas scaffolding protein family member 4 (CASS4) [129]. Cas was first isolated from v-Src and v-Crk transformed rat fibroblasts, and like BCAR3, was found in a molecular screen of genes driving antiestrogen resistance in ER+ breast cancers [115,130]. Cas is an adaptor molecule that contains a Src homology 3 (SH3) domain, as well as clusters of SH2-binding motifs [130]. Knockout of Cas in mice has been demonstrated to be synthetically lethal, with Cas-deficient embryos appearing smaller in size and exhibiting cardiovascular defects [131]. Numerous studies have shown that Cas can be found in complex with Src, and this interaction

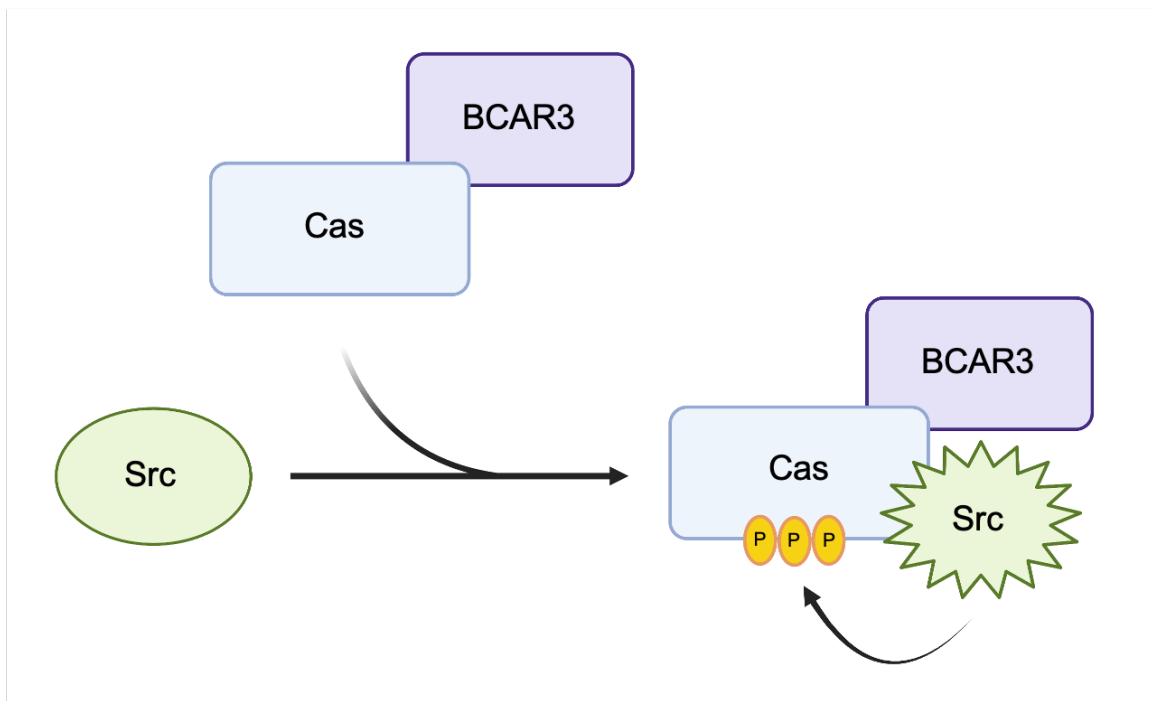


**Figure 1-6. Schematic diagram of a potential BCAR3-Cas-Src complex.** The schematic representation of a potential BCAR3-Cas-Src complex shows that BCAR3-Cas binding stabilizes the interaction between Cas and Src. This interaction prevents formation of the Src autoinhibitory conformation, subsequently increasing Src activity. After binding to Cas, Src proceeds to phosphorylate Cas at multiple sites within the central domain in a processive manner, increasing the affinity of Src to Cas and generating additional SH2 binding sites for other SH2 domain-containing proteins. Figure created with BioRender.com.

promotes proliferation/survival in breast cancer cells cultured under conditions of antiestrogen therapy [130,132]. As stated above, BCAR3 and Cas together form a complex that regulates Src kinase activity and promotes cell migration [127]. Several studies have identified Cas as an important component of cellular responses to the environment. Extracellular mechanical stress has been reported to induce conformational changes in Cas that facilitate its association with Src [133]. Mechanical stress promotes focal adhesion assembly through clustering of integrins and regulates adhesion signaling [134]. Cas localizes with BCAR3 in focal adhesions where they regulate adhesion dynamics and promote cell migration and invasion of TNBC cells [125,126]. Given that Cas has been identified as a factor involved in mechanotransduction and is often complexed with BCAR3, a potential role for BCAR3 in mechanosensing cannot be ruled out.

### **1.5.3 Src**

c-Src (Src) is a non-receptor tyrosine kinase and one of the first proto-oncogenes discovered due to its homology to the v-Src gene product of the avian Rous sarcoma virus [135]. The structure of Src consists of an N-terminal Src Homology 4 domain (SH4), a Src Homology 3 domain (SH3), a Src homology 2 domain (SH2), a linker sequence, a tyrosine kinase domain, and a C-terminal inhibitory tail [136]. Src belongs to a large family of non-receptor kinases that exhibits structural similarities and amino acid sequence homology. Members of the Src family of protein tyrosine kinases include Fyn, Yes, Yrk, Blk, Fgr, Hck, Lck, Lyn, and the Frk subfamily of proteins (Frk/Rak and Iyk/Bsk) [137]. Src kinase

activity has been reported to be an important driver of cell proliferation, cell differentiation, migration, angiogenesis, and cell survival [136].

Src is generally found in a closed (autoinhibitory) conformation that is stabilized by intramolecular interactions that engage its SH3 and SH2 domains[138]. The adaptor molecule Cas binds to both the SH2 and SH3 domains of Src, preventing formation of the autoinhibitory conformation and thus increasing Src activity [139]. Following binding to Cas, Src promotes processive multisite phosphorylation of Cas, increasing the affinity of Src to Cas and ultimately enhancing Src kinase activity through displacement of its SH3 domain [140]. As previously stated, BCAR3 stabilizes Cas-Src binding, further enhancing Src activity and driving cell migration (Figure 1-6) [127].

In TNBC, Src protein levels have been reported to be elevated compared to non-triple negative breast cancer [141]. Multiple studies show that inhibition of Src activity by dasatinib and other small molecule inhibitors of Src reduces TNBC cell growth as well as migration and invasion [141,142]. Together, this suggests that Src could be a reasonable therapeutic target for patients with TNBC. Clinical data thus far have failed to show efficacy of the Src inhibitor, dasatinib, in unselected breast cancer patients [143]. However, some patients with TNBC exhibited complete responses when treated with the Src inhibitor dasatinib combined with chemotherapy [143,144]. Based on these data, it is clear that more studies are needed to identify biomarkers that can be used to select breast cancer patients that may benefit from Src inhibition.

## 1.6 Autocrine/paracrine signaling in TNBC

### 1.6.1 HGF/MET signaling

HGF is reported to be aberrantly expressed in about 51% of breast tumors derived from African American females compared to 15% of breast tumors from women of mixed European descent [145]. HGF has been reported to be primarily produced by mesenchymal cells like fibroblasts, whereas MET is reported to be primarily expressed in epithelial cells *in vitro*. This underscores the importance of the tumor microenvironment in enabling an environment that promotes tumor growth [100,146]. MET and HGF are frequently co-expressed, with the strongest expression detected at the advancing edge of tumors, suggesting that their co-expression is important for tumor progression [147]. Further, high levels of HGF in breast cancer tissue extracts is associated with reduced relapse-free and overall survival [148].

Together, MET and HGF have been shown to form an autocrine/paracrine signaling loop that drives tumor growth and metastasis of various cancers [149,150]. To recapitulate the tumor microenvironment present in TNBC, studies have utilized a 3D model system called MAME (Mammary Architecture and Microenvironment Engineering) where TNBC cell lines are co-cultured with cancer-associated fibroblasts (CAFs) in a 3-D setting [151]. In these studies, CAFs with HGF overexpression induced TNBC cell growth and invasion, and this effect was inhibited with the MET kinase inhibitor cabozantinib. *In vivo*, inhibition of MET with cabozantinib abrogated TNBC tumor growth and metastasis. Together, these data show that 1) the tumor microenvironment influences TNBC cell growth and

invasion in an HGF-dependent manner and that 2) targeting MET reduces tumor growth *in vitro* and *in vivo*. Interestingly, MET activation may have different roles in different compartments of the mammary gland, as studies have shown that MET exhibits differential expression between luminal cells and myoepithelial cells [152]. Additionally, HGF has been found to elicit differential effects in these cells, inducing proliferation in luminal cells and branching morphogenesis in myoepithelial cells. Furthermore, co-cultures using CAFs have shown that HGF signaling is induced in basal-like but not luminal-like breast cancer cells [151]. These observations together underscore the potential value of MET as a therapeutic target for patients with TNBC as well as the importance of future studies to understand how the contribution of MET/HGF signaling to tumor progression may vary based on TNBC molecular subtype.

### **1.6.2 TGF $\beta$ signaling**

TGF $\beta$  is a cytokine that has an important role in cell proliferation, differentiation, apoptosis, and embryogenesis [153]. TGF $\beta$  elicits downstream effects by binding to type II TGF $\beta$  receptors. Upon binding, type I and type II receptors form large complexes consisting of a ligand dimer and four receptor molecules. Both type I and type II receptors consist of an N-terminal extracellular ligand binding domain, a transmembrane domain, and a C-terminal serine/threonine kinase domain. These complexes enable type II receptors to phosphorylate the kinase domain of type I receptors, initiating downstream

signaling by phosphorylating SMAD proteins. The SMAD proteins are part of large family that include receptor SMADs (SMADs 1, 2, 3, 5, and 8), a co-mediator SMAD (SMAD 4), and inhibitory SMADs (SMADs 6 and 7). Briefly, upon activation, type I TGF $\beta$  receptors activate the receptor SMADs, which can form complexes with SMAD 4. Together, this complex then translocates to the nucleus to act on transcriptional targets. Signaling is negatively regulated by the inhibitory SMADs, which compete for SMAD 4 binding. This signaling cascade has been implicated in regulating a variety of biological processes. The TGF $\beta$  family of ligands (TGF $\beta$  1, TGF $\beta$  2, TGF $\beta$  3) have been identified as having roles in the regulation of mesenchymal cell growth and differentiation, cell cycle arrest in epithelial cells, wound healing, extracellular matrix production, and immunosuppression [154].

Importantly, in breast cancer, tumor growth is associated with reduced TGF $\beta$  signaling [155]. However, TGF $\beta$  is known to be a strong promoter of the EMT transition, which as previously stated, is a process that enables epithelial cells to acquire migratory properties. TGF $\beta$  signaling regulates EMT transcriptional networks that include gene targets such as SNAIL1, SNAIL2 (SLUG), ZEB1, TCF3, and TWIST [156]. Studies using human mammary epithelial cells have shown that TGF $\beta$  induces EMT, which in turn generates cells with properties of stem cells, suggesting that these signaling dynamics may have a role in breast cancer initiation [157].

TGF $\beta$  ligands are produced in the tumor microenvironment by tumor cells, tumor associated stromal cells, and immune cells, which together modulate tumor-

suppressing or tumor-promoting mechanisms [158]. Studies have found that TGF $\beta$  plays a role in chemotherapeutic drug resistance by promoting the expansion of cancer stem-like cells (CSCs) in TNBC cell lines and mouse xenografts treated with paclitaxel [159]. Inhibition of TGF $\beta$  signaling in TNBC cells was found to reduce the presence of CSCs and tumor-initiating potential *in vivo*. While the tumor-suppressing and tumor-promoting roles of TGF $\beta$  remain complex and somewhat intertwined, further studies can help identify the context under which TGF $\beta$  receptor inhibitors may be beneficial.

### **1.7 Significance and overview**

The main goal of this dissertation is to determine the function of the adaptor molecule BCAR3 in TNBC. While our group has previously identified BCAR3 as an important promoter of breast tumor cell adhesion, migration, and invasion [125–127], the mechanisms by which BCAR3 regulates aggressive cell behaviors are not fully understood. Our group and others have shown that BCAR3 enhances Src kinase activity through the formation of a BCAR3-Cas-Src complex and this regulation contributes to enhanced migration and adhesion signaling [127,160,161]. BCAR3 has also been reported to bind to EGFR and regulate EGF-mediated DNA synthesis in breast cancer cells [121]. Like EGFR, the MET receptor is a receptor tyrosine kinase involved in regulating cell growth, migration, and invasion through interaction with HGF [162–164]. The focus of **Chapter 2** is to explore BCAR3-mediated regulation of the MET receptor and implications in

TNBC cell growth. The data presented in this chapter show that BCAR3 protein expression is elevated in DCIS and invasive carcinomas compared to normal mammary tissue and is associated with poor survival of TNBC patients with tumors that contain elevated BCAR3 mRNA. This chapter also shows for the first time that BCAR3 and the MET receptor participate in a single pathway to control proliferation and migration of TNBC cells, and that this functional coupling appears to take on unique features depending on the genetic background of the TNBC. **Chapter 3** expands on the differential regulation of MET by exploring BCAR3-MET coupling in basal-like TNBC. These data show for the first time that BCAR3 negatively regulates MET expression in basal-like TNBC and that this regulation is likely to occur post-transcriptionally.

The signaling networks regulated by BCAR3 that may be involved in regulating aggressive phenotypes are further explored in **Chapter 4**. Computational approaches are used to analyze gene and pathway enrichment as a function of BCAR3 expression. The effects of the extracellular microenvironment on these BCAR3-dependent networks are also investigated. This study shows that TNBC cells and mouse mammary organoids with reduced BCAR3 expression exhibit altered gene expression and pathway enrichment, with an overlap of 33 genes among all three conditions. In addition, this analysis shows that these broad network changes are influenced by the extracellular microenvironment in TNBC. Finally, the implications of this work to the field are discussed, with proposed follow-up studies that will help shed light on the value of BCAR3 as a prognostic tool, therapeutic biomarker, or as a therapeutic target in TNBC (**Chapter 5**).

Overall, the data and analysis presented in this dissertation offer a view of the mechanistic and transcriptional landscape regulated by BCAR3. It reveals for the first time a novel functional relationship between BCAR3 and MET and explores the establishment of distinctive transcriptional networks by BCAR3 in the setting of TNBC. Most importantly, it sets the stage for future work focused on molecular pathways and targets that inform new therapeutic approaches for patients with TNBC.

## **Chapter 2: Breast Cancer Antiestrogen Resistance 3 (BCAR3) promotes tumor growth and progression in triple-negative breast cancer**

(Adapted from Arras, *et al.*, *AJCR*, 2021)

### **2.1 Abstract**

Triple-negative breast cancers (TNBCs) constitute roughly 10-20% of breast cancers and are associated with poor clinical outcomes. Previous work from our laboratory and others has determined that the cytoplasmic adaptor protein Breast Cancer Antiestrogen Resistance 3 (BCAR3) is an important promoter of cell motility and invasion of breast cancer cells. In this study, we use both *in vivo* and *in vitro* approaches to extend our understanding of BCAR3 function in TNBC. We show that BCAR3 is upregulated in ductal carcinoma *in situ* (DCIS) and invasive carcinomas compared to normal mammary tissue, and that survival of TNBC patients whose tumors contained elevated BCAR3 mRNA is reduced relative to individuals whose tumors had less BCAR3 mRNA. Using mouse orthotopic tumor models, we further show that BCAR3 is required for efficient TNBC tumor growth. Analysis of publicly available RNA expression databases revealed that MET receptor signaling is strongly correlated with BCAR3 mRNA expression. A functional role for BCAR3-MET coupling is supported by data showing that both proteins participate in a single pathway to control proliferation and migration of TNBC cells. Interestingly, the mechanism through which this functional interaction operates appears to differ in different genetic backgrounds of TNBC, stemming in one case from potential differences in the strength of downstream signaling by the

MET receptor and in another from BCAR3-dependent activation of an autocrine loop involving the production of HGF mRNA. Together, these data open the possibility for new approaches to personalized therapy for individuals with TNBCs.

## 2.2 Introduction

With the advent of the genomic era, it has become increasingly clear that breast cancers comprise a collection of diseases influenced by distinct molecular and genetic drivers as well as systemic and microenvironmental factors. Cell-intrinsic signaling networks play a critical role in integrating external cues with genetic programs that contribute to tumor growth and progression. Previous work from our group has shown that the adaptor molecule Breast Cancer Antiestrogen Resistance 3 (BCAR3) functions within these signaling networks to control cell adhesion, migration, and invasion of breast cancer cells [125,165]. BCAR3 was originally identified in a screen for genes implicated in resistance to antiestrogens in estrogen receptor-positive (ER+) breast cancer cell lines [115]. At its N-terminus, BCAR3 contains a Src-homology 2 (SH2) domain that has been reported to bind to protein tyrosine phosphatase  $\alpha$  (PTP $\alpha$ ) and human epidermal growth factor receptor 3 (HER3). Its C-terminus contains a domain that mediates binding to the adaptor molecule p130<sup>Cas</sup> (Cas) and has homology to the guanine nucleotide exchange factor (GEF) domain of Cdc25 [115,117,118,122,123]. This domain adopts a closed catalytically inactive conformation that impedes GEF activity while facilitating binding to Cas [118]. BCAR3-Cas interactions enhance the activity of the non-receptor tyrosine kinase c-Src (Src) and positively regulate cell adhesion, invasion, proliferation, and activation of the small GTPase Rac1 [125–127,160,161,166].

Similar to BCAR3, Cas, and Src, the MET receptor tyrosine kinase modulates cell migration, invasion, and growth through its interactions with

hepatocyte growth factor/scatter factor (HGF/SF) [162–164]. MET and HGF/SF have also been reported to create an autocrine signaling loop that is important for the tumorigenic functions associated with MET in cancers [167]. MET receptor protein expression is elevated in 15-20% of breast cancer cases and is associated with poor outcomes across several breast cancer subtypes, including triple-negative breast cancer (TNBC) [109–112]. Elevated levels of active (autophosphorylated) and total MET protein correlate with a poor prognosis in patients with breast cancer [168]. In addition, over-expression of MET and HGF/SF has been reported in patient-derived invasive breast cancer tissues [169], and elevated levels of circulating HGF/SF in patient serum is associated with recurrence and reduced survival in patients with breast cancer [148].

In the current study, we extend our understanding of BCAR3 function in TNBC. We show that BCAR3 is upregulated in ductal carcinoma *in situ* (DCIS) and invasive TNBC compared to normal mammary tissue, and that BCAR3 mRNA expression is associated with poor survival for patients with TNBC. In mice, BCAR3 is required for TNBC tumor growth. Finally, using multiple cell models, we show that BCAR3 promotes TNBC cell proliferation, autocrine growth control, and migration through signaling pathways that include the MET receptor. These data underscore the potential utility of BCAR3 as a gateway into new targetable pathways for the treatment of TNBC.

## **2.3 Materials and methods**

### **2.3.1 Histological staining and microarray analysis**

Formalin-fixed, paraffin-embedded (FFPE) mammary tumor samples were obtained from the Biorepository and Tissue Research Facility at UVA. Serial sections were stained with hematoxylin and eosin (H&E) or immunostained with BCAR3 antibodies. Specificity was established by parallel staining of control and BCAR3-depleted MDA-MB-231 FFPE cell pellets. Microarrays containing core biopsies were described in Dill *et al.* [170]

### **2.3.2 Patient survival analysis**

The Kaplan-Meier Plotter algorithm [171] was used to compare survival of patients whose tumors fell in the top quartile of BCAR3 expression to the remaining patients in the full dataset of 255 TNBC patients.

### **2.3.3 Cell culture**

Breast cancer cell lines used in this study are shown in Table 2-1.

### **2.3.4 Ectopic expression and knockdown of BCAR3**

Stable MDA-MB-231 and Hs578T BCAR3 knockdown and re-expression cell lines were generated via lentiviral transduction using small hairpin RNAs targeting BCAR3 [125]. shBCAR3-1 and shBCAR3-2 oligonucleotides targeting

**Table 2-1.** Cell lines used in this study

Cell line	Source	Media <sup>1</sup>	Supplements <sup>1</sup>
Hs578T	ATCC <sup>5</sup>	High-glucose DMEM <sup>2</sup>	0.01mg/mL bovine insulin <sup>3</sup> ; 10% FBS <sup>4</sup> ; 1% penicillin-streptomycin
MDA-MB-231	ATCC	High-glucose DMEM	10% FBS; 1% penicillin-streptomycin
BT-549	ATCC	High-glucose DMEM	10% FBS; 1% penicillin-streptomycin
MDA-MB-157	ATCC	Leibovitz's L-15 (CO <sub>2</sub> -free)	10% FBS; 1% penicillin-streptomycin
MDA-MB-468	ATCC	Leibovitz's L-15 (CO <sub>2</sub> -free)	10% FBS; 1% penicillin-streptomycin
MDA-MB-436	ATCC	Leibovitz's L-15 (CO <sub>2</sub> -free)	0.01mg/mL bovine insulin; 16µg/mL glutathione; 10% FBS; 1% penicillin-streptomycin
HCC1937	ATCC	RPMI <sup>2</sup>	10% FBS; 1% penicillin-streptomycin
HCC1143	ATCC	RPMI	10% FBS; 1% penicillin-streptomycin
HCC1187	ATCC	RPMI	10% FBS; 1% penicillin-streptomycin
HCC1395	ATCC	RPMI	10% FBS; 1% penicillin-streptomycin
BT-20	ATCC	Eagle's MEM	10% FBS; 1% penicillin-streptomycin

<sup>1</sup>All media and supplements were purchased from Gibco Life Technologies, Carlsbad, CA, USA unless otherwise noted.

<sup>2</sup>DMEM: Dulbecco's Modified Eagle's Medium; RPMI: Roswell Park Memorial Institute

<sup>3</sup>Bovine insulin from Sigma-Aldrich, St. Louis, MO, USA

<sup>4</sup>FBS: fetal bovine serum

<sup>5</sup>ATCC: American Type Culture Collection, Manassas, VA, USA

BCAR3 were generated and cloned into the TRC2-pLKO-puro vector (Sigma-Aldrich, St. Louis, Mo, USA). The following hairpin sequences were used:

shBCAR3-1 shRNA ID: TRCN0000364816, sequence:

5'-

CCGGTAACTGCCCTCTCGCGTAAATCTCGAGATTTACGCGAGAGGGCAGTT  
ATTTTTG-3'

shBCAR3-2 shRNA ID: TRC0000376503, sequence:

5'-

CCGGTCGGCATTGCAGTGGACATTCCTCGAGGAATGTCCACTGCAATGCCG  
ATTTTTG-3'.

shBCAR3-1 knockdown cell lines were used to generate control and BCAR3 re-expression cells by viral transduction with empty vector (pLV-Venus; shBCAR3 + Ctl) or vector encoding a wobble mutant of wildtype (WT) Venus-BCAR3 (shBCAR3 + WT BCAR3) [125]. Wildtype (WT) BCAR3 complementary DNA was cloned into the *NotI* and *SpeI* sites of the pLV-Venus vector. The QuikChange II XL Site-Directed Mutagenesis Kit (Agilent Technologies, Santa Clara, CA, USA; 200521) was used to perform site directed mutagenesis. The primer sequence used are as follows:

shB3wobble1 forward:

5'-CCAGATTTTAACTGCGCTGTCCGAAAATTGGAACCTCCTCCTG-3',

shB3wobble1 reverse:

5'-CAGGAGGAGGTTCCAATTTICGGGACAGCGCAGTTAAAATCTGG-3'

(Changed nucleotides are underlined, and all constructs were confirmed by sequencing). shBCAR3 + Ctl and shBCAR3 + WT BCAR3 cells were then sorted by flow cytometry to obtain the population of cells with the highest expression of Venus. All engineered cell lines were cultured as stated above and maintained in 0.5 $\mu$ g/ml (MDA-MB-231 cells) and 1 $\mu$ g/ml (Hs578T cells) puromycin (MP Biomedicals, Santa Ana, CA, USA; 100552). Doxycycline (Dox)-inducible shBCAR3 knockdown constructs were generated using the Tet-on 3G bidirectional inducible expression system (Takara, San Jose, CA, USA). BCAR3 knockdown was induced in cells with these constructs by the addition of 1 $\mu$ g/ml Dox (MP Biomedicals, Irvine, CA, USA; ICN19895505) in the medium (*in vitro*) or 1mg/mL Dox plus 0.4% sucrose in the drinking water of mice (*in vivo*).

### **2.3.5 Tumor xenografts**

Six-week-old homozygous Foxn1<sup>nu/nu</sup> female mice (Jackson Laboratories, Bar Harbor, ME, USA) were anesthetized by intraperitoneal (IP) injection of 6mg/25g body weight tribromoethanol and injected bilaterally with 2x10<sup>6</sup> tumor cells into each 4<sup>th</sup> inguinal mammary fat pad. To induce conditional knockdown of BCAR3, drinking water was supplemented with 1mg/mL Dox plus 0.4% sucrose when tumors reached 200mm<sup>3</sup>. Tumor growth was monitored weekly by caliper until tumors became palpable, and then three times a week thereafter. Mice were euthanized once humane endpoints were reached. Tumors were then excised and processed for immunohistochemistry. All animal work was performed in

accordance with established guidelines, and following approval by, the University of Virginia Animal Care and Use Committee

### **2.3.6 Immunoblotting**

Immunoblots were performed as described previously [125,165]. Antibodies are shown on Table 2-2.

### **2.3.7 Organoid cultures**

Primary mammary organoids were generated using epithelial cells obtained from mouse mammary glands isolated from WT and BCAR3 KO (gift from Dr. Adam Lerner) [120] 8-week-old mice as described by Nguyen-Ngoc, *et al.* [172]. Epithelial cell suspensions were plated on growth factor-reduced matrigel (Corning, Corning, NY, USA; 354230) and cultured in DMEM/F12 media supplemented with 2.5nM FGF2 (PeproTech, Rocky Hill, NJ, USA; 100-18B) or 9nM TGF $\alpha$  (Sigma, T7924) for seven days with a media change every 3-4 days.

### **2.3.8 Cell proliferation and colony growth**

Cells were plated in eight separate 96-well plates at a density of 1000 cells per well for analysis using the CyQUANT NF Cell Proliferation Assay Kit (Invitrogen, Waltham, MA, USA; C35007). Samples were processed at 6 hours post-plating and every day thereafter for seven days with no media changes. Fold-change was determined by calculating the average fluorescence (excitation at

**Table 2-2.** Antibodies used in this study

Protein	Species	Catalog #	Company	Location
ERK1/2	Rabbit	9102	Cell Signaling Technology	Danvers, MA, USA
BCAR3	Rabbit	HPA 014858	Sigma-Aldrich	St. Louis, MO, USA
MET	Mouse	3127	Cell Signaling Technology	Danvers, MA, USA
pMET (pTyr <sup>1234/1235</sup> )	Mouse	3077	Cell Signaling Technology	Danvers, MA, USA
GAPDH	Mouse	Sc-32233	Santa Cruz	Dallas, TX, USA

~485nm and emission detection at ~530nm) of 4-6 technical replicates per cell line at each day relative to 6 hours.

To measure colony growth, 1000 cells were plated in triplicate wells of a 6-well plate and grown for 10 (MDA-MB-231 cells) or 15 (Hs578T cells) days with no media changes. Cells were fixed with 3% paraformaldehyde, stained with a 0.05% crystal violet solution in methanol overnight, washed with 1X PBS, and left to dry. Plates were scanned using the ChemiDoc imaging system (Bio-Rad, Hercules, CA, USA) and signal intensity per unit area was quantified by ImageJ (NIH, Bethesda, MD, USA; version 1.51).

To measure the effect of HGF on colony growth, cells were plated, allowed to adhere for 24 hours and treated with either 0.05% BSA (vehicle) or 50ng/mL HGF and supplemented every three days (MDA-MB-231) or one time three days after plating (Hs578T). Images were processed in ImageJ by applying a median filter of 2 pixels and a color threshold. The area of all detected colonies was measured in mm<sup>2</sup> using the ImageJ particle analysis tool. Colony areas for each condition were compiled and the distribution of colony size for each condition was analyzed. Using quartile data obtained from the distribution present in vehicle-treated Vector-control cells, colony sizes for each condition were separated into large, average, and small for statistical analysis.

To assess MET activation, cells were plated at a density of  $2.5 \times 10^5$ ,  $1.25 \times 10^5$ , and  $2.5 \times 10^4$  cells per 60mm dish and cultured for 2, 5, and 10 days, respectively, with no media changes.

### **2.3.9 Survival assay**

Cells were plated at a density of  $1.5 \times 10^5$  or  $2.5 \times 10^5$  cells per 6-well plate in the presence of DMSO (vehicle) or 50nM foretinib, and cultured for 72 hours and 24 hours, respectively. Cells were trypsinized and cell viability measured using Trypan Blue exclusion (Thermo Scientific; Waltham, MA, USA; SV30084.01).

### **2.3.10 Gene set variation analysis (GSVA)**

RNA expression data from the Cancer Cell Line Encyclopedia (CCLE) for 32 TNBC cell lines were downloaded from the Cancer Dependency Map (DepMap, release 21Q2; <https://depmap.org/portal/download/>). GSVA [173] was then used to calculate enrichment scores for the Reactome gene sets [174] related to receptor tyrosine kinase signaling. Spearman rank correlation coefficients were calculated for each set of GSVA scores against BCAR3 transcript expression from the 32 TNBC cell lines. Rank correlations and p-values were calculated using the Hmisc R package). R version 4.1.0 was used in these analyses. The codes for these analyses are available on GitHub under the username “pauljmyers.”

### **2.3.11 Transwell migration assay**

Transwell migration assays were performed as previously described [165]. Cells were suspended in FBS-free DMEM and seeded at  $2.5 \times 10^4$  cells per well in the upper chamber of the Transwell chamber (Costar 3422, 8 $\mu$ m pore size) in the presence of DMSO (vehicle) or 50nM foretinib. The lower chamber was filled with DMEM supplemented with 10% FBS and 50ng/mL HGF (PeproTech, 100-39H).

Boyden chambers were incubated for 6 hours after which cells on the bottom surface were stained using Protocol HEMA 3 stain set (Fisher Scientific, Waltham, MA, USA; 122-911) and quantified under the microscope. Data were normalized relative to DMSO-treated Vector-control.

### **2.3.12 Drug inhibitor assays**

Cells were plated at half volume in 12-well plates at a density of 500 cells per well, allowed to adhere for 24 hours, and supplemented with media containing either DMSO (vehicle) or foretinib (ChemCruz, Dallas, TX, USA; sc-364492) to a final concentration of 50nM. Cells were cultured in the presence or absence of foretinib, for 10 days (MDA-MB-231 cells) or 15 days (Hs578T cells) and processed as described above.

### **2.3.13 Quantitative real-time PCR**

Quantitative real-time PCR was performed with the Applied Biosystems StepOnePlusReal-Time PCR System (StepOne Software v2.2.2) (Waltham, MA, USA) and the Power SYBR Green PCR Master Mix (Applied Biosystems, Waltham, MA, USA; 4367659). Cells were plated at a density of  $2.5 \times 10^5$  cells per 60mm dish and cultured for 48 hours. mRNA was extracted according to the manufacturer's protocol using the Zymo Research Quick RNA Microprep Kit (Zymo Research, Irvine, CA, USA; R1050). For each sample, 1 $\mu$ g of mRNA was reverse-transcribed into cDNA in a 20 $\mu$ l reaction according to the manufacturer's protocol using the iScript cDNA Synthesis Kit (Bio-Rad, 1708890). The final cDNA product

was diluted 5X and subjected to quantitative real-time PCR performed with the Applied Biosystems StepOnePlusReal-Time PCR System (StepOne Software v2.2.2) (Waltham, MA, USA) and the Power SYBR Green PCR Master Mix (Applied Biosystems, Waltham, MA, USA; 4367659) using the following thermal cycling conditions: one initial cycle at 95°C for 10 min; 40 cycles of 15 sec at 95°C and 1 min at 60°C; followed by a melt-curve stage of 95°C for 15 sec, 60°C for 1 min, and 95°C for 15 sec. Relative mRNA expression was calculated using the  $2^{-\Delta\Delta Ct}$  method where transcript expression was normalized to GAPDH mRNA levels. The sequences of the primers used to amplify the genes are shown in Table 2-3.

#### **2.3.14 Statistical analysis**

For the non-inducible mouse tumor xenograft experiment (Figure 2-2A), the average volume of the left and right tumors was used as a unit of analysis. Comparisons between groups for the average tumor volume were made with the two-part models discussed in Albert and Shih [175]. Quadratic mixed models were used for tumor volume after the first detectable tumor. The p-values were computed from permutation tests based on 2000 permutations. For the Dox-inducible mouse tumor xenograft experiments (Figure 2-2B), quadratic mixed models were fit to the post-treatment average tumor volumes. The models included random effects for the intercept, linear, and quadratic terms. F-tests based on contrasts were used to compare groups. The analyses treated the left and right tumors as independent.

**Table 2-3.** Primer sequences for qRT-PCR

Gene	Forward (F) Reverse (R)	Primer Sequences (5'-3')
<i>BCAR3</i>	F	CCACATCTTCTGGACCCAAC
<i>BCAR3</i>	R	CTCCTCCTCCAGCTCCTTCT
<i>HGF</i>	F	CGAGGCCATGGTGCTATACT
<i>HGF</i>	R	ATTGACAGTGCCCCTGTAGC
<i>MET</i>	F	CAGTCGGAGGTTCACTGCAT
<i>MET</i>	R	AATCTGGCTTGCTTTGTGCG
<i>GAPDH</i>	F	AACGTGTCAGTGGTGGACCT
<i>GAPDH</i>	R	TCGCTGTTGAAGTCAGAGGA

For all other experiments, normal distribution of residuals was tested before performing one-way ANOVA followed by either Tukey or Sidak post hoc tests to determine p-values. Chi-squared tests were used in experiments that tested distributions. In experiments where proportions were compared, the test of 2-proportions was used followed by the Holm method to correct for multiple testing.

## **2.4 Results**

### **2.4.1 BCAR3 is upregulated in breast cancer tumor samples and TNBC cell lines**

While BCAR3 protein has been readily detected in breast cancer cell lines, its expression in clinical breast tumor samples has not been rigorously evaluated. Patient-derived tumor sections and microarrays obtained from the UVA Biorepository and Tissue Research Facility were evaluated by immunohistochemistry (IHC) for BCAR3 protein expression. The intensity of BCAR3 staining was scored by 2-3 individuals using a scale from 0 (no staining) to 3+ (high staining) (Figures 2-1A and 1B). Average BCAR3 expression was elevated in DCIS as well as invasive ductal carcinoma (IDC) (Figures 2-1A), and in both ER+/progesterone receptor (PR)+ and TNBC tumors relative to normal mammary tissue (Figure 2-1B). Focusing specifically on TNBCs, BCAR3 was readily detected by Western blot analysis in both claudin-low and basal-like TNBC cells [34,176,177] (Figure 2-1C). Kaplan-Meier survival curves generated using the top quartile of BCAR3 mRNA expression in 255 TNBC patients show that elevated BCAR3 expression correlates with worse patient outcomes (Figure 2-1D). These

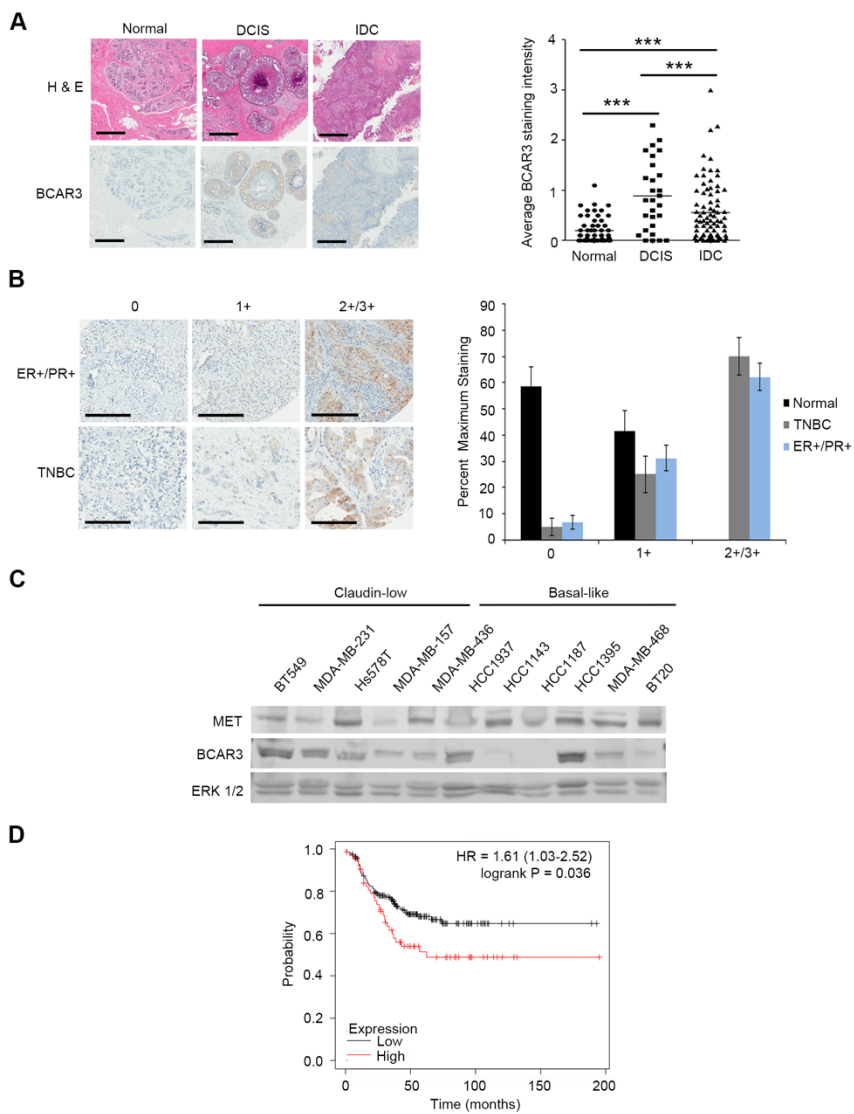


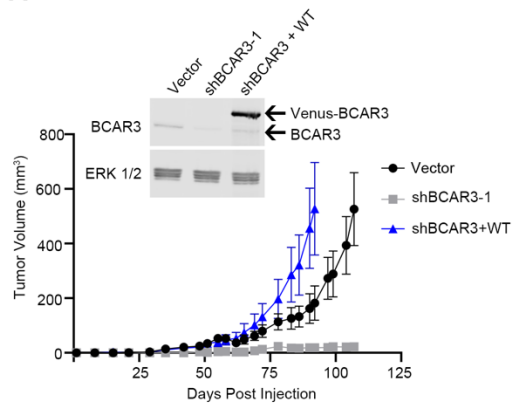
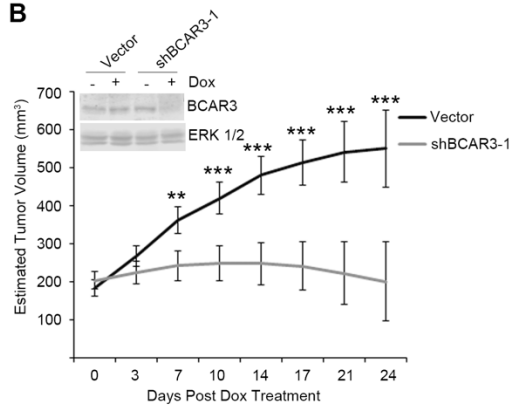
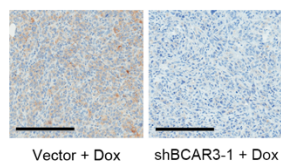
**Figure 2-1. BCAR3 is upregulated in breast cancer samples and TNBC tumor cell lines.** (A) Human tissue samples were obtained from the University of Virginia Biorepository and Tissue Research Facility (BTRF) and stained for H&E and BCAR3. Scale bars represent 200 $\mu$ m. Staining intensity was evaluated by 2-3 investigators on a scale of 0 (no staining) to 3+ (high intensity) (see Panel B below). Data shown are the average of 10 fields per sample for 56 normal breast tissues samples, 28 DCIS samples, and 82 IDC samples. The Kruskal-Wallis test was used to determine differences between groups. \*\*\* indicates  $p < 0.0001$ . (B) Examples of BCAR3 staining intensities from breast tissue microarray samples obtained from the BTRF. Scale bars represent 200 $\mu$ m. The maximum intensity for BCAR3 staining was assessed by 2-3 investigators in 41 normal samples, 40 TNBC samples and 91 ER+/PR+ samples. Data shown are the percentage of samples exhibiting the indicated maximum staining intensities +/- SEM. (C) Representative immunoblot from 11 TNBC cell lines. Lysates from 40,000 cells were separated by SDS-PAGE and immunoblotted for BCAR3, MET, and ERK 1/2. Samples were derived from the same experiment and processed in parallel on multiple blots. (D) Kaplan–Meier plot showing survival data for 255 TNBC patients separated by the top (red) or remaining (black) quartiles of BCAR3 expression in the primary tumor (<https://kmplot.com/analysis/index.php?p=service&start=1>) [171]. Panels A-D provided by Kristen Atkins, Amy Bouton, and Keena Thomas.

results provide the rationale for exploring a potential role for BCAR3 in TNBC tumor growth and progression.

#### **2.4.2 BCAR3 promotes TNBC tumor growth *in vivo***

The correlation between BCAR3 expression and poor outcomes in patients with TNBC led us to hypothesize that BCAR3 might influence TNBC tumor growth *in vivo*. This was tested using orthotopic tumor models in which MDA-MB-231 TNBC cells that express endogenous BCAR3 (Vector), reduced levels of BCAR3 (shBCAR3-1), or ectopic Venus-BCAR3 in the background of the BCAR3 knockdown (shBCAR3 + WT) (Figure 2-2A, inset) were injected into the 4<sup>th</sup> inguinal fat pads of Foxn1<sup>nu/nu</sup> mice. While the control cells readily formed tumor masses, the shBCAR3-1 knockdown cells uniformly failed to produce measurable tumors (Figure 2-2A). This deficiency was reversed when ectopic Venus-BCAR3 was expressed in the shBCAR3-1 cells. In fact, tumor growth in cells with ectopic BCAR3 expression was significantly greater than in the presence of endogenous BCAR3, possibly due to the over-expression of Venus-BCAR3 relative to endogenous BCAR3 (see inset, Figure 2-2A; note that ectopic expression of Venus-BCAR3 may also stabilize endogenous BCAR3 as seen by the lower-migrating BCAR3 band).

We reasoned that the absence of tumor growth exhibited by shBCAR3-1 cells could be due to an inability of the cells to establish tumors and/or a decrease in tumor cell proliferation/survival in the mouse. To address these possibilities, tumor studies were repeated using a doxycycline (Dox)-inducible system to

**A****B****C**

**Figure 2-2. BCAR3 promotes tumor growth in orthotopic MDA-MB-231 mouse xenograft models.** (A)  $2 \times 10^6$  MDA-MB-231 cells were injected into both the left and right 4<sup>th</sup> inguinal mammary fat pad. Corresponding cells were lysed and immunoblotted for BCAR3 and ERK 1/2 to verify BCAR3 knockdown (shBCAR3-1) and re-expression of WT Venus-BCAR3 (shBCAR3+WT) (inset). Tumors were measured by caliper three times a week. Data shown are the average  $\pm$  SEM of 15 control tumors, 13 shBCAR3-1 tumors and 13 shBCAR3+WT tumors. A permutation test using 2000 permutations was used to determine p-values. (B)  $2 \times 10^6$  Dox-inducible MDA-MB-231 control and BCAR3 knockdown cells were injected into the left and right 4<sup>th</sup> inguinal mammary fat pad. Corresponding cells were lysed and immunoblotted for BCAR3 and ERK 1/2 to verify regulated expression of BCAR3 under the shBCAR3+Dox conditions (inset). Doxycycline was added to the animals' drinking water once the tumors reached 200 mm<sup>3</sup>. The data represent an average of 10 (Vector) and 8 (shBCAR3-1) tumors. An F-test based on contrasts was used to compare groups and determine p-values. \*\* indicates  $p < 0.001$ , \*\*\* indicates  $p < 0.0001$ . (C) Tumors were excised at the endpoint of the experiment, formalin fixed, embedded in paraffin, and stained for BCAR3. Panels A-C provided by Keena Thomas.

regulate expression of the shBCAR3 construct. Dox-inducible control and shBCAR3 MDA-MB-231 cells were inoculated as described above and Dox was introduced into the drinking water to knock down BCAR3 once tumors reached 200 mm<sup>3</sup>. While the control tumors continued to grow in the presence of Dox, tumors generated from the conditional knockdown cells failed to progress once BCAR3 knockdown was initiated (Figure 2-2B). Immunohistochemistry performed on tumor samples isolated 24 days post-Dox treatment confirmed the knockdown of BCAR3 (Figure 2-2C). Together, these data strongly support a role for BCAR3 in promoting tumor growth *in vivo*.

#### **2.4.3 BCAR3 promotes TNBC cell proliferation**

To investigate a potential role for BCAR3 in TNBC cell proliferation, MDA-MB-231 cells containing either empty vector or one of two shBCAR3-encoding lentiviral constructs were plated at low density and growth was assessed every day for a period of seven days using the CyQUANT assay. Western blot analysis confirmed knockdown of BCAR3 (Figure 2-3A, inset). Cell numbers were reduced under conditions of BCAR3 knockdown compared to control cells (Figure 2-3A). This effect appeared to be dependent on the expression level of BCAR3, as the shBCAR3-1 cells that featured a more robust BCAR3 knockdown exhibited a greater deficiency in cell number than did the shBCAR3-2 cells that exhibited a more modest BCAR3 knockdown. To further assess the contribution of BCAR3 to cell proliferation, long-term growth assays were performed. Cells were plated at low density, allowed to grow for 10 days with no media changes, and stained with

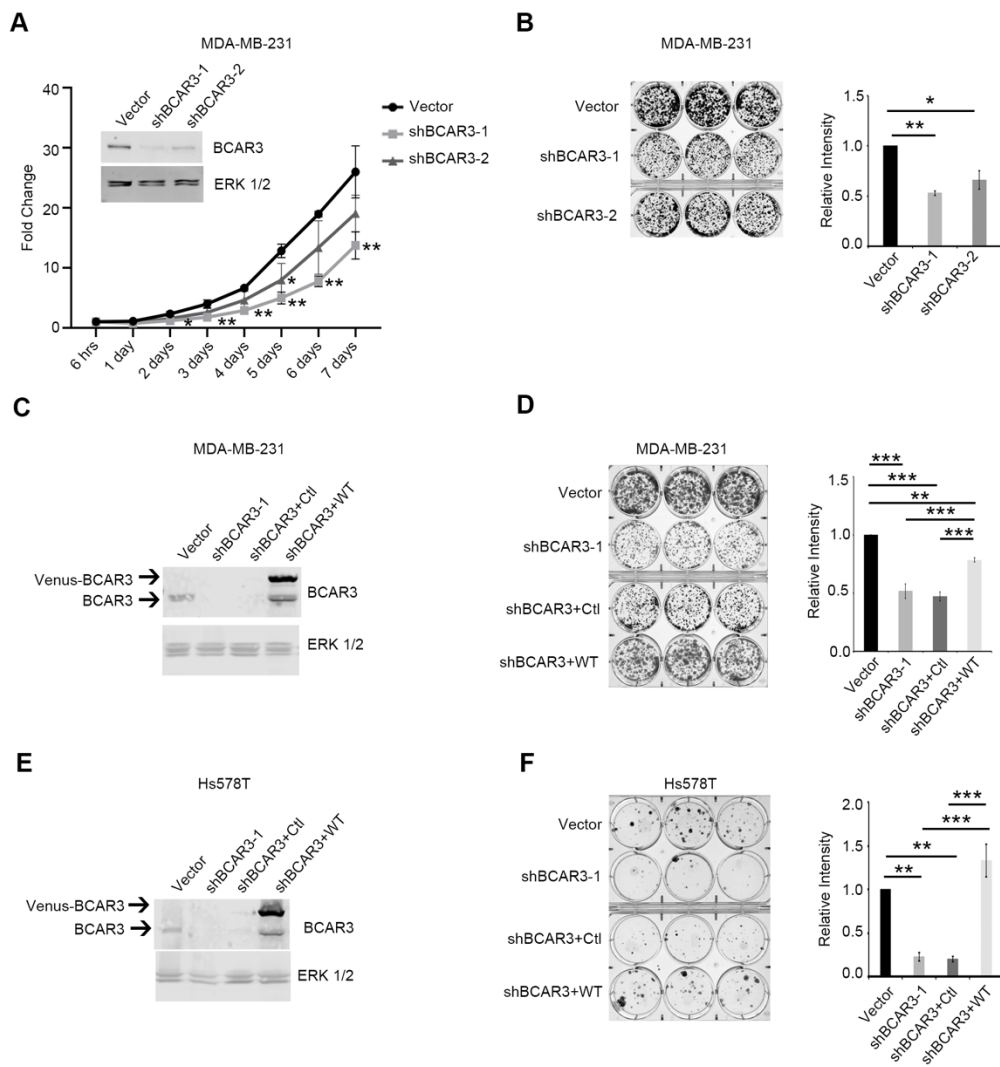


**Figure 2-3. BCAR3 promotes TNBC cell proliferation.** (A) CyQUANT NF cell proliferation assays were performed using control (Vector), shBCAR3-1 and shBCAR3-2 MDA-MB-231 cells. BCAR3 expression levels are shown in the inset. Each point on the graph represents the average fold change +/- SEM relative to a 6-hour baseline. Data were collected from three independent biological replicates. ANOVA analysis comparing the three cell lines for each day followed by a Tukey's post hoc test was used to determine p-values. (B) Long-term colony growth assays. 1000 cells/well were plated in triplicate in 6-well plates, allowed to grow for 10 days, and staining intensity was quantified. Data from the three technical replicates were averaged for each experiment and normalized to control cells. The average of three independent experiments +/- SEM was plotted on the graph. (C) Representative immunoblot showing endogenous BCAR3 and ectopic Venus-BCAR3 expression in the indicated MDA-MB-231 cell lines. (D) Cells were cultured in triplicate for 10 days and analyzed as described in Panel B. Data shown are the average +/- SEM of five independent experiments. (E) Representative immunoblot showing endogenous BCAR3 and ectopic Venus-BCAR3 expression in the indicated Hs578T cell lines. (F) Cells were cultured in triplicate for 15 days and analyzed as described for Panel B. Data shown are the average +/- SEM of three independent experiments. For all long-term colony growth assays, ANOVA analysis followed by Tukey's post hoc tests were used to determine p-values. \* indicates  $p < 0.05$ , \*\* indicates  $p < 0.01$ , \*\*\* indicates  $p < 0.001$ . Panels C and E provided by Keena Thomas. Panel F was provided by Amare Osei.

crystal violet. Colony growth as determined by the intensity of the crystal violet signal was significantly reduced in shBCAR3 cultures grown under these conditions and, similar to the previous experiment, inhibition of colony growth appeared slightly greater in the shBCAR3-1 cells than in the shBCAR3-2 cells (Figure 2-3B). This difference was unlikely to be due to cell death, as the number of viable cells at early times after plating (24 and 72 hours) was similar for Vector-control and shBCAR3-1 cells (Figure 2-4A).

To verify that the reduced colony size exhibited by BCAR3 knockdown cells was a consequence of BCAR3 depletion, constructs encoding shRNA-resistant ectopic Venus-BCAR3 (shBCAR3+WT), or the empty vector (shBCAR3+Ctl) were expressed in shBCAR3-1 cells (Figure 2-3C; again, note that ectopic expression of Venus-BCAR3 may stabilize endogenous BCAR3 as seen by the lower-migrating BCAR3 band). As before, colony growth was reduced in cells expressing lower amounts of BCAR3 (shBCAR3-1 and shBCAR3+Ctl) (Figure 2-3D). However, this deficiency was largely alleviated when ectopic Venus-BCAR3 was expressed in the knockdown cells. A similar result was observed in a second TNBC cell line, Hs578T (Figures 2-3E, 2-3F, and 2-4B). Together, these data show that, under long-term growth conditions, BCAR3 promotes TNBC colony expansion.

#### **2.4.4 BCAR3 is required for budding of mouse mammary epithelial organoids in response to growth factors**

Mammary branching morphogenesis is a dynamic process involving cell proliferation, remodeling, and response to external cues [178,179], all of which also

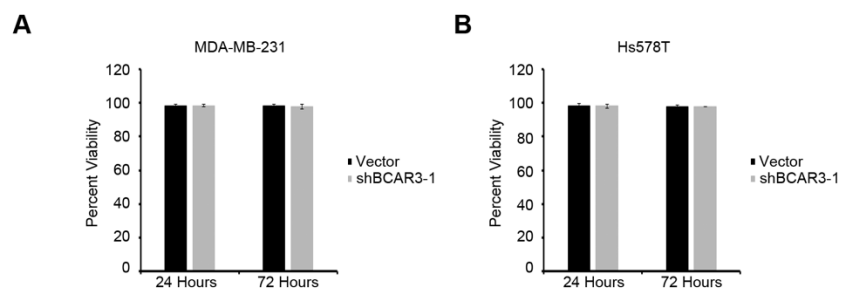


**Figure 2-4. BCAR3 knockdown does not impact cell viability at 24 or 72 hours.** MDA-MB-231 (Panel A) or Hs578T (Panel B) cells were cultured for a period of 24 or 72 hours. Viability was measured using Trypan Blue exclusion. Data shown are the average of 3-4 independent experiments. ANOVA followed by Sidak post hoc tests were used to determine differences. Panels A and B provided by Keena Thomas.

contribute to TNBC tumor growth and progression. To further explore proliferation as a function of BCAR3 expression, we used a mouse mammary epithelial organoid system as a tool to measure mammary epithelial cell proliferation. Primary organoids were generated using epithelial cells isolated from mammary glands obtained from wildtype (WT) and BCAR3 knock-out (B3KO) mice (Figure 2-5A). Epithelial cells were suspended in matrigel to establish primary mammary organoids and treated for seven days with two growth factors that have historically been used to stimulate branching morphogenesis, fibroblast growth factor 2 (FGF2) and transforming growth factor  $\alpha$  (TGF $\alpha$ ) [172,180] (Figure 2-5B). Organoid budding was then quantified as a measure of proliferation. Organoids generated from BCAR3 KO mice exhibited less budding when treated with FGF2 or TGF $\alpha$  compared to organoids generated from WT mice (Figures 2-5C and 2-5D). BCAR3 KO organoids treated with FGF2, but not TGF $\alpha$ , were also smaller in size compared to those generated from WT mice (Figure 2-5E), suggesting that BCAR3 may modulate differential growth responses depending on the nature of external growth factors.

#### **2.4.5 BCAR3-MET coupling regulates TNBC cell proliferation and migration**

To gain a more complete understanding of the signaling pathways that might partner with BCAR3 to drive TNBC phenotypes, we performed gene set variation analysis (GSVA). Publicly available mRNA expression data from a panel of 32 TNBC cell lines in the Cancer Cell Line Encyclopedia (CCLE) were used to identify receptor tyrosine kinase gene sets whose enrichment correlated positively

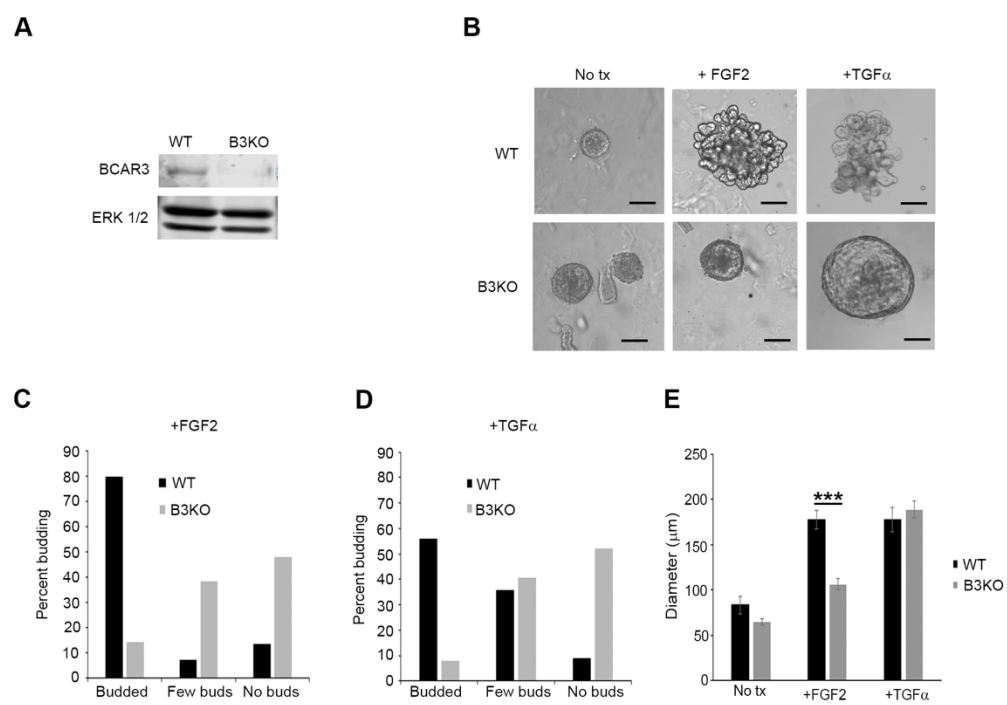
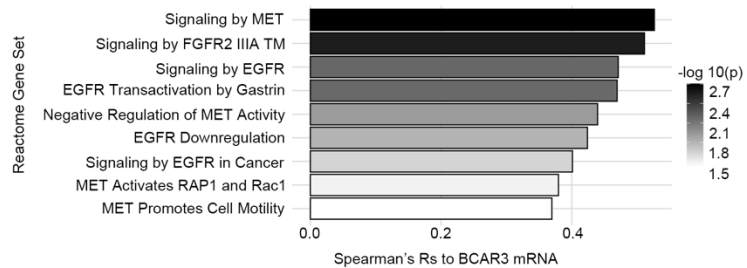


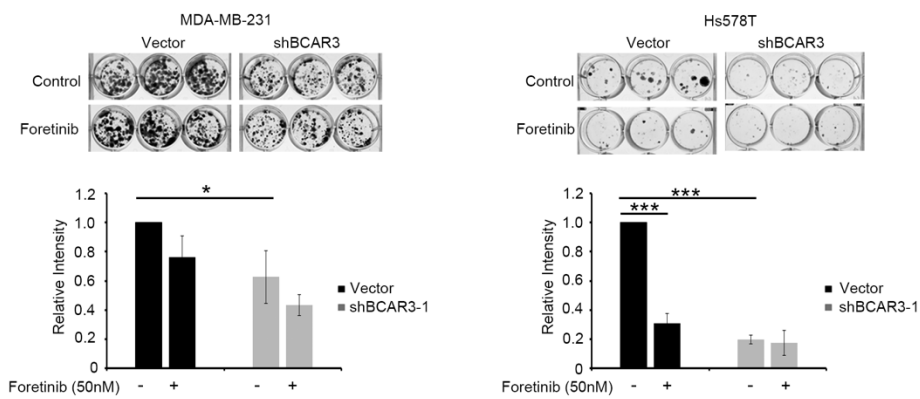
**Figure 2-5. BCAR3 promotes budding of mammary organoids under conditions of FGF2 and TGF $\alpha$  treatment.** (A) Representative immunoblot from organoids generated from 8-week old wildtype (WT) and BCAR3 knockout (B3KO) mice cultured *in vitro* for seven days. (B) Representative images of organoids cultured in the absence (no tx) or presence of FGF2 (2.5 nm) or TGF $\alpha$  (9nM) for seven days. Scale bar represents 50 $\mu$ m. (C and D) Quantification of organoids that exhibited robust budding (budded; >10), few buds ( $\leq$ 10 buds), or no buds. Data were generated from 1255 WT and 1015 B3KO organoids gathered from seven independent experiments (FGF2), and 790 WT and 822 B3KO organoids gathered from three independent experiments (TGF $\alpha$ ). Chi-squared tests were used to determine differences between groups ( $p < 0.001$ ). (E) The average diameter of organoids  $\pm$  SEM is shown for WT and B3KO organoids (37–46 organoids over multiple independent experiments) cultured under the indicated conditions. ANOVA followed by a Sidak post hoc test was used to determine differences. \*\*\* indicates  $p < 0.001$ . Panels A-E provided by Keena Thomas.

with BCAR3 transcript abundance. Fibroblast growth factor receptor (FGFR) and epidermal growth factor receptor (EGFR) signaling pathways, which were shown to be impaired in the absence of BCAR3 for FGF2- and TGF $\alpha$ -induced organoid budding, respectively, were positively correlated with BCAR3 mRNA abundance (Figure 2-6A). In addition, gene sets associated with the MET receptor signaling showed a strong correlation with BCAR3 mRNA expression. MET was readily detected by Western blot analysis in both claudin-low and basal-like TNBC cells (see Figure 2-1C). This prompted us to investigate the potential role of MET in BCAR3-dependent cell proliferation. MDA-MB-231 and Hs578T cells were treated with 50nM of the MET inhibitor, foretinib; this concentration produces a significant reduction in MET autophosphorylation (pTyr1234/1235) following HGF stimulation (Figure 2-7A) and is 50-100-fold below the reported IC<sub>50</sub> (dose at which there is a 50% reduction in cell survival) for MDA-MB-231 cells [181]. Importantly, neither Vector-control nor BCAR3-depleted cells demonstrated a loss in viability in the presence of 50nM foretinib during the early stages of this assay (Figure 2-7B). While MDA-MB-231 cells expressing the vector failed to exhibit a significant decrease in colony growth in the presence of foretinib, colony growth of the analogous Hs578T cells was reduced under these conditions (Figure 2-6B; black bars). The greater sensitivity of Hs578T cells to foretinib may be explained in part by the higher expression of MET receptor in these cells (see Figure 2-1C). However, although depletion of BCAR3 again resulted in a decrease in colony growth for both MDA-MB-231 and Hs578T cells (gray bars, no inhibitor), treatment of shBCAR3 cells with foretinib did not cause any additional growth-inhibitory effect

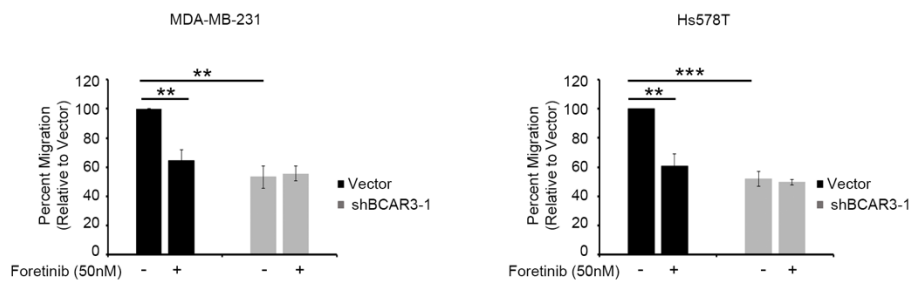
A



B

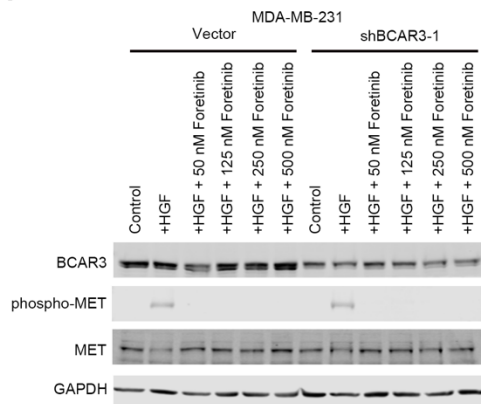
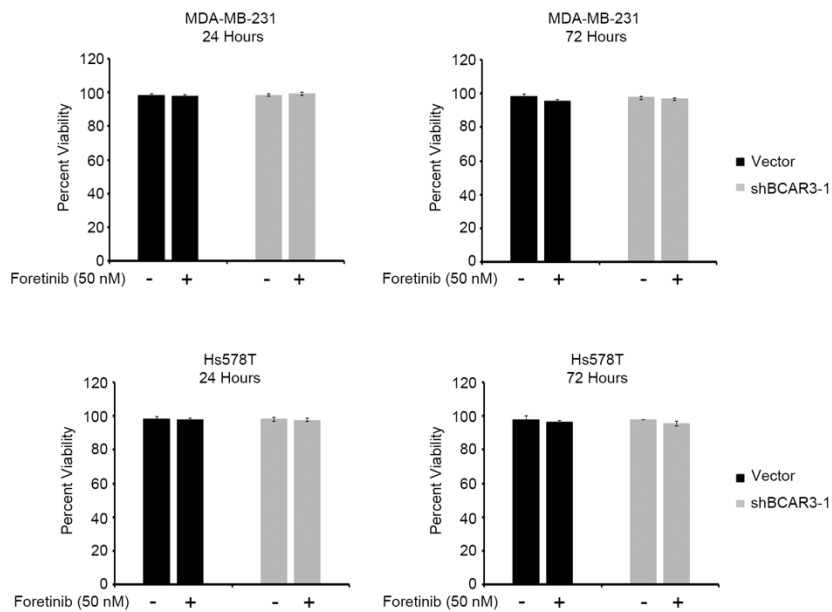


C



**Figure 2-6. BCAR3 and MET function in the same proliferation and migration pathways.** (A) Gene set variation analysis (GSVA) was used to calculate enrichment scores for the Reactome gene sets related to receptor tyrosine kinase signaling using mRNA transcript abundance data from 32 TNBC cell lines from the Cancer Cell Line Encyclopedia (CCLE). Spearman rank correlations and associated p-values ( $-\log_{10}(p)$ ) were then calculated between the GSVA scores and BCAR3 transcript abundance from the same TNBC cell lines. (B) Long-term colony growth assays. 500 cells/well were plated in triplicate in 12-well plates and allowed to grow in the presence or absence of 50nM foretinib. MDA-MB-231 cells were treated with the inhibitor 24 hours post-plating, re-treated on days three and six after initial treatment, and stained at day 10. Hs578T cells were treated with inhibitor 24 hours post-plating, re-treated on day three after initial treatment, and stained at day 15. Staining intensity was quantified and data from three technical replicates were averaged for each experiment. Data were normalized relative to the DMSO-treated Vector-control sample and the average  $\pm$  SEM of 3-4 independent experiments was plotted on the graph. (C) Transwell migration assays. Percent migration of MDA-MB-231 and Hs578T cells toward 50ng/ml HGF. 25,000 cells were plated in the top well of Boyden chambers in the presence of DMSO or 50nM foretinib and incubated for 6 hours. Data shown are the average  $\pm$  SEM of three independent experiments. ANOVA followed by Sidak post hoc tests were used to determine differences. Asterisks indicate a significant difference from the Vector-control, no drug condition. \* indicates  $p < 0.05$ , \*\* indicates  $p < 0.01$ ,

\*\*\* indicates  $p < 0.001$ . Panel A provided by Paul Myers and Panel C provided by Keena Thomas.

**A****B**

**Figure 2-7. Foretinib inhibits MET receptor activation but does not impact viability at 50nM.** (A) Representative immunoblot from MDA-MB-231 cells treated as indicated. Phospho-MET antibodies recognize pTyr1234/1235. (B) Viability in the presence or absence of foretinib was measured at 24 and 72 hours using Trypan Blue exclusion. Data shown are the average of 3-4 experiments +/- SEM. ANOVA followed by Sidak post hoc tests were used to determine differences. Panel B provided by Keena Thomas.

beyond what was observed in vehicle-treated cells. These data suggest that MET and BCAR3 may function in the same pathway to control cell growth, at least in the case of Hs578T cells where inhibition of MET alone caused a reduction in cell growth.

Considering that both the MET receptor and BCAR3 have been implicated in migration of cancer cells [163,164], we next sought to explore whether these proteins functioned together to regulate cell migration. Vector-control and BCAR3-depleted MDA-MB-231 and Hs578T cells were plated in Boyden chambers and allowed to migrate toward HGF in the presence or absence of 50nM foretinib. Inhibition of MET in control cells reduced migration by approximately 40-50% (Figure 2-6C; black bars), similar to the reduced migration observed in BCAR3 knockdown cells in the absence of foretinib (gray bar). However, as was the case for proliferation, foretinib had no added effect beyond BCAR3 depletion alone, again supporting a model in which BCAR3 and MET function in the same regulatory pathway.

To further explore the functional relationship between BCAR3 and MET, we next examined MET receptor activation in cells plated for 2 to 10 days with no media changes. Phosphorylation of MET at Tyr1234/1235 was observed after 10 days in culture in MDA-MB-231 cells expressing endogenous BCAR3 (Vector) and in knockdown cells expressing high levels of ectopic Venus-BCAR3 (Figure 2-8A; lanes 9 and 12). While Hs578T cells containing the vector did not show a similar elevation of MET phosphorylation, BCAR3-depleted cells that re-expressed Venus-BCAR3 exhibited robust MET activation after 5 and 10 days in culture

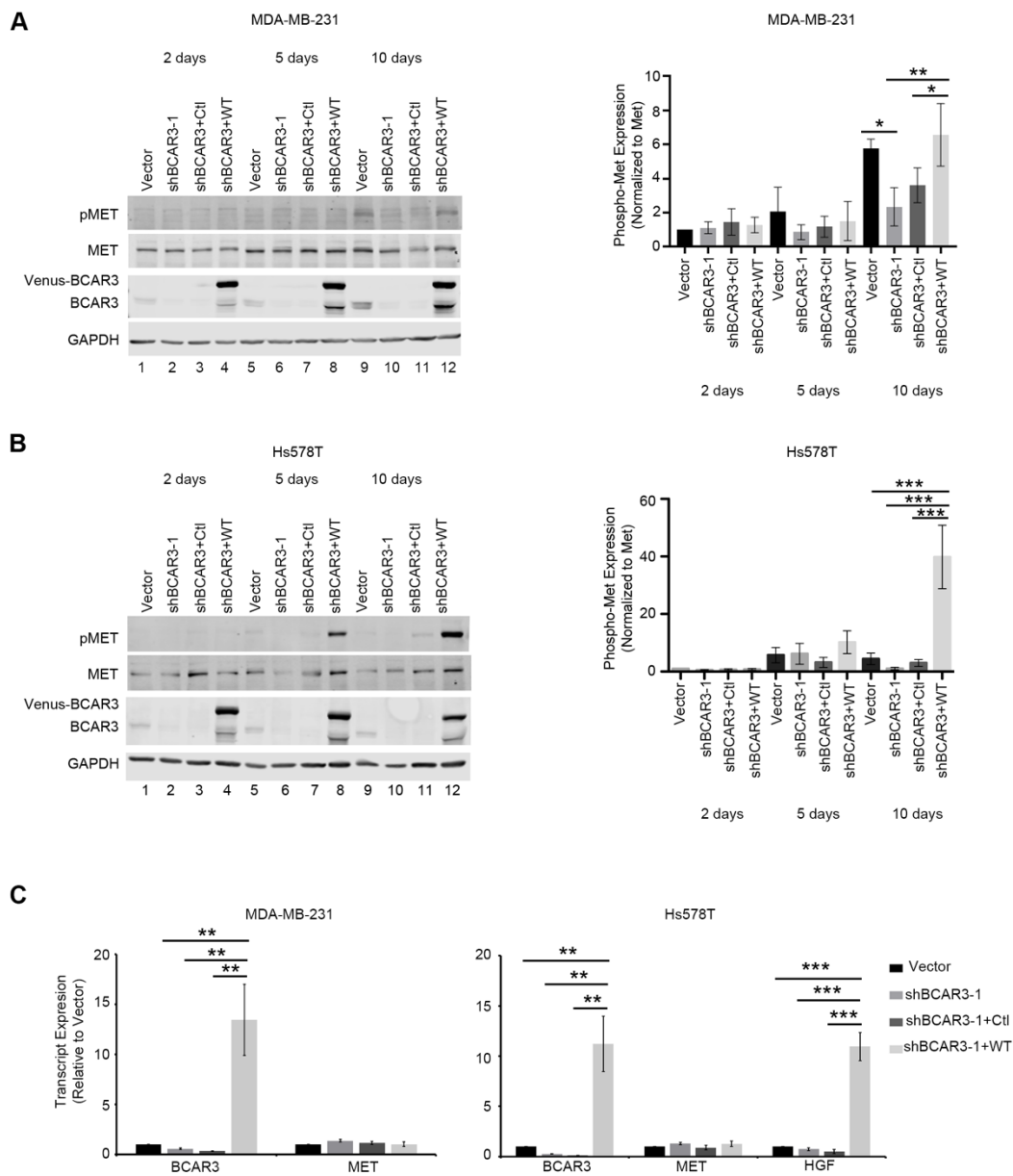


**Figure 2-8. BCAR3 regulates MET receptor activation in cells cultured long-term.** (A and B) Representative immunoblot analysis and quantification of MET activation in MDA-MB-231 (Panel A) or Hs578T (Panel B) cells with endogenous, depleted, or re-expressed BCAR3 expression. Cells were cultured for 2, 5, and 10 days with no media changes. Cells were lysed and protein expression/phosphorylation was evaluated with the indicated antibodies. Phospho-MET (Tyr1234/1235) was normalized to total MET and fold-change was quantified relative to Vector-control cells cultured for two days. (C) Quantitative real-time PCR analysis of BCAR3, MET and HGF transcript levels in the MDA-MB-231 and Hs578T cell panels cultured for 48 hours. RT-PCR was conducted with technical duplicates for three independent experiments. Data shown are the average +/- SEM of three biological replicates. ANOVA followed by Sidak post hoc tests were used to determine differences. \* indicates  $p < 0.05$ , \*\* indicates  $p < 0.01$ , \*\*\* indicates  $p < 0.001$ .

(Figure 2-8B, lanes 8 and 12). Note that the level of Venus-BCAR3 present in these cells is significantly elevated compared to endogenous BCAR3.

Based on these data, we hypothesized that BCAR3 may contribute to autocrine signaling through the MET receptor. To test this hypothesis, HGF mRNA levels were measured by quantitative real-time PCR (RT-PCR) in the full panel of MDA-MB-231 and Hs578T cells. As expected, BCAR3 transcripts were decreased in shBCAR3-1 cells and elevated in cells overexpressing Venus-BCAR3 (Figure 2-8C). MET transcript levels were not significantly impacted by BCAR3 depletion or overexpression in either cell line. HGF mRNA levels were below the level of detection in MDA-MB-231 cells. However, HGF mRNA was detectable in Hs578T cells, and shBCAR3-1+WT cells expressing robust levels of Venus-BCAR3 harbored significantly elevated HGF mRNA. Thus, in the presence of elevated BCAR3, HGF mRNA is upregulated in Hs578T cells.

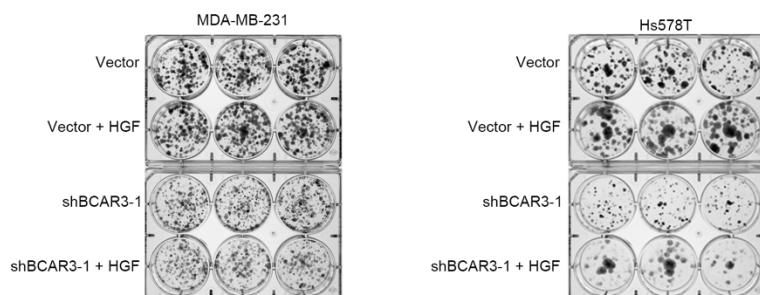
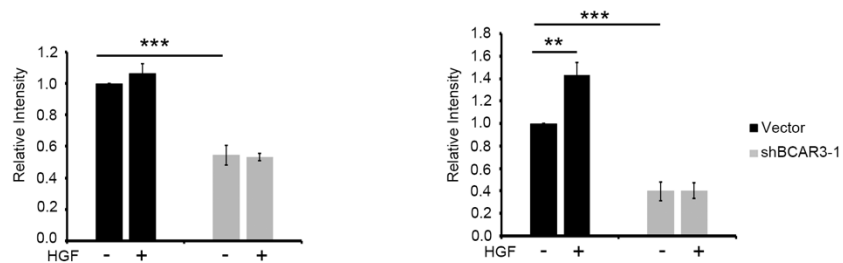
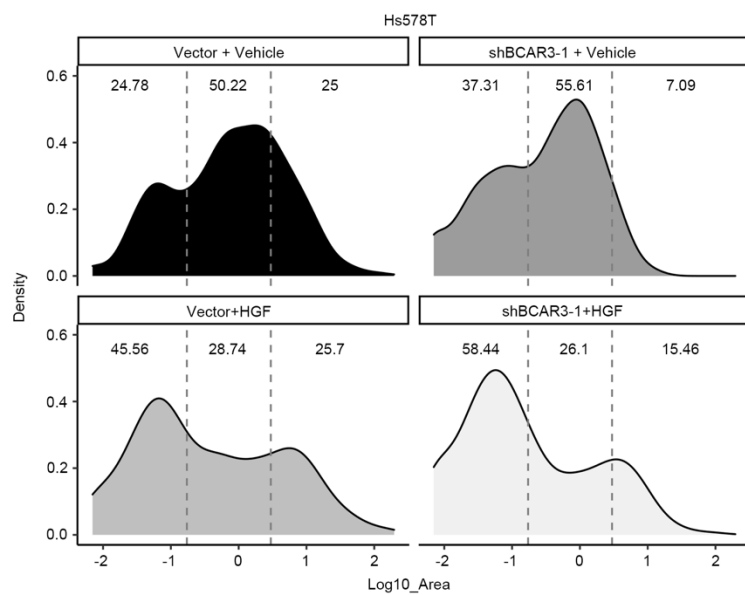
#### **2.4.6 HGF promotes colony growth in Hs578T cells**

In light of the evidence for BCAR3-MET functional coupling in both MDA-MB-231 and Hs578T cells and the possibility that the increase in HGF mRNA seen in Hs578T cells overexpressing BCAR3 may contribute to the enhanced proliferation seen under these conditions, we sought to determine whether exogenous HGF could rescue the defect in colony growth observed under conditions of BCAR3 depletion. We reasoned that, if MET activation was due to autocrine signaling in a BCAR3-dependent fashion, then exogenous HGF would at least partially rescue the phenotype caused by BCAR3 depletion. Vector-control

and BCAR3-depleted MDA-MB-231 and Hs578T cells were cultured long-term in the presence or absence of 50ng/ml HGF. Irrespective of BCAR3 status, the average colony growth of MDA-MB-231 cells was not impacted by exogenous HGF (Figures 2-9A and 2-9B). HGF induced a slight increase in the average colony density of Hs578T Vector-control but not shBCAR3 cells.

Interestingly, the distinctive variability in colony size exhibited by Hs578T cells appeared to be augmented upon treatment with HGF (Figure 2-9A). This prompted us to enumerate the proportion of Hs578T colonies falling into small, average, and large sizes as defined by the top (large) and bottom (small) quartiles of colony size for untreated Vector-control cells. HGF treatment of the Vector-control cells resulted in a shift from average to smaller colonies (Figure 2-9C). One possible explanation for this increase in smaller colonies could be the “scatter” effect of HGF [98,182,183], leading to a more dispersed colony phenotype. In the shBCAR3 cells, HGF induced a bimodal change in colony size marked by an increase in both small and large colonies at the expense of the average cohort. This suggests that HGF may induce both scatter/migration of the shBCAR3 cells (leading to the colonies appearing smaller in size) as well as proliferation (leading to a larger colony size).

While autocrine signaling through upregulation of HGF mRNA may contribute to BCAR3-dependent regulation of proliferation and migration in Hs578T cells, our data suggest that this is not the case for MDA-MB-231 cells. Instead, we hypothesized that MET receptor activation may be differentially regulated in Vector-control compared to shBCAR3 MDA-MB-231 cells. To test this

**A****B****C**

**Figure 2-9. HGF treatment differentially impacts colony size distribution of**

**Hs578T cells as a function of BCAR3.** (A) Long-term colony growth assays under conditions of HGF stimulation. MDA-MB-231 and Hs578T cells were plated at a density of 1,000 cells/well in triplicate in a 6-well plate and treated with either vehicle (0.05% BSA) or 50ng/mL HGF the day after plating. MDA-MB-231 cells were re-treated with HGF on days three and six after initial treatment and stained at day 10. Hs578T cells were re-treated with HGF on day three after initial treatment and stained at day 15. (B) Staining intensity was quantified and data from the three technical replicates were averaged for each experiment. Data were normalized relative to the vehicle-treated Vector-control sample and the average  $\pm$  SEM of 3-5 independent experiments was plotted on the graph. ANOVA followed by Sidak post hoc tests were used to determine p-values. (C) Quartile data obtained from the colony size distribution of untreated Vector-control cells were used to bin colonies into large ( $\geq 2.975\text{mm}^2$ ), average ( $< 2.975\text{mm}^2 \geq 0.172\text{mm}^2$ ), or small ( $< 0.172\text{mm}^2$ ) groupings. Data were generated from 904 Vector-control no treatment colonies, 856 Vector-control +HGF colonies, 1115 shBCAR3-1 no treatment colonies, and 705 shBCAR3-1 +HGF colonies obtained from five independent experiments. The chi-squared test was used to determine differences between groups ( $p < 0.001$ ). A test of 2-proportions was performed to compare small, average, and large colonies in cells of the same background treated with vehicle or HGF. The Holm method was used to correct for any errors that might have arisen from performing multiple tests across the comparisons analyzed.  $p = 3.26 \times 10^{-19}$  and  $4.82 \times 10^{-19}$  comparing vehicle to HGF-treated

Vector-control cells for average and small colonies, respectively.  $p = 7.13 \times 10^{-18}$ ,  $3.39 \times 10^{-8}$ ,  $6.36 \times 10^{-34}$  comparing vehicle to HGF treatment of shBCAR3 cells for small, large, and average colonies, respectively.

hypothesis, MET phosphorylation at Tyr1234/1235 was measured following acute stimulation with HGF. Both the magnitude and duration of MET phosphorylation was attenuated under conditions of BCAR3 knockdown (Figure 2-10A), supporting a role for BCAR3 in regulating MET receptor activation in MDA-MB-231 cells.

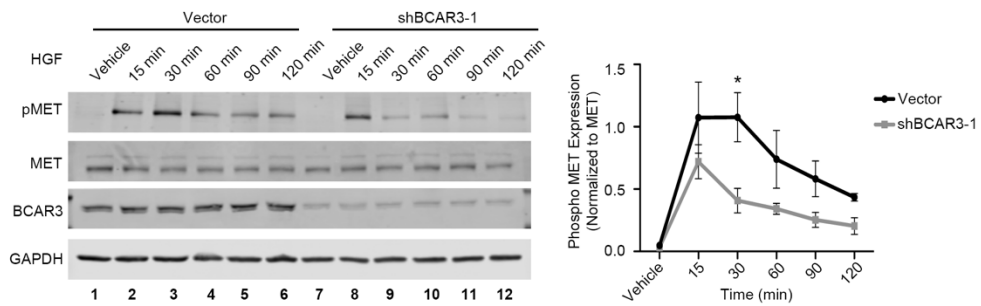
## **2.5 Discussion**

In this report, we used both *in vivo* and *in vitro* approaches to probe the function of BCAR3 in TNBC tumor growth, proliferation, and migration. Our study is the first to show that BCAR3 regulates growth of TNBC xenografts in mouse models and that this correlates with its upregulation and association with poorer outcomes in patients with TNBC. In addition, we show that BCAR3-MET receptor coupling plays a key role in BCAR3-dependent proliferation and migration of TNBC cells, and that the mechanisms through which this functional interaction operates may differ in different genetic backgrounds of TNBC. Most importantly, these data open the possibility for new approaches to personalized therapy for individuals with TNBCs.

### **2.5.1 BCAR3 is a regulator of MET signaling**

Like BCAR3, MET has been shown to drive cell proliferation, migration and invasion [163,164]. It has also been shown to induce branching morphogenesis through its interaction with the adaptor molecule Gab1 [103]. Despite having similar functions in breast cancer, however, a connection between MET and BCAR3 has not been explored prior to this study. Using publicly available data,

**A**



**B**

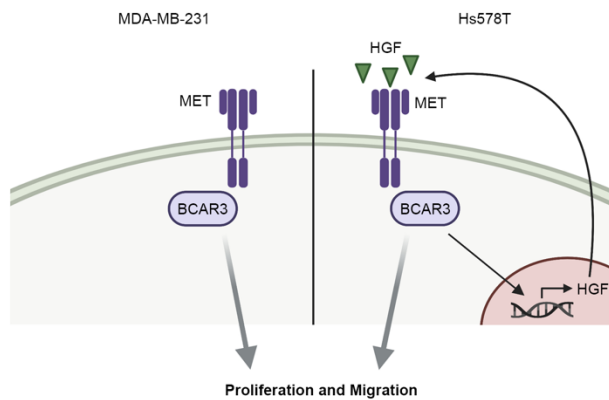


**Figure 2-10. BCAR3-MET coupling in TNBC cells.** (A) Representative immunoblot analysis of MDA-MB-231 cells with control or stable BCAR3 knockdown that were serum-starved and stimulated with 50ng/mL HGF over a time-course ranging from 0-120 min. Cells were lysed and protein expression/phosphorylation was evaluated with the indicated antibodies. Data shown are the average  $\pm$  SEM of four independent experiments. ANOVA followed by Sidak post hoc test was used to determine differences. Samples were derived from the same experiment and processed in parallel on multiple blots. \* indicates  $p < 0.05$ . (B) Model for functional BCAR3-MET coupling in MDA-MB-231 and Hs578T cells. Figure created with BioRender.com.

we showed that, among receptor tyrosine kinases, expression of the MET receptor signaling gene set correlated most strongly with BCAR3 mRNA expression in a panel of 32 TNBCs (Figure 2-6A). Our biological studies support a functional interaction between BCAR3 and MET that contributes to cell proliferation and migration (Figures 2-6B and 2-6C). However, our data suggest that BCAR3-MET coupling may be mediated through distinct mechanisms in TNBCs depending on their genetic profiles. As suggested by Figures 2-8C and 2-9, an autocrine loop generated through BCAR3-dependent expression of the MET receptor ligand HGF may help drive proliferation and migration of Hs578T cells (Figure 2-10B). Of note, studies have reported that exposure of luminal breast cancer cells to HGF induces increased growth with no morphological changes, while exposure of myoepithelial cells to HGF does not impact cell growth but rather induces morphological changes [152]. Considering that HGF elicits contrasting effects on luminal epithelial cells compared to myoepithelial cells, it will be interesting to compare the regulatory functions of BCAR3 on MET signaling between basal-like and claudin-low TNBC.

There is no evidence of autocrine signaling through BCAR3-MET receptor for MDA-MB-231 cells. While BCAR3 appears to be necessary in these cells for maximal MET receptor activation (Figure 2-10A), the inability of HGF to rescue the proliferation defect observed in BCAR3-depleted cells (Figure 2-9B) suggests that impairment of the BCAR3-MET axis under conditions of BCAR3 depletion may arise independently of ligand binding to the receptor (Figure 2-10B). Instead, BCAR3 could regulate the availability or activity of phosphatases, intracellular kinases, or adaptor molecules that control downstream signaling. While the

mechanism through which this enhanced signaling is mediated through BCAR3 remains to be determined, the resultant increase in signal flux could account for the differences in cell migration and proliferation observed in MDA-MB-231 cells as a function of BCAR3.

### **2.5.2 Targeting BCAR3 signaling pathways for the treatment of TNBC**

We have shown that BCAR3 expression is elevated in both ductal carcinoma in situ (DCIS) and invasive ductal carcinoma (IDC) compared to normal mammary tissue. Interestingly, the average BCAR3 expression was higher in DCIS than in IDC. Since BCAR3 is an important regulator of cell motility and invasion [125,126,165], its increased expression in a subset of DCIS lesions may reflect an early step in the transition to invasive disease. This possibility is further supported by the heterogeneity in BCAR3 expression that was observed in tumor tissue, suggestive of functional microdomains with high BCAR3 expression. Using publicly available patient data, we also found that high BCAR3 mRNA expression specifically in TNBC correlates with poorer outcomes. This is in contrast to several reports evaluating patients with hormone receptor-positive cancers that show that BCAR3 expression is a predictor of better outcomes [184,185]. Our finding that BCAR3 protein expression was elevated in a subset of both TNBCs and ER+/PR+ tumors suggests that hormone status may help determine the impact of BCAR3 expression on the tumor. Beyond hormone status alone, the fact that BCAR3 may function in different regulatory pathways even within individual TNBCs underscores the importance of also considering the receptor tyrosine kinases that

coordinate with BCAR3 when developing personalized treatment strategies to control tumor progression for breast cancer patients.

While the data presented in this work are the first to describe the functional role of BCAR3-MET coupling in TNBC, there are some limitations to the study. These include 1) experimental use of only two claudin-low TNBC cell lines, 2) the lack of a quantitative approach to measure growth following HGF stimulation, and 3) the lack of additional functional assays to test the effects of HGF on migration and invasion, which are phenotypes known to be altered with HGF stimulation. Since the only claudin-low TNBC cell lines tested in this study were MDA-MB-231 and Hs578T cells, it would be interesting to test if other claudin-low cell lines show similar results as a function of BCAR3 knockdown or overexpression. In this study, only colony growth assays were used to measure the effects of HGF on cell growth; it would be interesting to utilize a more quantitative approach to measure daily cell accumulation or proliferation following HGF treatment. These approaches could perhaps show greater BCAR3-dependent effects of HGF on MDA-MB-231 and Hs578T cells. It would also be interesting to test the effects of HGF stimulation using additional functional assays, such as transwell migration and 3D matrigel invasion assays in response to HGF.

Despite the limitations, overall, our data provide the beginnings of a roadmap for this type of analysis by considering BCAR3-MET coupling as one axis to target therapeutically. Even more broadly, BCAR3 could serve as a potential biomarker for additional therapeutic avenues that exploit the distinct functional interactions through which BCAR3 contributes to tumor phenotypes. Further

analysis of these interactions could help identify new molecular targets and drug combinations to enhance the clinical management of patients with TNBC.

## **Chapter 3: BCAR3-MET coupling in triple-negative breast cancer**

### **3.1 Abstract**

**Chapter 2** showed that BCAR3 is elevated in breast cancer samples and regulates MET receptor signaling dynamics that promote aggressive cell behaviors in TNBC. Using publicly available RNA expression databases, we found that when MET-curated gene sets are analyzed, most TNBC cell lines separate based on their molecular subtype. In this study, we use biochemical techniques to extend our understanding of BCAR3 regulatory functions specifically in basal-like TNBC. Immunoblot and quantitative real-time polymerase chain reaction (RT-PCR) analyses were performed in breast tumor cells representative of the basal-like molecular subtype of TNBC under conditions of endogenous, depleted, or overexpressed BCAR3 protein. These data revealed that, under conditions of BCAR3 depletion, MET receptor protein expression and phosphorylation are elevated, but MET receptor mRNA levels were not altered. Conversely, when BCAR3 was over-expressed in a basal-like cell line with low endogenous levels of BCAR3 expression, MET receptor protein expression and phosphorylation are reduced again without any change in mRNA levels. Interestingly, similar changes in MET receptor phosphorylation were not observed in the claudin-low molecular subtype of TNBC. Together, our data show that BCAR3 may differentially regulate MET signaling depending on the genetic profile of the TNBC cell studied.

### 3.2 Introduction

Using gene expression analysis and molecular profiling, numerous subtypes of breast cancer have been identified including luminal subtype A, luminal subtype B, luminal subtype C, normal breast-like, basal-like, HER2+, and claudin-low [31,33]. Basal-like breast cancer encompasses a group of tumors that exhibit broad heterogeneity. Microarray analysis of these breast tumors demonstrate high expression of genes characteristic of breast epithelial cells [30]. On histology, basal-like breast cancers show aggressive features such as elevated mitotic index, tumor necrosis, and an invading tumor border [78]. Most basal-like breast cancers demonstrate immunoreactivity to vimentin, EGFR, cytokeratin 8/18, and cytokeratin 5/6, and are negative for the estrogen receptor (ER), progesterone receptor (PR), and human epidermal growth factor receptor 2 (HER2) [78,186,187]. Further, gene expression analysis shows that most ER-/PR-/HER2- (triple-negative) breast cancers align with the basal-like molecular subtype [75]. Like the basal-like group, most breast cancer tumors characterized as claudin-low also exhibit triple-negative status and both subtypes show a lower pathological complete response after chemotherapy [33]. Claudin-low breast cancers have been identified as having stem-cell features and enrichment of genes involved in the epithelial-to-mesenchymal transition (EMT).

Molecular profiling of breast cancer cell lines identified two subtypes within the basal group termed basal A and basal B. The basal A subtype was found to be more consistent with the expression profile of the originally identified “basal-like” group and these cells were found to display epithelial characteristics. On the other

hand, studies have found that cells with the basal B subtype display a less differentiated phenotype with a more mesenchymal-like appearance and have similar expression profiles to “claudin-low” tumors [34,75].

In **Chapter 2**, we found that BCAR3 protein is expressed in patient-derived TNBC tumor samples and TNBC cell lines of different gene profiles and is associated with poor outcomes in patients with TNBC. We also found that BCAR3 couples with MET to promote aggressive phenotypes in MDA-MB-231 and Hs578T cells, a subset of claudin-low TNBC cell lines that are grouped as basal B. As stated in **Chapter 2**, MET is a receptor tyrosine kinase that has been implicated in driving migration and invasion in cancers through autocrine/paracrine signaling involving hepatocyte-growth factor (HGF), a known ligand of the MET receptor [188]. Elevated phosphorylated (active) MET and total MET protein levels have been reported to correlate with a poor prognosis in patients with breast cancer [168]. Of note, breast cancer cell lines of the “intrinsic” basal-like subtype have elevated MET mRNA and protein levels compared to breast cancer cell lines of the “intrinsic” luminal-like subtype [189].

Studies have shown that human luminal and myoepithelial cells express MET differentially and exhibit differential responses to HGF [152,190]. When treated with exogenous HGF, luminal breast cells exhibit increased growth with no morphological changes, while exposure of myoepithelial cells to HGF does not impact cell growth but rather induces morphological changes [152]. Mouse models show that myoepithelial cells and stromal cells produce HGF whereas luminal progenitor cells express MET [190]. Further, HGF stimulation has been shown to

induce basal cell features in luminal progenitor cells, including upregulation of basal-specific genes such as CDH3 (encoding P-cadherin), TRP63 (encoding transformation-related protein 63), and SNAI2 (encoding snail family transcriptional repressor 2), and downregulation of luminal-specific genes such as ELF5 (encoding E74-like factor 5), HEY1 (encoding hairy/enhancer-of-split related with YRPW motif protein 1), and GATA3 (encoding GATA binding protein 3). Together, these data suggest that MET signaling may be differentially regulated depending on the genetic profile of the breast cancer cell.

In this chapter, we set out to investigate the role of BCAR3-MET coupling in regulating cellular behaviors that promote tumor progression in basal-like triple negative breast cancers.

### **3.3 Materials and methods**

#### **3.3.1 Cell culture**

All breast cancer cells were purchased from American Type Culture Collection (Manassas, VA, USA) except for HCC1937 and Hs578T, which were kindly provided by Dr. Kevin Janes (UVA). All media and supplements unless otherwise noted were purchased from Gibco, Life Technologies, Carlsbad, CA, USA. MDA-MB-231 and BT-549 cells were cultured in high-glucose Dulbecco's modified Eagle's medium (DMEM). MDA-MB-468, and MDA-MB-436 cells were cultured in a CO<sub>2</sub>-free environment in Leibovitz's L-15 medium; media for MDA-MB-436 cells was supplemented with 10µg/ml of insulin and 16µg/ml of glutathione. HCC1937 and HCC1187 cells were cultured in Roswell Park Memorial

Institute (RPMI) medium. Hs578T cells were cultured in high glucose DMEM supplemented with 0.01mg/mL bovine insulin (Sigma-Aldrich, St. Louis, MO, USA). All media was supplemented with 10% fetal bovine serum (FBS) and 1% penicillin-streptomycin.

### **3.3.2 Principal component analysis (PCA)**

RNA expression data from the Cancer Cell Line Encyclopedia (CCLE) for all available TNBC cell lines were downloaded from the Cancer Dependency Map (DepMap, release 21Q2; <https://depmap.org/portal/download/>). Genes contained within the Pathway Interaction Database (PID) MET Pathway curated gene set were then obtained [191]. Principal component analysis (PCA) was performed with genes as “loadings” and cell lines as “scores” using the pcaMethods R package. R version 4.1.0 was used in these analyses.

### **3.3.3 Small-interfering RNA transfection**

Cells were plated at a density of  $1 \times 10^6$  –  $2 \times 10^6$  cells per 100mm dish and reverse transfection was performed using Lipofectamine RNAiMAX Reagent (Invitrogen, Waltham, MA; 13778150). Cells were transfected with either negative control siRNA (siCtrl) (Ambion, Austin, Tx; AM4635) or BCAR3 siRNA ID: s15973 (Ambion; 4392420) at a concentration of 10 $\mu$ mol/ $\mu$ l and 20 $\mu$ mol/ $\mu$ l. Cells were cultured 24 hrs before plating for experiments.

### **3.3.4 Immunoblotting**

Immunoblots were performed as described previously [125,165]. Antibodies used for immunoblotting were as follows: Phospho-AKT (Ser473) (Cell Signaling Technology, Danvers, MA, USA; 9018), AKT (Cell Signaling Technology, Danvers, MA, USA; 2920), BCAR3 (Sigma-Aldrich, HPA014858), MET (Cell Signaling Technology, 3127), Phospho-MET (Tyr1234/1235) (Cell Signaling Technology, 3077), and GAPDH (Santa Cruz, Dallas, TX, USA; sc-32233).

### **3.3.5 Growth factor and inhibitor assays**

For all experiments measuring the effects of HGF (PeproTech, Rocky Hill, NJ; 100-39H) on protein or gene expression, cells were treated with either vehicle control (0.05% BSA) or 50ng/mL of HGF for 1-120 min, 24 hrs, or 72 hrs. For experiments testing protein expression following HGF treatment or Src inhibition with dasatinib (ChemCruz, sc-358114), cells were treated with either vehicle control (0.05% BSA + DMSO) or 50ng/mL of HGF, 5nM dasatinib, or combination of HGF + dasatinib.

### **3.3.6 Quantitative real-time PCR analysis**

mRNA was extracted according to the manufacturer's protocol using the Zymo Research Quick RNA Microprep Kit (Zymo Research, Irvine, CA, USA; R1050). For each sample, 1 $\mu$ g of mRNA was reverse-transcribed into cDNA in a 20 $\mu$ l reaction according to the manufacturer's protocol using the iScript cDNA Synthesis Kit (Bio-Rad, 1708890). The final cDNA product was diluted 5X and

subjected to quantitative real-time PCR performed with the Applied Biosystems StepOnePlusReal-Time PCR System (StepOne Software v2.2.2) (Waltham, MA, USA) and the Power SYBR Green PCR Master Mix (Applied Biosystems, Waltham, MA, USA; 4367659) using the following thermal cycling conditions: one initial cycle at 95°C for 10 min; 40 cycles of 15 sec at 95°C and 1 min at 60°C; followed by a melt-curve stage of 95°C for 15 sec, 60°C for 1 min, and 95°C for 15 sec. Relative mRNA expression was calculated using the  $2^{-\Delta\Delta Ct}$  method where transcript expression was normalized to GAPDH mRNA levels. Data were combined from 3 biological replicates. The sequences of the primers used to amplify the genes are shown in Table 2-3 (**Chapter 2**).

### **3.3.7 Ectopic expression of BCAR3**

Stable HCC1187 and MDA-MB-436 BCAR3 overexpression cell lines were generated by viral transduction using the pLV-Venus vector (HCC1187) or via plasmid transduction using the pEGFP-C1 vector (MDA-MB-436) as described in Cross *et al.* [125].

### **3.3.8 Statistical analysis**

Normal distribution of residuals was tested before performing one-way ANOVA followed by Sidak post hoc tests to determine p-values.

### **3.4 Results**

#### **3.4.1 MET signaling gene sets differentially align with the Basal A and Basal B TNBC subtypes.**

Given that previous reports have shown differential expression and functions of MET in mammary glands [190], we sought to further investigate MET gene expression in breast cancer. A principal component analysis was performed using a panel of 32 breast cancer cell lines and gene sets from the Pathway Interaction Database (PID) MET signaling pathway (Figure 3-1). Based on this analysis, we found that TNBC cells cluster based on their molecular profile when looking at genes from the MET signaling pathway, with basal A “basal-like” breast cancer cell lines clustering together and basal B “claudin-low” cells clustering together. Together, these data support previous reports showing that MET is differentially expressed based on molecular subtype of breast cancer [189].

#### **3.4.2 BCAR3 regulates MET protein levels and phosphorylation in basal-like TNBC cells**

Previously, our lab performed gene set variation analysis using publicly available mRNA expression data from a panel of 32 TNBC cell lines in the Cancer Cell Line Encyclopedia (CCLE) and found that gene sets associated with the MET receptor signaling showed a strong correlation with BCAR3 mRNA expression (**Chapter 2**). Based on these results and the data presented above, we wanted to further investigate the role of BCAR3-MET signaling in basal-like TNBC. To address this, immunoblot analysis was performed using the basal-like TNBC cell

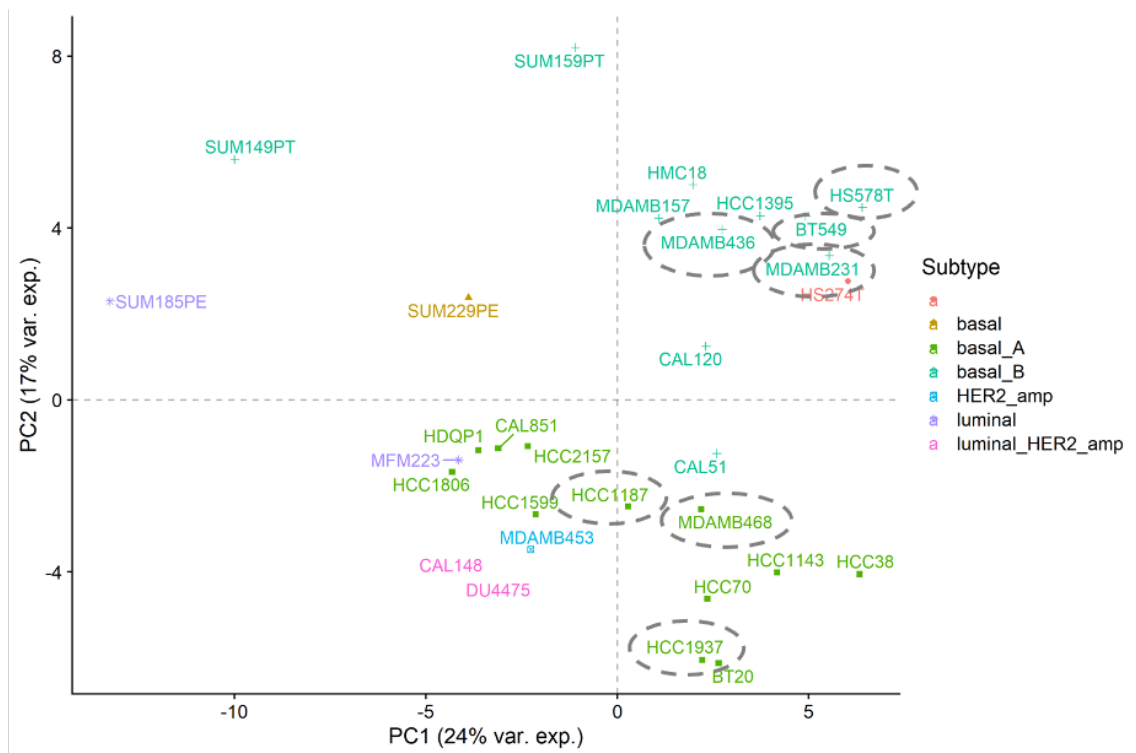


**Figure 3-1. TNBC cell lines cluster based on their molecular profile when MET pathway genes are analyzed.** Principal component analysis (PCA) was used to analyze genes within the Pathway Interaction Database (PID) MET Pathway in relation to mRNA expression data for all available TNBC cell lines obtained from the Cancer Cell Line Encyclopedia (CCLE). The analysis was performed by using genes as loading and cell lines as scores using the `pcaMethods` R package. PCA panel provided by Paul Myers.

line HCC1937. Cells were treated with control (siCtrl) or BCAR3-specific (siBCAR3) small interfering RNAs (siRNA) to promote transient BCAR3 knockdown. Cycling cells depleted of BCAR3 exhibited both elevated MET receptor expression as well as phosphorylation on Tyr1234/1235, which is an indicator of MET activity [99] (Figures 3-2A and B). AKT activation is also a common downstream indicator of MET receptor activity. However, phosphorylated (activated) AKT at Ser473 did not appear to be markedly elevated in cycling cells under conditions of BCAR3 depletion.

Because MET receptor protein and phosphorylation were significantly elevated in cycling cells depleted for BCAR3, we next investigated whether loss of BCAR3 also impacted phosphorylation of MET in response to acute stimulation by HGF. In contrast to cycling cells, serum-starved siBCAR3 HCC1937 cells exhibited a more modest elevation in MET expression compared to control cells, and phosphorylated MET was not detected in either case (Figure 3-3A, compare lanes 1 and 7). MET and AKT phosphorylation were significantly elevated at 15 minutes of HGF stimulation, which continued with a slow decline over the 120-minute time course in both control and BCAR3-depleted cells (lanes 2-6, 8-12). The increase in total MET expression appears to be largely responsible for the increase in MET phosphorylation in BCAR3 knockdown cells, as the specific activity of MET (phosphoMET/total MET) appears to be similar in control and siBCAR3 cells (middle panel). The specific activity of AKT was similarly not affected by BCAR3 knockdown (lower panel). Together, these data suggest that BCAR3 may serve a regulatory function to inhibit MET protein expression/turnover in HCC1937 cells.

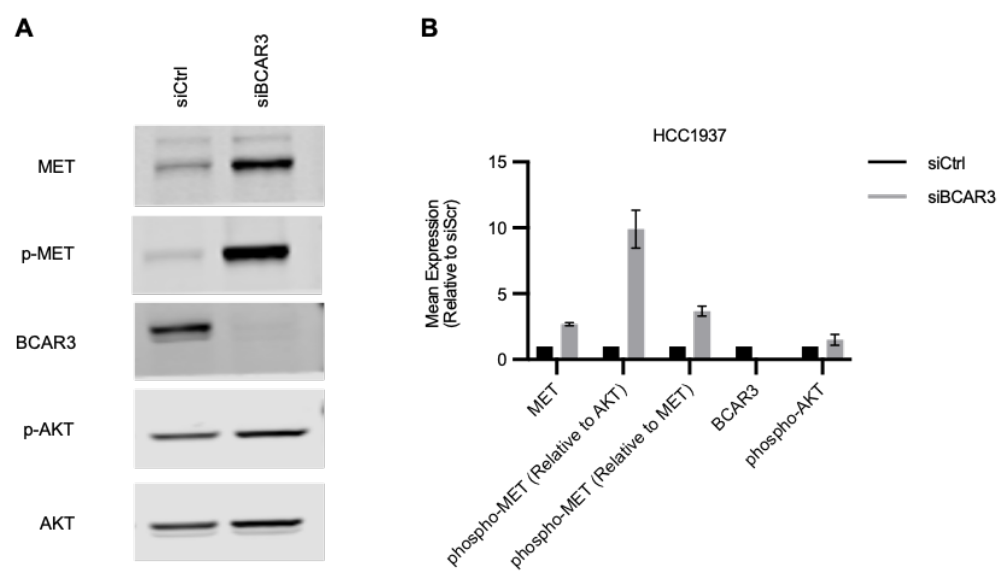


**Figure 3-2. BCAR3 regulates MET receptor protein expression in HCC1937 cells.** (A) Representative immunoblot showing HCC1937 cells with control or transient BCAR3 knockdown cultured under full serum conditions for 72 hrs. Cells were lysed and protein expression/phosphorylation was evaluated with the indicated antibodies. (B) Immunoblot quantification of endogenous protein levels. Phospho-MET (Tyr1234/1235) was normalized to total MET or AKT, and MET, BCAR3, and phospho-AKT (Ser473) were normalized to total AKT. Fold-change was quantified relative to siCtrl cells. Data shown are the average +/- SEM of two biological replicates.

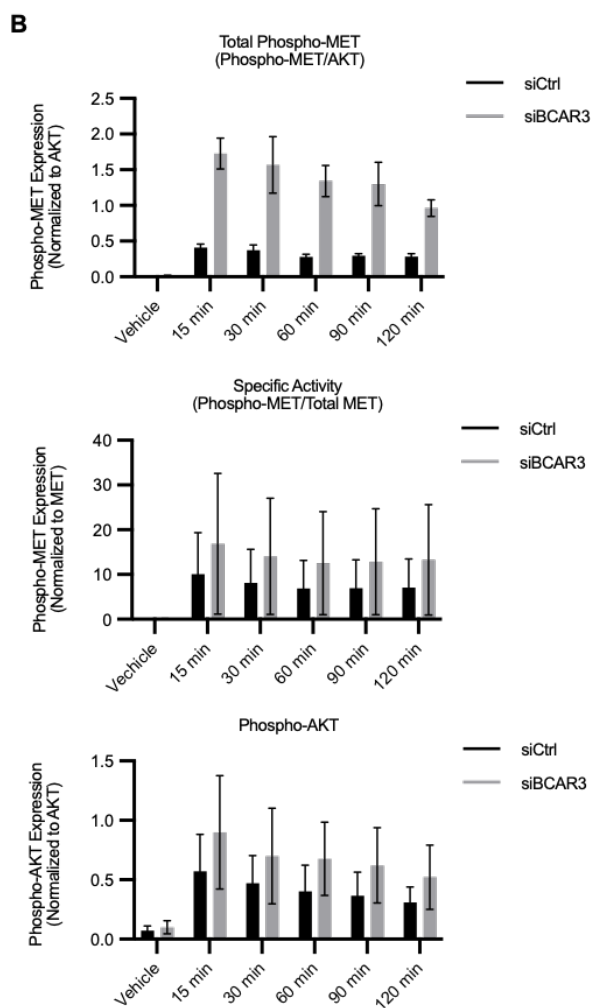
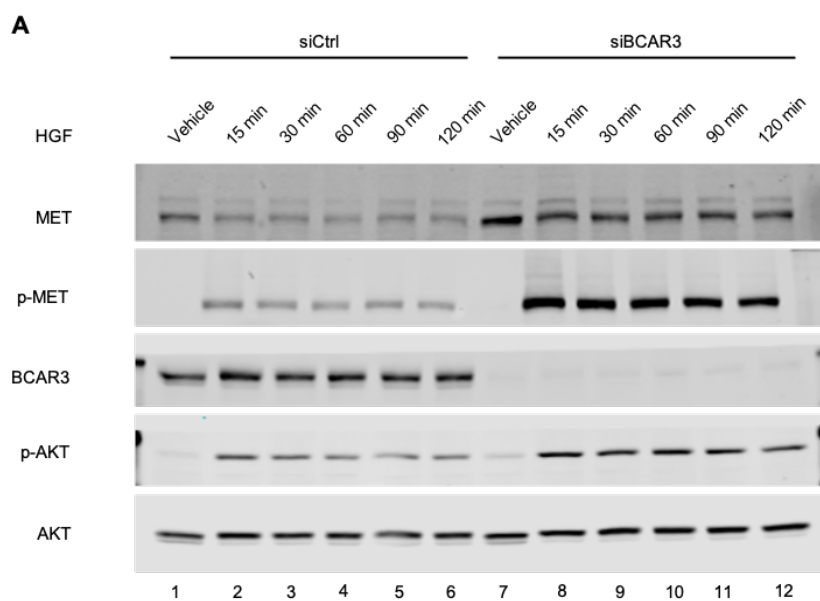


**Figure 3-3. HCC1937 cells exhibit elevated levels of MET phosphorylation following acute HGF stimulation.** (A) Representative immunoblot analysis of HCC1937 cells with control or transient BCAR3 knockdown that were serum-starved and stimulated with either vehicle control (0.05% BSA) or 50ng/mL HGF over a time-course ranging from 0-120 min. Cells were lysed and protein expression/phosphorylation was evaluated with the indicated antibodies. (B) Immunoblot quantification showing phospho-MET (Tyr1234/1235) levels normalized to total MET or AKT, and phospho-AKT (Ser473) normalized to total AKT. Fold-change was quantified relative to vehicle treated cells for each transfection condition. Data shown are the average +/- SEM of two biological replicates.

Tumor cells are often exposed to growth factors present in the tumor microenvironment for prolonged periods of time. Thus, we next sought to test the effects of prolonged HGF stimulation in HCC1937 cells under full serum conditions. As was the case with cycling cells, total and phosphorylated MET levels were elevated in siBCAR3 cells treated with vehicle (Figure 3-4A, compare lanes 1 and 3). MET expression was significantly reduced in both control and siBCAR3 cells following three-day treatment with HGF, with equivalent levels of expression in both cells (compare lanes 2 and 4). This is likely due to ligand-dependent downregulation of the MET receptor as reported by Hammond, *et al.* [192]. MET phosphorylation was slightly elevated in control cells following three days of HGF treatment but significantly reduced in BCAR3-depleted cells (Figure 3-4B). However, considering the changes in MET expression, the specific activity of MET was not significantly changed in response to HGF in the siBCAR3 cells. Similarly, AKT phosphorylation was not significantly altered as a function of BCAR3 expression in either cell type.

During this analysis, we noticed that BCAR3 protein levels were significantly elevated in control cells in the presence of HGF (Figure 3-4C). This suggested a possible reciprocal relationship between MET and BCAR3, with increased MET under conditions of BCAR3 depletion and increased BCAR3 coincident with downregulation of MET following the three-day HGF treatment. To test whether the changes in protein expression of either MET and/or BCAR3 were a consequence of transcriptional regulation, quantitative real-time PCR (RT-PCR) was performed to measure the gene expression. As expected, BCAR3 mRNA was

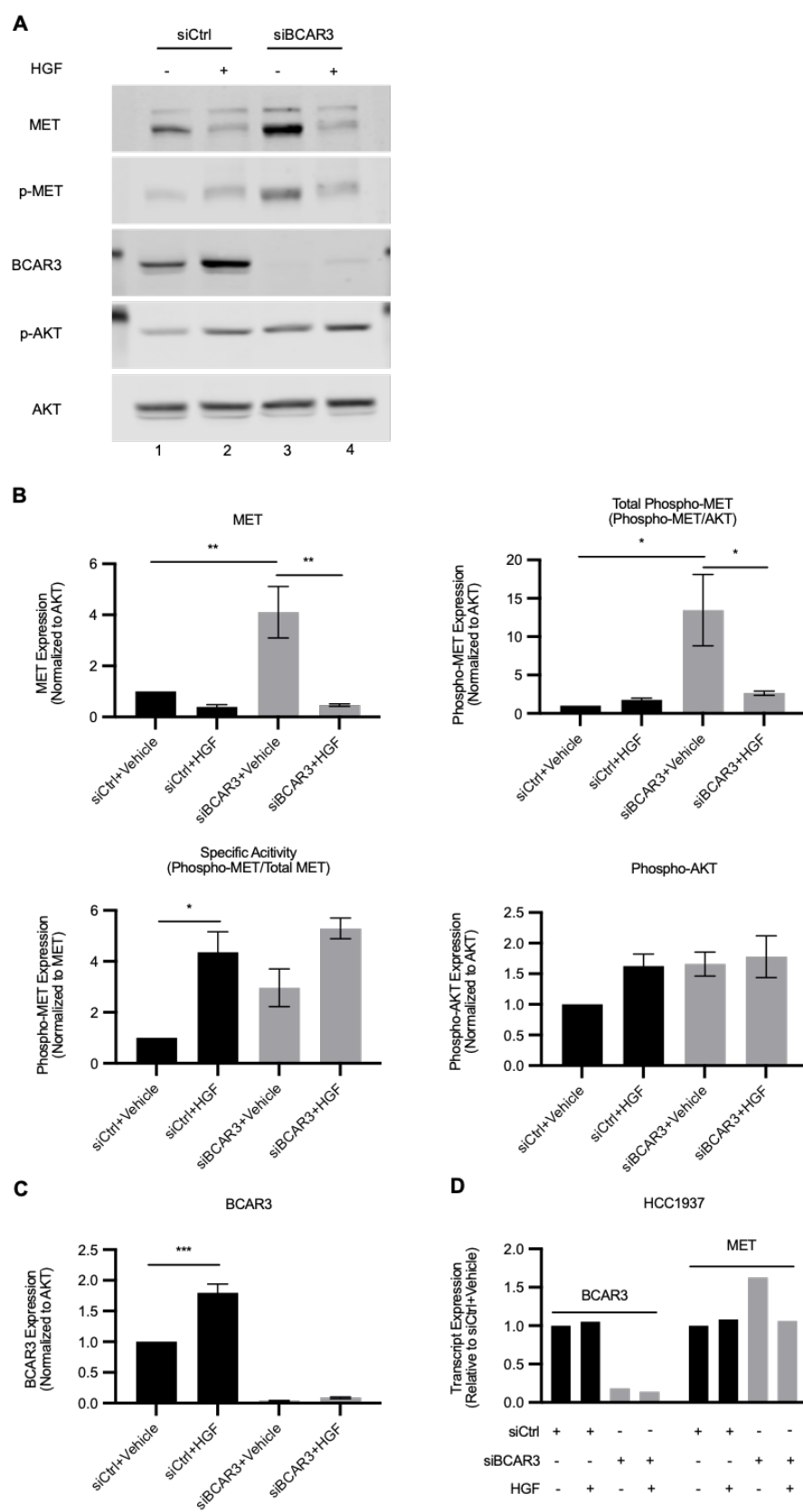


**Figure 3-4. BCAR3 expression is elevated in HCC1937 cells following prolonged HGF treatment.** (A) Representative immunoblot showing HCC1937 cells with control or transient BCAR3 knockdown cultured in the presence of either vehicle control (0.05% BSA) or 50ng/mL HGF for 72 hours. (B and C) Immunoblot quantification. Phospho-MET (Tyr1234/1235) levels were normalized to total MET or AKT, and MET, BCAR3, and phospho-AKT (Ser473) were normalized to total AKT. Fold-change was quantified relative to siCtrl cells treated with vehicle. Data shown are the average +/- SEM of three biological replicates. \* indicates  $p < 0.05$ , \*\* indicates  $p < 0.01$ , \*\*\* indicates  $p < 0.001$ . (D) RT-PCR analysis of BCAR3 and MET gene expression in HCC1937 cells with control or transient BCAR3 knockdown cultured under conditions above. Data shown are from one experiment.

reduced in cells with BCAR3 knockdown (Figure 3-4D). However, BCAR3 mRNA levels did not change in control cells as a function of HGF treatment. Similarly, MET mRNA levels were not affected by HGF treatment in control cells. However, as was the case for MET protein, mRNA expression was elevated in siBCAR3 compared to control cells in the absence of HGF and then decreased following treatment with HGF for three days. While it is not possible to make any firm conclusions from these data since the gene expression analysis was performed only once, the data suggest preliminarily that 1) the increase in MET protein expression observed in cells depleted for BCAR3 may arise due at least in part to transcriptional control, and 2) the changes in BCAR3 expression found in control cells following prolonged treatment with HGF may be due to post-transcriptional regulation.

Given the apparent reciprocal relationship between MET receptor and BCAR3 in HCC1937 cells, we next sought to determine whether a second basal-like TNBC cell line exhibited similar patterns of regulation. Like HCC1937 cells, the basal-like MDA-MB-468 cell line showed an increase in MET expression under conditions of BCAR3 knockdown (Figure 3-5A, compare lanes 1 and 3) and a possible increase in BCAR3 expression when control cells were treated with HGF for three days (compare lanes 1 and 2). Long-term treatment with HGF resulted in downregulation of MET receptor in both control and BCAR3 knockdown cells (Figure 3-5B). Unlike the HCC1937 cells, MET phosphorylation was still elevated after three days of HGF treatment, trending similarly in control and siBCAR3 cells. AKT phosphorylation was also slightly elevated in HGF-treated cells for both

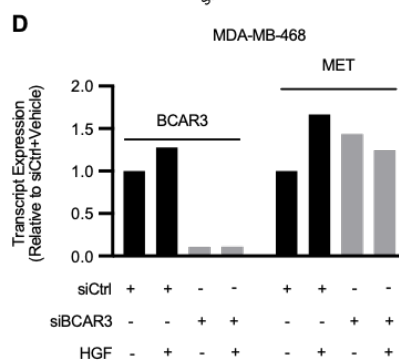
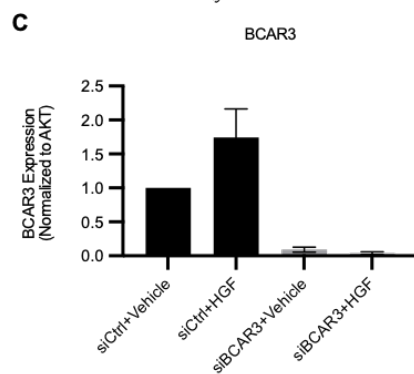
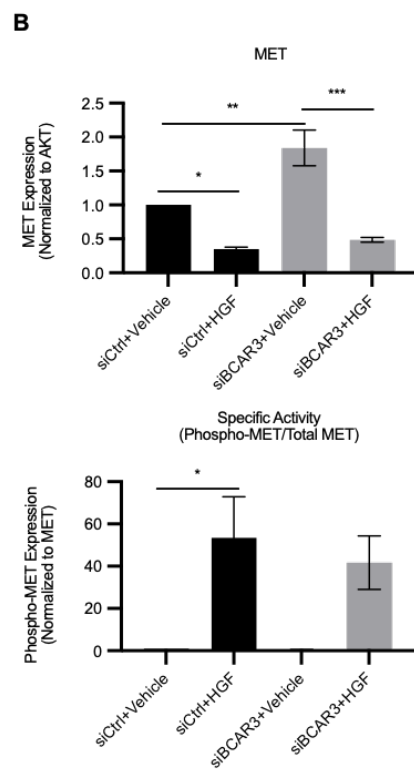
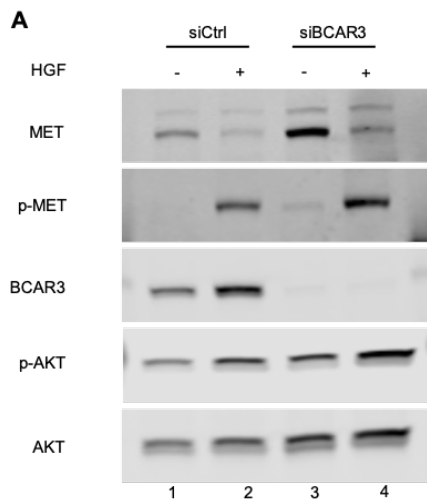


**Figure 3-5. MDA-MB-468 cells exhibit sustained MET and AKT phosphorylation following prolonged HGF treatment.** (A) Representative immunoblot showing MDA-MB-468 cells with control or transient BCAR3 knockdown cultured in the presence of vehicle control (0.05% BSA) or 50ng/mL HGF for 72 hours in full serum conditions. (B) Immunoblot quantification. Phospho-MET (Tyr1234/1235) levels were normalized to total MET or AKT, and MET, BCAR3, and phospho-AKT (Ser473) were normalized to total AKT. Fold-change was quantified relative to siCtrl cells treated with vehicle. Data shown are the average +/- SEM of three biological replicates. \* indicates  $p < 0.05$ , \*\* indicates  $p < 0.01$ , \*\*\* indicates  $p < 0.001$ . (C) RT-PCR analysis of BCAR3 and MET gene expression in MDA-MB-468 cells with control or transient BCAR3 knockdown cultured under conditions above. Data shown are from one experiment.

control and siBCAR3 cells. The slight difference in MET regulation between HCC1937 and MDA-MB-468 cells may be due to 1) a slower decay in MET receptor phosphorylation in MDA-MB-468 cells compared to HCC1937 and/or 2) greater responsiveness of AKT to HGF stimulation in these cells. As was the case for the HCC1937 cells, the increase in MET receptor expression observed in non-stimulated siBCAR3 cells could potentially arise from an ~1.4-fold increase in mRNA (Figure 3-5D). However, the difference between BCAR3 mRNA levels in vehicle and HGF-treated control cells was even less, suggesting that transcriptional regulation was unlikely to account for any change in BCAR3 protein expression. Taken together, data from both HCC1937 and MDA-MB-468 support an interaction between BCAR3 and MET signaling in basal-like TNBC.

### **3.4.3 “Gain of function” approach supports reciprocal co-regulation of BCAR3-MET expression**

The two basal-like cells used above, HCC1937 and MDA-MB-468, express relatively high levels of BCAR3 (see Figure 2-1C). Since loss-of-function studies with BCAR3 showed increased MET expression in these cells, we hypothesized that overexpression of BCAR3 in a basal-like breast cancer cell line that expresses little to no BCAR3 would result in decreased MET expression. Stable overexpression of BCAR3 was established in the basal-like cell line HCC1187 and protein of the previously described targets was analyzed (Figure 3-6). Ectopic overexpression of BCAR3 resulted in a decrease in total and phosphorylated MET in cycling cells, with limited effect on AKT phosphorylation (Figure 3-6). These data

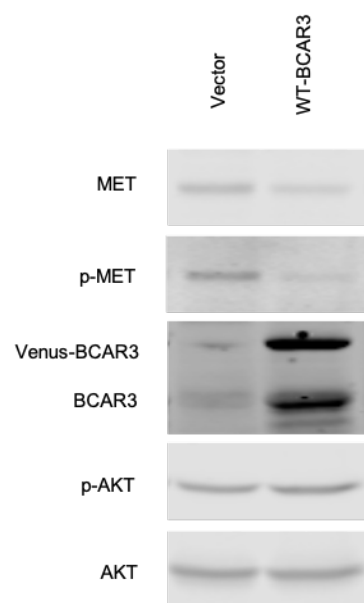


**Figure 3-6. MET receptor expression and phosphorylation is reduced in HCC1187 cells with BCAR3 overexpression.** (A) Representative immunoblot showing HCC1187 cells stably transfected with vector or plasmids encoding Venus-BCAR3 and cultured for five days in full serum conditions with no media changes. (B) RT-PCR analysis of the previously described HCC1187 cells cultured for 48 hrs in full serum conditions. Data shown are from one experiment. Panel A courtesy of Keena Thomas.

provide further support for a reciprocal BCAR3-dependent regulation of MET expression and phosphorylation in basal-like TNBC cells.

#### **3.4.4 MET expression does not exhibit BCAR3-dependent regulation in claudin-low TNBC cells**

Considering that MET expression was altered as a function of BCAR3 expression in basal-like cells, we sought to test whether BCAR3 similarly induced changes in MET expression in claudin-low cells. BT549, a cell line characterized as being claudin-low, was subjected to siRNA transfection, cultured under full serum conditions, stimulated with HGF for three days, and protein and gene expression analyzed as described above. MET expression, MET phosphorylation, and AKT phosphorylation were unchanged as a function of BCAR3 before or after HGF stimulation (Figure 3-7A). Additionally, endogenous BCAR3 expression was unchanged following HGF stimulation. Gene expression analysis supported these findings (Figure 3-7B). A similar study was performed in two additional claudin-low cell lines, MDA-MB-231 and Hs578T, under conditions of serum starvation followed by a shorter period of HGF stimulation (24 hrs) to determine whether the BCAR3-dependent regulation of MET might be shortened in these cells. In these cases, stable BCAR3 knockdowns were performed with shRNAs as previously described in **Chapter 2**. Again, no changes in total MET, MET phosphorylation, or AKT phosphorylation were observed as a function of BCAR3 expression either before or after HGF stimulation in either cell line tested (Figure 3-8).

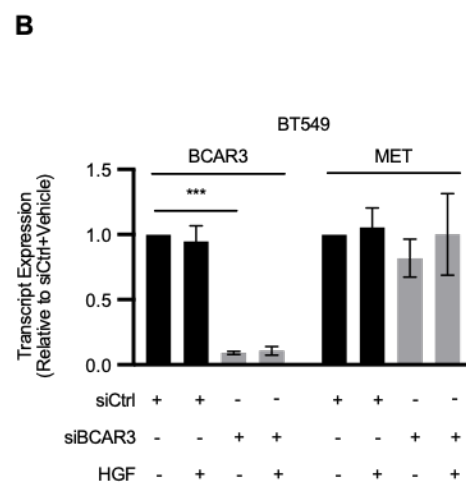
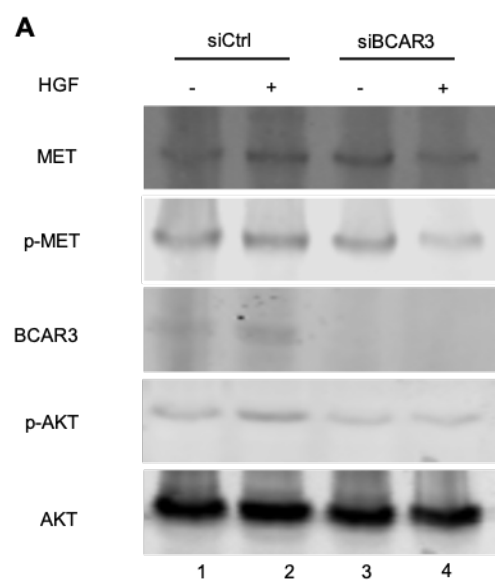


**Figure 3-7. MET receptor expression and phosphorylation are not altered in claudin-low TNBC cells following prolonged HGF treatment.** (A)

Representative immunoblot showing BT549 cells with control or transient BCAR3 knockdown cultured in vehicle control (0.05% BSA) or 50ng/mL HGF for 72 hours in full serum conditions. (B) RT-PCR analysis of BCAR3 and MET gene expression in BT549 cells with control or transient BCAR3 knockdown cultured under the conditions above. Data shown are the average +/- SEM of three biological replicates. \*\*\* indicates  $p < 0.001$ .

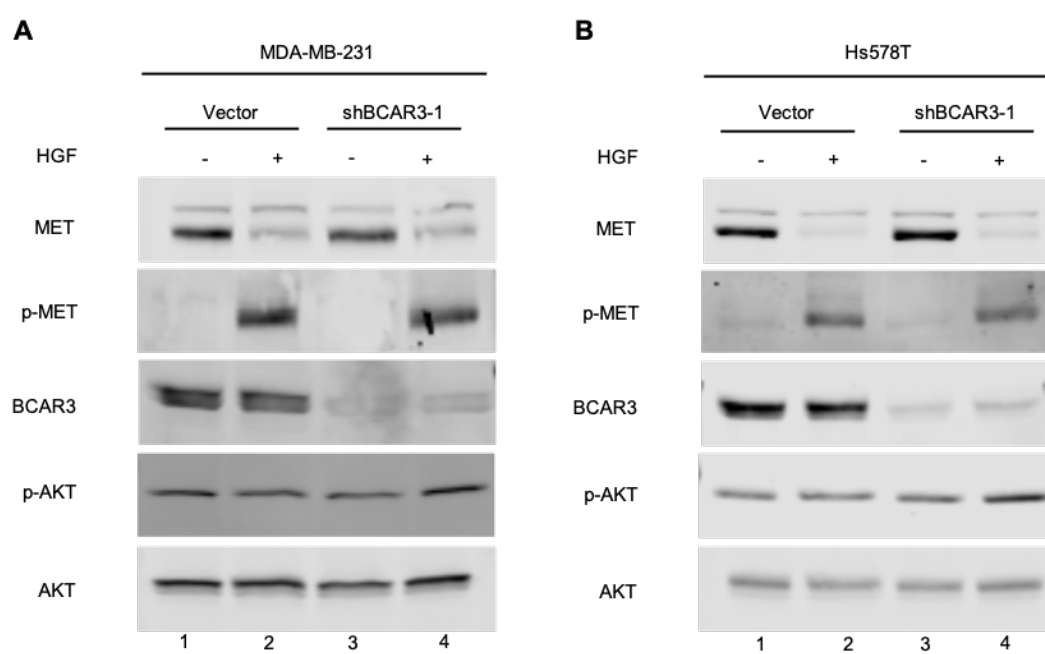


**Figure 3-8. MET receptor expression and phosphorylation are not altered in claudin-low TNBC cells following short-term HGF stimulation.** (A)

Representative immunoblot showing MDA-MB-231 cells with control or stable BCAR3 knockdown that were serum-starved and stimulated with either vehicle control (0.05% BSA) or 50ng/mL HGF for 24 hrs. Data shown are from one experiment. (B) Representative immunoblot showing Hs578T cells with control or stable BCAR3 knockdown cultured as described above. Data shown are from one experiment.

Finally, we took a gain-of-function approach to determine whether expression of MET would be altered under conditions of ectopic BCAR3 overexpression in MDA-MB-436 cells, a claudin-low cell line with low endogenous expression of BCAR3 (see Figure 2-1C). No changes in MET expression or AKT phosphorylation were observed in cells with BCAR3 over-expression either before or after HGF stimulation (Figure 3-9A). Similarly, no changes in endogenous BCAR3 and MET mRNA were observed following HGF stimulation (Figure 3-9B). Together, these data indicate that BCAR3 differentially regulates MET expression and phosphorylation based on the genetic profile of TNBC cells, functioning as a negative regulator of MET signaling in basal-like but not claudin-low TNBC cells.

#### **3.4.5 Src reduces MET upregulation in HCC1937 cells**

Previous work from our lab and others has established BCAR3 as a regulator of the non-receptor tyrosine kinase c-Src (Src) through interaction with the adaptor molecule Cas [161,166]. As mentioned previously, BCAR3 and Cas together regulate Src activity and enhance cell adhesion, invasion, proliferation, and activation of the small GTPase Rac1 [125–127,160,161,166]. If BCAR3 functions through Src to modulate MET expression, we hypothesized that Src inhibition would phenocopy the elevation of MET expression observed in basal-like cells under conditions of BCAR3 depletion. To test this hypothesis, HCC1937 control and BCAR3-depleted cells were treated with either the Src inhibitor dasatinib, HGF, or a combination of both for 72 hrs and protein levels were measured. As previously shown, cells with reduced BCAR3 expression contained

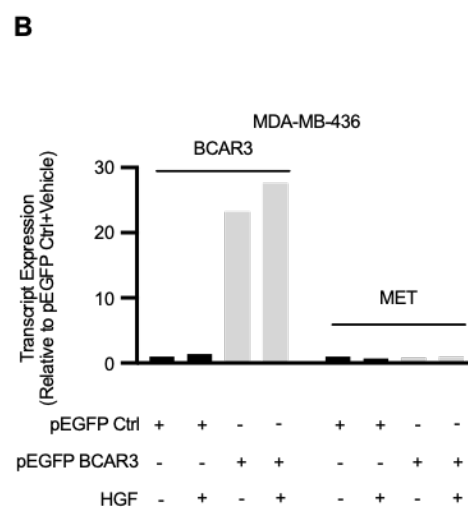
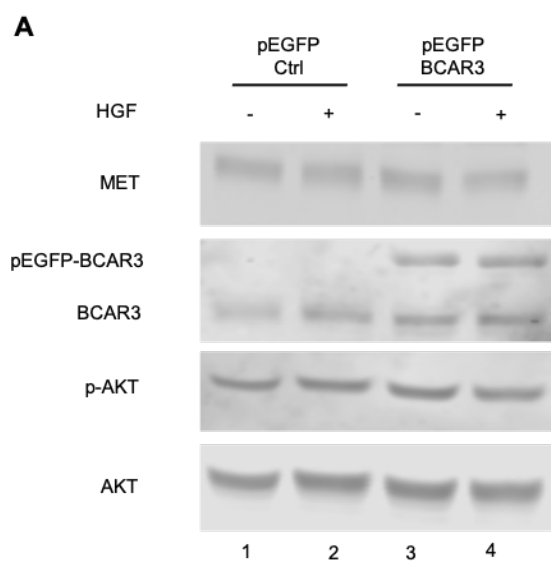


**Figure 3-9. BCAR3 overexpression does not alter MET receptor expression and phosphorylation in claudin-low MDA-MB-436 cells.** (A) Representative immunoblot showing MDA-MB-436 cells with plasmids encoding EGFP (pEGFP ctrl) or EGFP-BCAR3 (pEGFP BCAR3) cultured in vehicle control (0.05% BSA) or 50ng/mL HGF for 72 hours in full serum conditions. (B) RT-PCR analysis of BCAR3 and MET gene expression in MDA-MB-436 cells with pEGFP control or BCAR3 overexpression cultured under conditions above. Data shown are from one experiment. Panels A and C were provided by Keena Thomas.

elevated levels of total and phosphorylated MET (Figure 3-10A, compare lanes 1 and 5). Additionally, as was the case previously, prolonged HGF stimulation elicited a downregulation of MET expression and phosphorylation in these cells (Figure 3-10B). Interestingly, siBCAR3 cells showed increases in MET expression and phosphorylation compared to control cells when treated with dasatinib (compare lanes 3 and 7), although the magnitude of these change was substantially reduced. The addition of dasatinib with HGF had no further effect on MET expression or phosphorylation than HGF alone. These data suggest that the elevation of MET expression and phosphorylation observed in cells with reduced BCAR3 expression may in part require Src, but that Src inhibition alone is not sufficient to upregulate MET expression. One caveat to these experiments is that Src autophosphorylation (pTyr419) was not measured to confirm inhibition of the kinase activity by dasatinib. Additionally, this experiment was performed one time, so it is difficult to make definitive conclusions.

### 3.5 Discussion

This study demonstrates for the first time that BCAR3 can serve as a negative regulator of MET receptor expression in basal-like TNBC. We show that depletion of BCAR3 in basal-like TNBC cells results in an upregulation of MET protein and phosphorylation of MET. Together with the observations in **Chapter 2**, these data establish BCAR3 as an adaptor molecule with broad functional roles that influence TNBC molecular dynamics. Understanding the regulatory functions

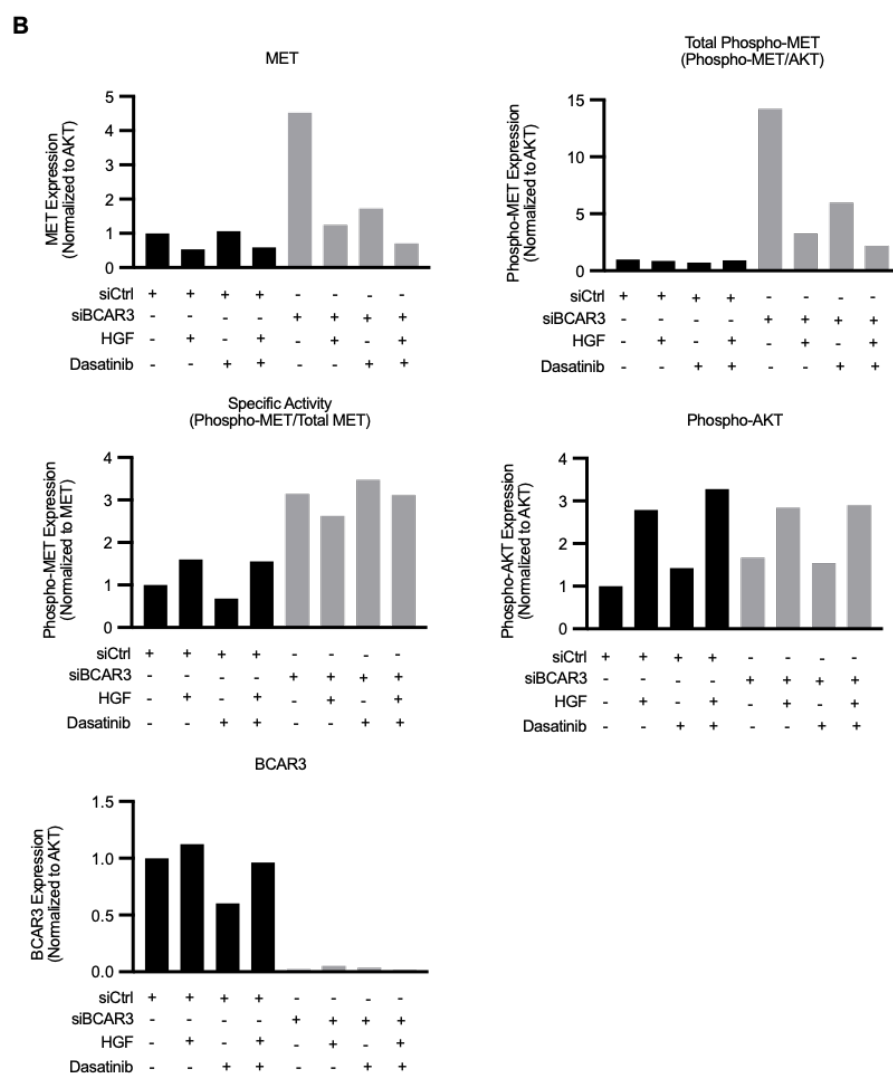
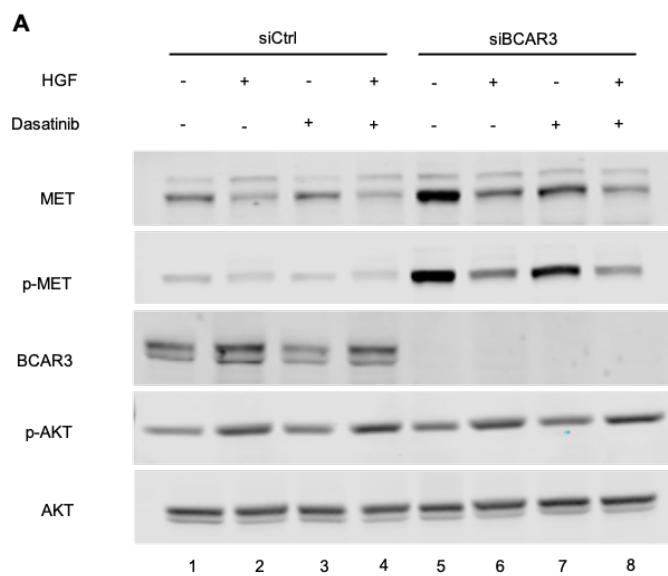


**Figure 3-10. Src inhibition reduces MET receptor elevation in HCC1937 cells with BCAR3 knockdown.** (A) Representative immunoblot showing HCC1937 cells with control or transient BCAR3 knockdown cultured in vehicle control (0.05% BSA + DMSO), 50ng/mL HGF, Src inhibition 5nM dasatinib, or combination for 72 hours under full serum conditions. (B) Immunoblot quantification. Phospho-MET (Tyr1234/1235) levels were normalized to total MET, and MET, BCAR3, and phospho-AKT (Ser473) were normalized to total AKT. Fold-change was quantified relative to siCtrl cells treated with Vehicle. Data shown are from one experiment.

of BCAR3 can help enhance the clinical management of patients by identifying mechanistic characteristics between subtypes of TNBC that can inform therapeutic strategies.

In **Chapter 2**, we showed that functional interactions between BCAR3 and MET in claudin-low TNBC cells contribute to cell proliferation and migration. In claudin-low Hs578T cells, this functional interaction generates an autocrine loop involving BCAR3, MET, and HGF that drives aggressive cellular behaviors. The data in this chapter highlight the heterogeneity of dysregulated mechanisms present in TNBC and how adaptor molecules like BCAR3 are important contributors to these mechanisms. Our signaling studies support a role of BCAR3 as a negative regulator of MET expression and phosphorylation in basal-like but not in claudin-low TNBC. Further exploration of the functional implication of the MET phosphorylation in our studies is needed to 1) determine whether this phosphorylation is indicative of MET biological activity and 2) uncover the mechanisms that negatively regulate this phosphorylation.

Cocultures using HGF-expressing cancer-associated fibroblasts show that HGF induces signaling in cell lines belonging to the original “intrinsic” basal-like broad classification but not in luminal-like breast cancer cells, suggesting that the response to HGF differs based on molecular profile [151]. These studies, together with the data presented in this chapter, suggest that even within the broad “intrinsic” basal group, there is heterogeneity in the way MET signaling may be regulated (comparing basal-like cells to claudin-low cells), and BCAR3 may have a role in this regulation.

One of the interesting aspects of the data presented in this study is the reciprocal nature of MET-BCAR3 expression in basal-like TNBC cells. Depletion of BCAR3 in cells that express relatively high levels of this molecule resulted in increased MET expression (Figures 3-2, 3-4, and 3-5), while forced ectopic expression of BCAR3 in cells that typically express very low levels resulted in decreased MET expression (Figure 3-6). Moreover, coincident with downregulation of MET following long-term (three day) treatment with HGF, BCAR3 expression was elevated (Figure 3-4B). Based on these findings, continuous and/or cyclic exposure to HGF in the tumor microenvironment [190] could impact the biological activity of the tumor cells, causing a feedback loop that promotes MET and BCAR3 activities with alternating periodicities. Intermittent activation of these pathways, in turn, could lead to distinct functional outcomes for the tumor. In support of this notion, BCAR3 expression is elevated in ductal carcinoma *in-situ* (DCIS) compared to invasive ductal carcinoma (IDC) (see Figure 2-1A), suggesting that BCAR3 may serve as an important molecule in the progression of aggressive phenotypes in cells that have not yet acquired, or are in the process of acquiring, aggressive traits (e.g., those associated with the epithelial-to-mesenchymal transition). It will be interesting to determine how this differential expression tracks with basal-like compared to claudin-low TNBC. Preliminary studies have also shown that HCC1937 cells with reduced BCAR3 have a faster wound healing phenotype compared to control cells (Personal communication with Paul Myers). This contrasts with extensive data in claudin-

low and ER+ cells showing that BCAR3 is a positive regulator of cell migration [125,165], highlighting again the impact of genetic background on the function of BCAR3.

The data presented in this study provide initial insight into the role of BCAR3 as a regulator of MET signaling in basal-like TNBC, but the data are limited in that many of the experiments were preliminary with only one or two biological replicates performed and conclusions are difficult to make. As stated previously, this study is also limited by the lack of functional assays testing migration, invasion, and proliferation to determine whether the upregulation of MET protein and phosphorylation of MET observed in cells with reduced BCAR3 expression is biologically relevant. More studies are also needed to understand if the MET phosphorylation observed is indicative of MET receptor activation and activation of downstream signaling.

Despite the limitations, our data suggest that overall, this adaptor molecule may serve as a valuable biomarker for 1) patient prognosis, 2) identifying patients who may benefit from targeted therapies against the MET receptor, and 3) identifying patients who may benefit from targeted neo-adjuvant therapy to ameliorate disease progression.

## **Chapter 4: Exploring the transcriptional landscape regulated by BCAR3**

### **4.1 Abstract**

The molecular mechanisms driving triple-negative breast cancers (TNBCs) remain largely unknown, leading to challenges in therapeutic treatment strategies for patients with this disease. As stated previously, work from our laboratory showed that BCAR3 is a potent activator of Src protein tyrosine kinase activity, and that BCAR3 regulates cell adhesion and motility through interaction with the adaptor molecule Cas. Data presented in **Chapter 2** show that patient-derived TNBC tumor samples contain elevated BCAR3 protein compared to normal mammary tissue. Further, BCAR3 expression was detected in TNBC cell lines and found to be required for maximal TNBC cell growth as well as tumor growth in an orthotopic xenograft model. Using mouse mammary epithelial organoid cultures from wild-type mice and BCAR3 knockout mice as a tool to measure cell growth, we determined that BCAR3 is required for mammary epithelial organoid branching in response to various growth factors. Despite these observations, signaling and transcriptional networks regulated by BCAR3 in TNBC or during mammary gland morphogenesis remain unclear. In this study, RNA sequencing and computational approaches were used to examine the transcriptome of the claudin-low MDA-MB-231 TNBC cell line as a function of BCAR3 expression when the cells were cultured in 2D (plastic) or 3D (matrigel) conditions. We show that 711 genes are altered as a function of BCAR3 expression in both conditions, and that pathway enrichment

analysis performed excluding the overlapping genes shows different enriched pathways in the conditions stated above. In parallel, the same approach was used in organoids generated from wildtype and BCAR3 knockout mice to understand how transcriptional and signaling networks present in normal mammary epithelial cells may contribute to tumor initiation. Comparisons of all three conditions revealed that 33 genes overlapped between all three conditions tested. Together, this study shows that BCAR3 may function as a signaling node driving cell growth pathways that may contribute to TNBC tumor initiation and progression.

## 4.2 Introduction

BCAR3 gene expression has been detected in normal mammary epithelial cells as well as in breast cancer cell lines and tumor tissues (**Chapter 2** and [193]). In non-tumorigenic mammary epithelial cells, BCAR3 has been shown to promote DNA synthesis in response to epidermal growth factor (EGF) stimulation [121]. In breast cancer, BCAR3 has been reported to regulate adhesion dynamics that promote invasion of cells [125,126]. We also showed that elevated BCAR3 mRNA expression in TNBC patients was found to correlate with worse patient outcomes and that BCAR3 is a promoter of TNBC cell growth (**Chapter 2**).

Physical as well as molecular properties of the extracellular matrix (ECM) engage cell-intrinsic molecules involved in growth factor and adhesion signaling, leading to dramatic changes in the migration, invasion, proliferation, and transcriptional programs of tumor cells [134,194,195]. Our lab previously demonstrated that BCAR3 is localized to focal adhesions and controls adhesion turnover through interaction with the adaptor molecule p130<sup>Cas</sup> (Cas) [125]. This BCAR3-dependent regulation of adhesion was implicated in driving TNBC cell invasion when cultured in 3D matrigel conditions. As discussed in **Chapter 1**, Cas is an adaptor molecule that plays an important role in cellular responses to the environment. For example, extracellular mechanical stress has been reported to induce conformational changes in Cas that facilitate association with c-Src (Src) and may enable downstream signaling [133].

Together, these studies provide evidence that BCAR3 has cell signaling implications in both normal mammary cells and in breast cancer. Despite this

evidence, however, the transcriptional networks regulated by BCAR3 that enable cell growth, migration, and invasion have never been explored. In this study, we analyzed the transcriptional landscape regulated by BCAR3 in TNBC cells and investigated whether the BCAR3-dependent transcriptional networks are altered as a function of the local microenvironment. In parallel, we analyzed the transcriptome of mouse mammary epithelial cells as a function of BCAR3 expression in an effort to understand the molecular functions of BCAR3 implicated in tumor initiation and growth.

## **4.3 Materials and methods**

### **4.3.1 Cell culture**

MDA-MB-231 breast cancer cells were purchased from American Type Culture Collection (Manassas, VA, USA). Media and supplements were purchased from Gibco, Life Technologies, Carlsbad, CA, USA. MDA-MB-231 cells were cultured in high-glucose Dulbecco's modified Eagle's medium (DMEM) supplemented with 10% fetal bovine serum (FBS) and 1% penicillin-streptomycin.

### **4.3.2 Stable knockdown of BCAR3**

Stable MDA-MB-231 knockdown cell lines were generated via lentiviral transduction using small hairpin RNAs targeting BCAR3 (shBCAR3-1 and shBCAR3-2) as previously described [125]. Cells were maintained in the presence of 0.5 $\mu$ g/ml puromycin.

#### **4.3.3 3D matrigel cell culture**

MDA-MB-231 cells were cultured in 3D matrigel as described by Cross *et al.* [125]. Growth factor-reduced matrigel (Corning, Corning, NY, USA; 354230) was spread evenly on the bottom of 8-well chamber slides. MDA-MB-231 cell suspensions were plated in the chamber slides with Dulbecco's modified Eagle's medium (DMEM) supplemented with 2% horse serum, 2% matrigel, 5ng/ml EGF, and 0.5 $\mu$ g/ml puromycin. Cells were cultured for eight days with media changes every four days.

#### **4.3.4 Organoid cultures**

Primary mammary organoids were generated using epithelial cells obtained from mouse mammary glands isolated from wildtype (WT) and BCAR3 knockout (B3KO) (gift from Dr. Adam Lerner) [120] 8-week-old mice as described by Nguyen-Ngoc, *et al.* [172]. Epithelial cell suspensions were plated on growth factor-reduced matrigel and cultured in DMEM/F12 media supplemented with 2.5nM fibroblast growth factor 2 (FGF2) (PeproTech, Rocky Hill, NJ, USA; 100-18B) for seven days with a media change every 3-4 days.

#### **4.3.5 RNA sequencing and differential gene expression analysis**

MDA-MB-231 cells with control shRNAs (Vector-control) or stable BCAR3 knockdown (shBCAR3-1) were plated at a density of 250,000 cells per 60mm and cultured on plastic for 48hrs or in matrigel for eight days. Mouse mammary organoids were cultured as described above for seven days. Cells were processed

for mRNA extraction according to the manufacturer's protocol using the Zymo Research Quick RNA Microprep Kit (Zymo Research, Irvine, CA, USA; R1050). Library preparation and Next Gen RNA sequencing (RNA-seq) at 400 million reads per run was performed by the University of Virginia Genome Analysis and Technology Core. RNA-seq processing and differential gene expression analysis was performed by Dr. Stephen Turner at the UVA Bioinformatics Core.

#### **4.3.6 Quantitative real-time PCR**

Quantitative real-time PCR was performed with the Applied Biosystems StepOnePlusReal-Time PCR System (StepOne Software v2.2.2) (Waltham, MA, USA) and the Power SYBR Green PCR Master Mix (Applied Biosystems, Waltham, MA, USA; 4367659). mRNA was extracted according to the manufacturer's protocol using the Zymo Research Quick RNA Microprep Kit (Zymo Research, Irvine, CA, USA). For each sample, 1 $\mu$ g of mRNA was reverse-transcribed into cDNA in a 20 $\mu$ l reaction according to the manufacturer's protocol using the iScript cDNA Synthesis Kit (Bio-Rad, 1708890). The final cDNA product was diluted 5X and subjected to quantitative real-time PCR performed with the Applied Biosystems StepOnePlusReal-Time PCR System (StepOne Software v2.2.2) (Waltham, MA, USA) and the Power SYBR Green PCR Master Mix (Applied Biosystems, Waltham, MA, USA; 4367659) using the following thermal cycling conditions: one initial cycle at 95°C for 10 min; 40 cycles of 15 sec at 95°C and 1 min at 60°C; followed by a melt-curve stage of 95°C for 15 sec, 60°C for 1 min, and 95°C for 15 sec. Relative mRNA expression was calculated using the 2(-

$\Delta\Delta\text{Ct}$ ) method where transcript expression was normalized to GAPDH mRNA levels. The sequences of the primers used to amplify the genes are shown in Tables 4-1 and 4-2.

#### **4.3.7 Identification of differentially expressed genes and pathway enrichment analysis**

Using the differential gene expression data obtained from the University of Virginia Genome Analysis and Technology Core, protein coding gene expression was analyzed using the “EnhancedVolcano” package in R [196]. The “VennDiagram” package in R was used to determine overlap of protein coding genes that were significantly altered ( $\text{padj} \leq 0.05$ ) between conditions [197]. Pathway enrichment was performed to assess enrichment of specific pathways within the Kyoto Encyclopedia of Genes and Genomes (KEGG) database using the “pathview” package in R [198,199]. The full extent of differential gene expression data for each condition was also used to perform pathway enrichment analysis with the fast gene set enrichment analysis “fgsea” package in R [200]. Fast gene set enrichment analysis was performed using 1000 permutations. R version 4.2.5033 was used in these analyses.

#### **4.3.8 Statistical analysis**

The unpaired Welch’s t-test was performed to determine p-values between comparisons.

**Table 4-1.** Human primer sequences for qRT-PCR

Gene	Forward (F) Reverse (R)	Primer Sequences (5'-3')
<i>GALNT14</i>	F	TGTCAGTCATCACCTTGTTTC
<i>GALNT14</i>	R	CATTGCTGTCGGTCATCT
<i>MAGEH1</i>	F	TTCTTTTGAAGTTGAAATACCCAGT
<i>MAGEH1</i>	R	TTCAGAAACGTCAGATATGAAGAAA
<i>CKMT1</i>	F	AGCTTCCTGATCTGGGTGAA
<i>CKMT1</i>	R	GAAGTCCAGTGCCCAGGTTA
<i>GABRE</i>	F	TCTCCCAGACCTGGTACGAC
<i>GABRE</i>	R	TCCTTGTAGATGCGGACCAT
<i>VCAM1</i>	F	TGTTGAGATCTCCCCTGGAC
<i>VCAM1</i>	R	AATTGGTCCCCTCACTCCTC
<i>EHF</i>	F	GGGCTCAGATCTCCATGACA
<i>EHF</i>	R	GTGCTTTTTGGTGTGGCACT
<i>GPR110</i>	F	G TTCAGGTCACCCAATTTTCG
<i>GPR110</i>	R	CACTCTGAAAGAGCCGTCTTC
<i>GPR116</i>	F	AAGAGGCACTGAGGCAAAAA
<i>GPR116</i>	R	TTCCCATGAATTGGAAAACCTG
<i>TMEM154</i>	F	TGGAAATTGAAATGGAAGAGC
<i>TMEM154</i>	R	TGGGTTGTGATTTGATTCCTT
<i>MIF</i>	F	ATCGTAAACACCAACGTGCC
<i>MIF</i>	R	CTGTAGGAGCGGTTCTGCG
<i>TNS3</i>	F	CATCCTCCGTTTCAGCCCAC
<i>TNS3</i>	R	GTTGCTGGAAATGGTGCAGG
<i>GAPDH</i>	F	AACGTGTCAGTGGTGGACCT
<i>GAPDH</i>	R	TCGCTGTTGAAGTCAGAGGA

**Table 4-2.** Mouse primer sequences for qRT-PCR

Gene	Forward (F) Reverse (R)	Primer Sequences (5'-3')
<i>B4GALNT12</i>	F	CCATGGCTCCTCAAGACATT
<i>B4GALNT12</i>	R	TCCTCAGATGCTCCTCTGGT
<i>CXCL13</i>	F	ATGAGGCTCAGCACAGCAAC
<i>CXCL13</i>	R	CAGGGGGCGTAACTTGAAT
<i>ENO1B</i>	F	TCTGGGGAAACTGAGGACAC
<i>ENO1B</i>	R	GATCTCCGGTCCATGCTTTA
<i>LPHN2</i>	F	GCAGAGCAGCCTTACCATT
<i>LPHN2</i>	R	GCATCAGGGAGGTAGCAGTC
<i>ST6GAL1</i>	F	CCCGGAAGTCAACTGAAATG
<i>ST6GAL1</i>	R	TGTTCTCCATGGGAAAGAGG
<i>TMPRSS11A</i>	F	CCAGAGGATAGCTGGTGAGG
<i>TMPRSS11A</i>	R	ACCACCATCATCAGGGAGAG
<i>GAPDH</i>	F	ACTCCACTCACGGCAAATTC
<i>GAPDH</i>	R	TCTCCATGGTGGTGAAGACA

## 4.4 Results

### 4.4.1 Identification of differentially expressed genes in MDA-MB-231 cells as a function of BCAR3 expression

BCAR3 has been implicated in regulating cell growth, migration, and invasion but the transcriptional networks that enable these cellular behaviors have not been studied. Given that BCAR3 has been reported to regulate cell growth when cells were grown on plastic (see Chapter 2) and promote cell invasion under 3D matrigel culture conditions, we sought to determine if transcriptional networks would be altered as a function of BCAR3 in cells cultured on plastic or 3D matrigel. To test this, MDA-MB-231 cells transduced with empty vector or constructs encoding short hairpins targeting BCAR3 were cultured on plastic or suspended in 3D matrigel. Following mRNA extraction and sequencing, differential gene expression analysis was performed and the “EnhancedVolcano” package in R was used to analyze differentially expressed protein-coding genes as a function of BCAR3 expression. In cells cultured on plastic, a total of 4680 protein coding genes were found to be significantly altered ( $p_{adj} \leq 0.05$ ), with 2401 genes downregulated ( $\log_2\text{FoldChange} < 0$ ) and 2279 genes upregulated ( $\log_2\text{FoldChange} > 0$ ) as a function of BCAR3 expression (Figure 4-1A; blue colored genes and red colored genes respectively, a  $\log_2\text{FoldChange}$  cutoff of  $\leq -0.5$  and  $\geq 0.5$  was applied for clarity). In cells cultured in 3D matrigel, a total of 1017 genes were found to be significantly altered as a function of BCAR3 expression ( $p_{adj} \leq 0.05$ ) with 549 genes downregulated ( $\log_2\text{FoldChange} < 0$ ) and 468 genes upregulated ( $\log_2\text{FoldChange} > 0$ ) (Figure 4-1B; blue colored genes

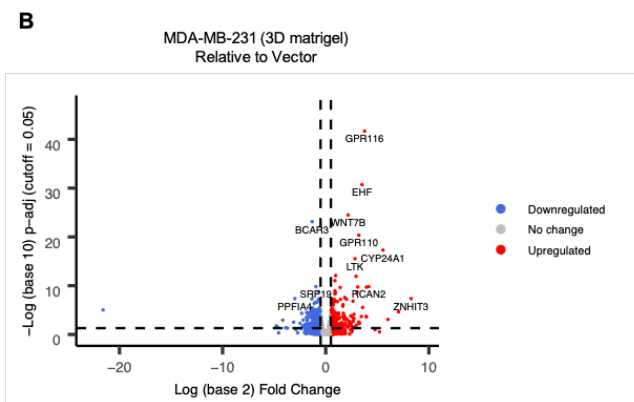
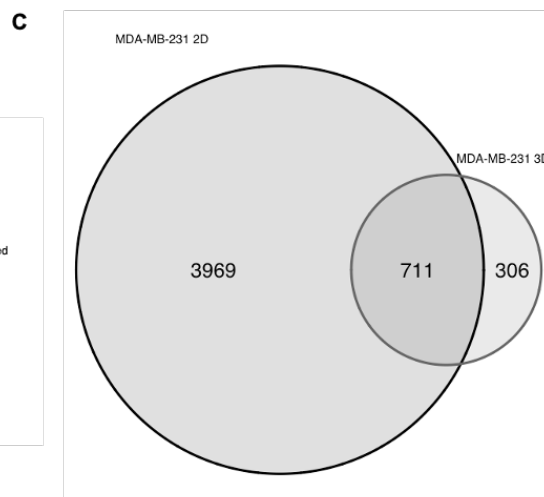
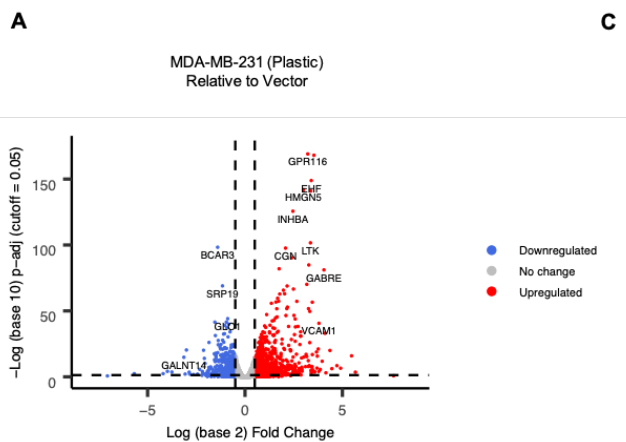


***Figure 4-1. Identification of differentially expressed genes in TNBC cells cultured on plastic and in matrigel as a function of BCAR3 expression.***

(A) Protein coding genes obtained from the differential gene expression analysis of MDA-MB-231 cells with stable BCAR3 knockdown relative to vector-control cells cultured on plastic were analyzed using the “EnhancedVolcano” package in R. For clarity, genes were marked as downregulated (blue color) if their Log2foldchange was  $< -0.5$ , no change (gray) if Log2foldchange was  $\geq -0.5$  and  $\leq 0.5$ , and upregulated (red color) if Log2foldchange was  $> 0.5$ . Only significantly altered genes ( $p_{adj} \geq 0.05$ ) were colored. (B) Protein coding genes obtained from the differential gene expression analysis of MDA-MB-231 cells with stable BCAR3 knockdown relative to vector-control cultured in matrigel were visualized and colored as stated above. (C) Overlap of differentially expressed protein coding genes was analyzed using the “VennDiagram” package in R. Only genes significantly altered ( $p_{adj} \leq 0.05$ ) were visualized.

and red colored genes respectively, a log<sub>2</sub>FoldChange cutoff of  $\leq -0.5$  and  $\geq 0.5$  was applied for clarity). In order to compare protein coding genes that were significantly altered ( $p_{adj} \leq 0.05$ ) between the two conditions analyzed, the “VennDiagram” package in R was used. 3969 genes were altered in cells cultured on plastic alone, 306 in cells cultured in 3D matrigel alone, and a total of 711 protein coding genes were found to overlap between the two conditions (Figure 4-1C). These overlapping genes thus appear to be regulated by BCAR3 independently of culture condition.

To validate BCAR3-dependent changes in gene expression identified by RNA sequencing, a subset of genes were analyzed in cells grown in the same culture conditions using RT-PCR (Figure 4-2A). Overall, BCAR3-dependent changes in gene expression identified by RNAseq were similarly altered when measured by RT-PCR. Moreover, genes that were found by RNAseq to be altered under both 2D and 3D culture conditions (GALNT14, MAGEH1, and EHF) exhibited similar directional trends when analyzed by RT-PCR (Figure 4-2A and Figure 4-2B). To test if these changes were consistent with the remainder of the dataset, the “geom\_tile” function within the “ggplot2” package in R was used to compare gene expression of the overlapping gene sets between conditions, and it was observed that most overlapping genes appeared to be changing in the same direction (Figure 4-2C). Together, this suggests that the genes exhibiting BCAR3-dependent changes in 2D and 3D showed consistent up- or down-regulation irrespective of culture condition.

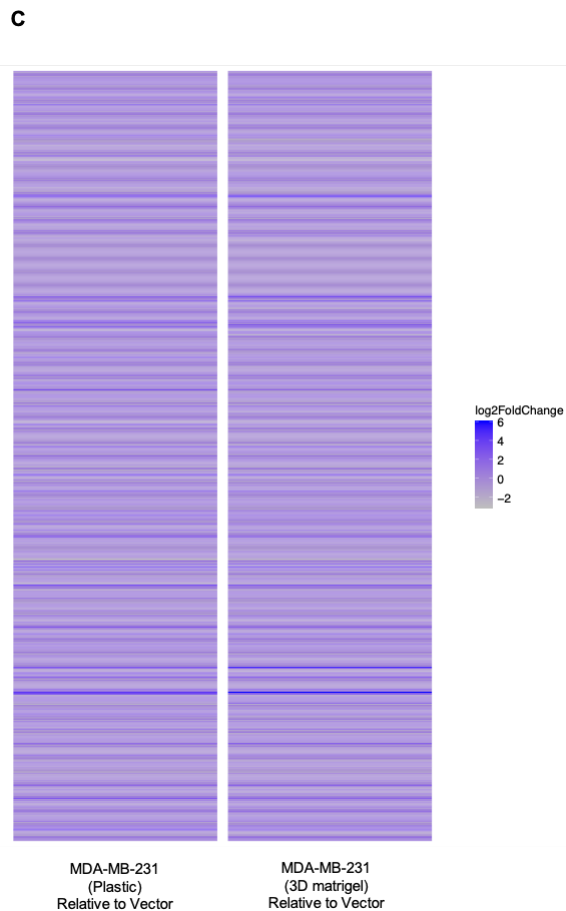
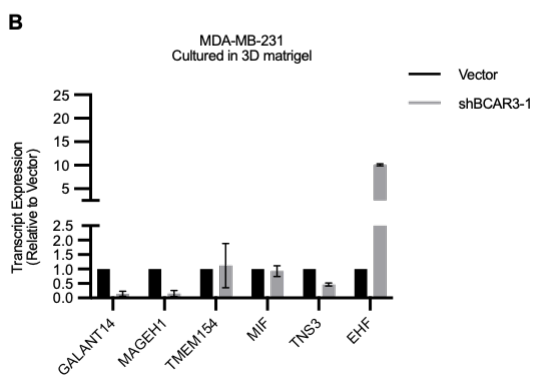
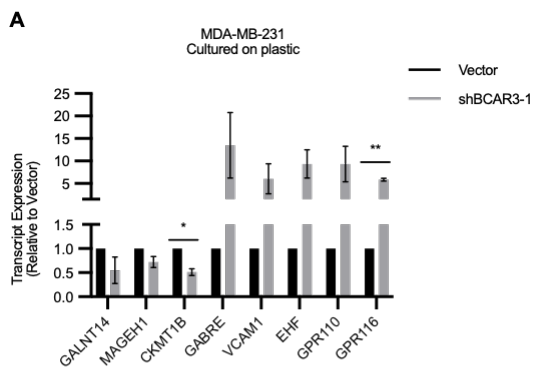


**Figure 4-2. BCAR3-dependent differentially expressed genes that were common to both plastic and matrigel culture conditions are altered in similar directions.** (A) Quantitative real-time PCR analysis of GALNT14, MAGEH1, CKMT1B, GABRE, VCAM1, EHF, GPR110, and GPR116 transcript levels in MDA-MB-231 vector-control or shBCAR3-1 cells cultured on plastic for 48 hours. RT-PCR was conducted with technical duplicates for 3-4 independent experiments. Data shown are the average +/- SEM of three biological replicates. The unpaired Welch's t-test was used to determine differences per gene. \* indicates  $p < 0.05$ , \*\* indicates  $p < 0.01$ . (B) Quantitative real-time PCR analysis of GALNT14, MAGEH1, TMEM154, MIF, TNS3, and EHF transcript levels in MDA-MB-231 vector-control or shBCAR3-1 cells cultured in matrigel. RT-PCR was conducted with technical duplicates for two independent experiments. Data shown are the average +/- SEM of two biological replicates. (C) Gene expression of overlapping genes between the two conditions was analyzed using the "geom\_tile" function in R. Blue color indicates high expression and gray color indicates low expression.

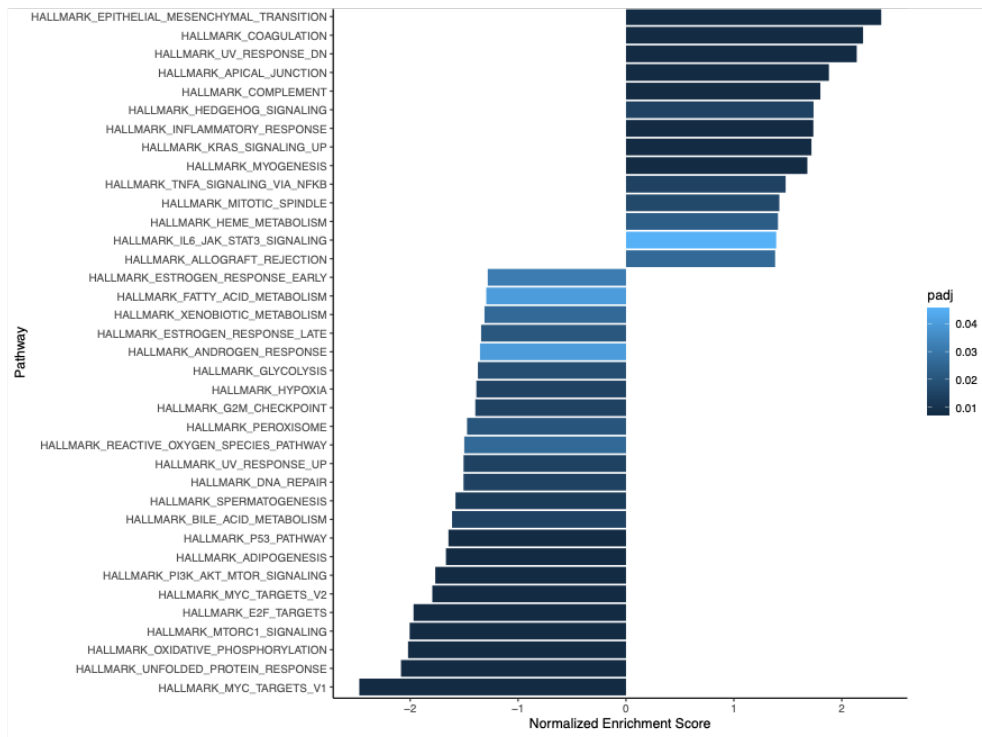
#### **4.4.2 Pathway enrichment in MDA-MB-231 cells reveals novel BCAR3-regulated pathways**

To gain a broad understanding of how BCAR3-dependent transcriptional changes affect signaling mechanisms in cells cultured on plastic, pathway enrichment was assessed using all genes altered in cells with reduced BCAR3 expression (Figure 4-3A). The “fgsea” package in R was used to perform gene set enrichment analysis based on hallmark genes. The top five pathways with significantly elevated enrichment in cells with reduced BCAR3 are pathways involved in the epithelial-to-mesenchymal transition, coagulation, negative regulation of ultra-violet response, apical junction, and complement (Figure 4-3A). The top five pathways with significantly reduced enrichment are MYC targets, unfolded protein response, oxidative phosphorylation, MTORC1 signaling, and E2F targets. While the range of pathways that were revealed by this analysis is very broad, it is interesting that some coincide with what is known about BCAR3 functions. For example, the downregulation of pathways involved in cell proliferation is consistent with the previous observation that cells with reduced BCAR3 expression exhibit reduced growth when cultured in plastic conditions (**Chapter 2**).

A similar analysis was performed to identify pathways impacted by reduced BCAR3 expression when cultured in matrigel (soft rigidity). In this analysis, the top five pathways with significantly elevated enrichment in cells with reduced BCAR3 are pathways involved in the mitotic spindle, epithelial-to-mesenchymal transition, negative regulation of ultra-violet response, inflammatory response, and TNF $\alpha$

**A**

MDA-MB-231 (Plastic)  
Relative to Vector



**B**

MDA-MB-231 (3D matrigel)  
Relative to Vector

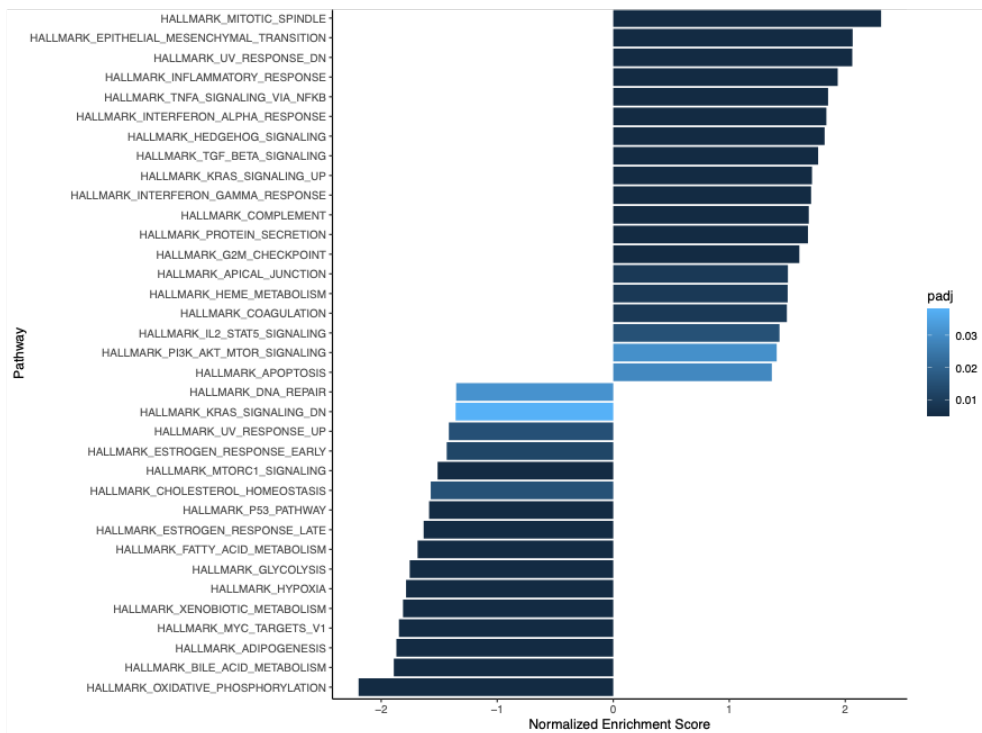


**Figure 4-3. Pathway enrichment in MDA-MB-231 cells with reduced BCAR3 expression.** (A) Differentially expressed genes in MDA-MB-231 cells with stable BCAR3 knockdown relative to vector-control cells cultured on plastic were used for pathway enrichment analysis using the “fgsea” package in R. Enrichment analysis was performed based on the Hallmark gene set using 1000 permutations. (B) Differentially expressed genes in MDA-MB-231 cells with stable BCAR3 knockdown relative to vector-control cells cultured in matrigel were used for pathway enrichment analysis as stated above. Only pathways that were significantly enriched were visualized ( $p_{adj} \leq 0.05$ ).

signaling via NF $\kappa$ B (Figure 4-3B). The top five pathways with significantly reduced enrichment are pathways involved in oxidative phosphorylation, bile acid metabolism, adipogenesis, MYC targets, and xenobiotic metabolism. Several of these pathways are similar to those identified for cells cultured on plastic such as reduced enrichment of MYC targets and MTORC1 signaling and positive enrichment in the EMT pathway.

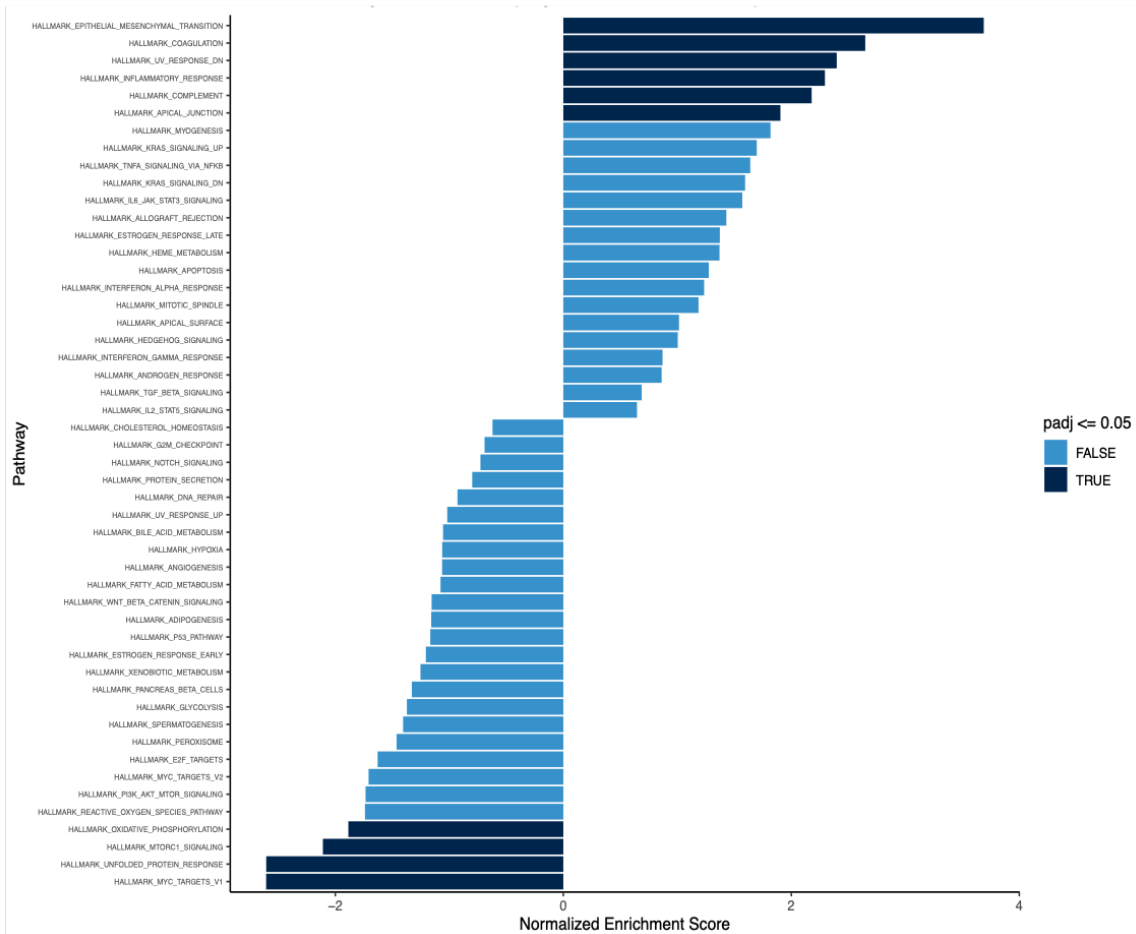
As previously stated, there are numerous reports that have demonstrated that increasing matrix rigidity activates signaling mechanisms that drive malignant phenotypes [134,194,195]. To gain a better understanding of rigidity-dependent pathways impacted by BCAR3 expression, a comparison in enrichment pathways was made between cells cultured on plastic and those cultured in matrigel after the 711 genes that were altered regardless of culture condition (overlapping) were removed from the datasets. Interestingly, while shBCAR3 cells cultured on plastic still exhibited enrichment of genes involved in EMT, this was not the case for cells cultured in matrigel (Figure 4-4A and Figure 4-4B). This is consistent with multiple studies that have reported the induction of EMT as a function of increased matrix rigidity [201,202]. Together, these data show that the pathway enrichment is different between culture conditions, suggesting that the microenvironment affects the enrichment of BCAR3-regulated pathways.

#### **4.4.3 BCAR3 regulates genes involved in cell adhesion**

Our lab has previously shown that BCAR3 is involved in the regulation of focal adhesions [125,126]. To test if the genes altered as a function of BCAR3

A

MDA-MB-231 (Plastic)  
Relative to Vector



**B**

MDA-MB-231 (3D matrigel)  
Relative to Vector

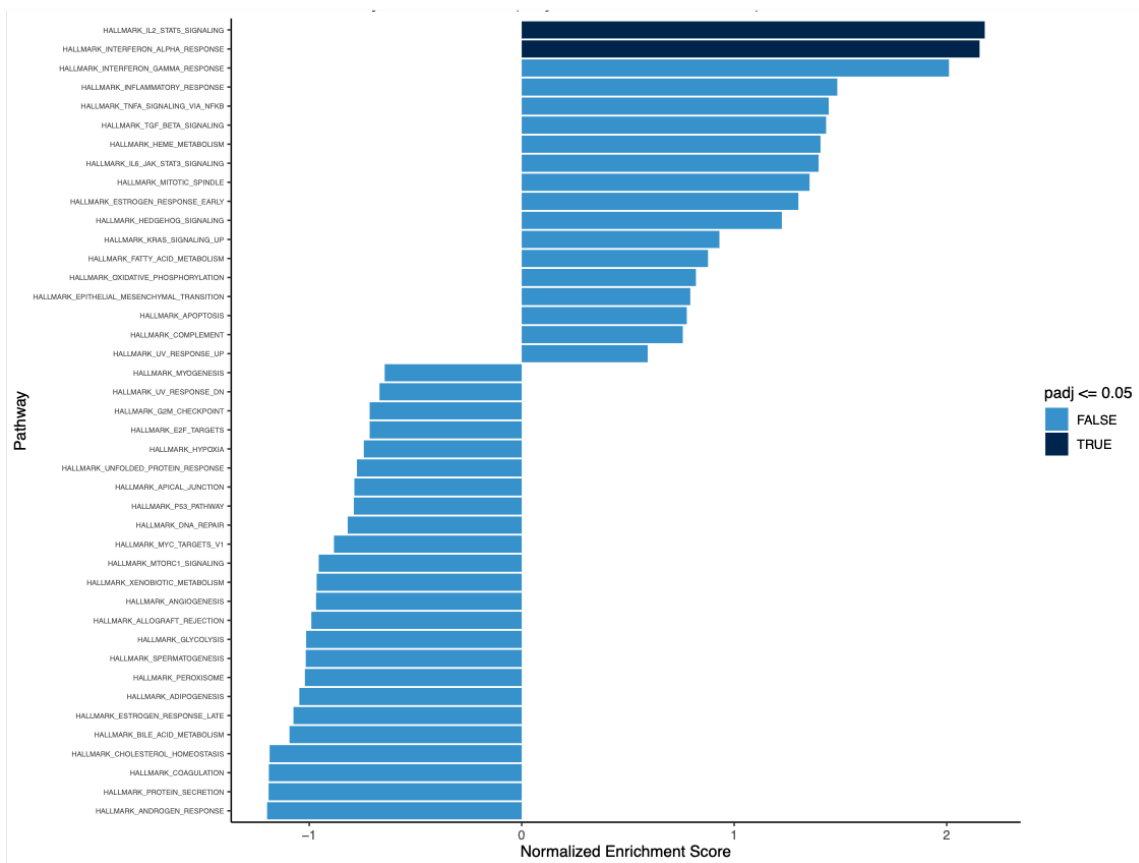


**Figure 4-4. Pathway enrichment of genes altered as a function of BCAR3 expression that are unique to each culture condition.** (A) Differentially expressed genes in MDA-MB-231 cells with stable BCAR3 knockdown relative to vector-control cells cultured on plastic that do not overlap with differentially expressed genes in cells cultured in matrigel were used for pathway enrichment analysis using the “fgsea” package in R. Enrichment analysis was performed based on the Hallmark gene set using 1000 permutations. Pathways that were significantly enriched ( $p_{adj} \leq 0.05$ ) are labeled as “TRUE”. (B) Differentially expressed genes in MDA-MB-231 cells with stable BCAR3 knockdown relative to vector-control cells cultured in 3D matrigel that do not overlap with differentially expressed genes in cells cultured on plastic were used for pathway enrichment analysis as described in part A.

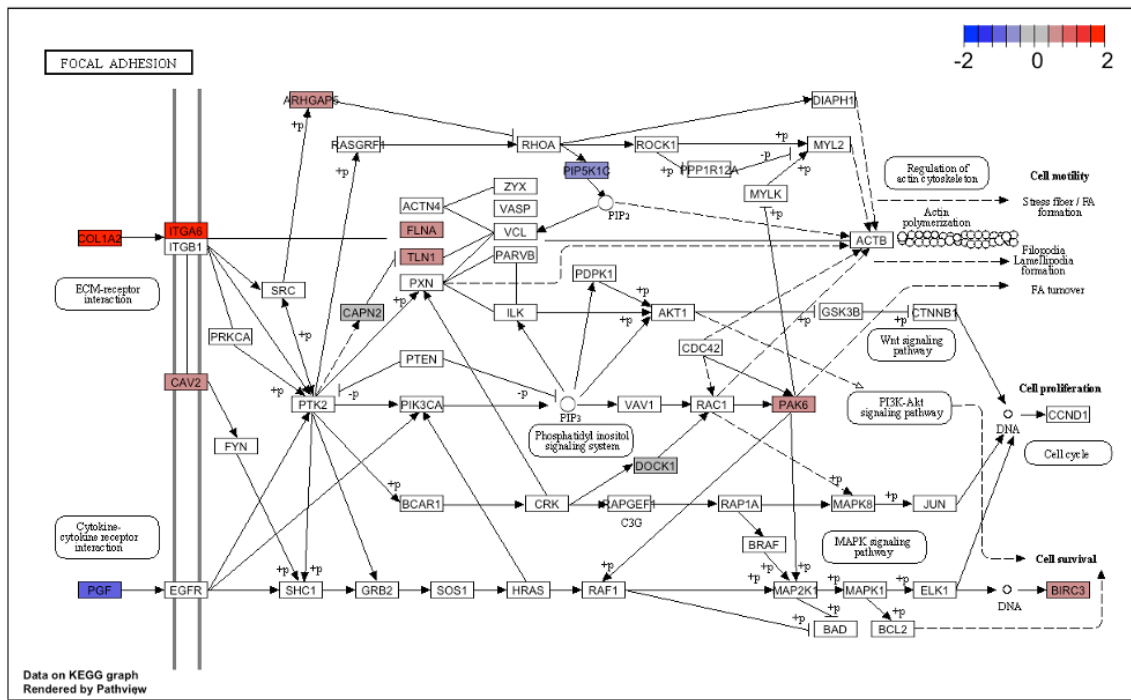
expression on both plastic and in 3D matrigel map to focal adhesion or cell adhesion pathways, the “pathview” package in R was used. Using differential gene expression data obtained from cells cultured on plastic, the 711 genes that were found to overlap between the two culture conditions (Figure 4-1C) were mapped to the Kyoto Encyclopedia of Genes and Genomes (KEGG) focal adhesion pathway (Figure 4-5A). The same approach was used for cells cultured in 3D matrigel (Figure 4-5B). As previously observed (Figure 4-2C), the genes that mapped to the focal adhesion pathway were altered in the same direction between the two conditions, with the same genes (e.g., ITGA6 and PGF and others) being upregulated and downregulated similarly. Likewise, the genes that mapped to cell adhesion molecules in the KEGG cell adhesion molecules curated set were altered in the same direction between the two conditions with genes like ITGB2 and ICAM2 among others being down regulated and upregulated similarly (Figure 4-6A and 6B). While the mechanisms through which BCAR3 affects transcription of genes in these pathways are not yet clear, the data indicate that genes altered as a function of BCAR3 expression regardless of culture condition are 1) regulated in similar ways and 2) map to pathways where BCAR3 has known functions, further supporting the role of BCAR3 in these functions.

#### **4.4.4 Identification of differentially expressed genes as a function of BCAR3 in mouse mammary organoids**

Mammary gland development is a process that involves activation of transcriptional networks that enable cell growth and differentiation [178,203,204].

A

MDA-MB-231 (Plastic)



B

MDA-MB-231 (3D matrigel)

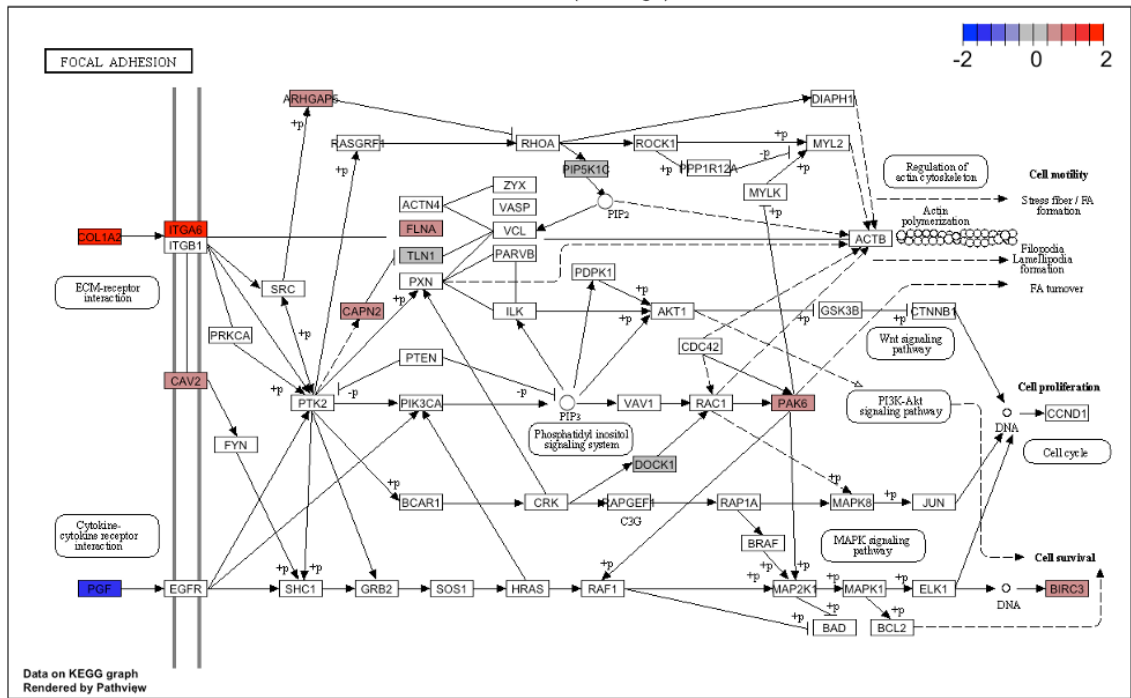


**Figure 4-5. BCAR3-dependent differentially expressed genes that overlap between MDA-MB-231 cells cultured on plastic or matrigel map to the focal adhesion pathway.** (A) Using differential gene expression data obtained from MDA-MB-231 cells with stable BCAR3 knockdown relative to vector-control cells cultured on plastic, the 711 genes found to overlap between culture conditions were mapped to the KEGG focal adhesion pathway using the “pathview” package in R. (B) The same approach was applied using differential gene expression data obtained from cells cultured in 3D matrigel to map the 711 genes that overlapped.



**Figure 4-6. BCAR3-dependent differentially expressed genes that overlap between MDA-MB-231 cells cultured on plastic or matrigel map to molecules involved in cell adhesion.** (A) Using differential gene expression data obtained from MDA-MB-231 cells with stable BCAR3 knockdown relative to vector-control cells cultured on plastic, the 711 genes found to overlap between culture conditions were mapped to KEGG cell adhesion molecules using the “pathview” package in R. (B) The same approach was applied using differential gene expression data obtained from cells cultured in 3D matrigel to map the 711 genes that overlapped.

Previously, we found that BCAR3 expression is required for budding of mouse mammary epithelial organoids in response to growth factors (**Chapter 2**). Based on this evidence, we sought to understand the transcriptional networks regulated by BCAR3 in normal mouse mammary epithelial cells that could potentially enable these responses. Primary organoids were generated using epithelial cells isolated from mammary glands obtained from wildtype (WT) and BCAR3 knockout (B3KO) mice. Epithelial cells were suspended in 3D matrigel to establish primary mammary organoids and treated for seven days with FGF2; this has been shown to induce budding in WT but not B3KO organoids (see **Chapter 2**) [172,180]. After seven days in culture, organoids were harvested, mRNA was extracted, RNA sequencing was performed, and differential gene expression was obtained. Using the “EnhancedVolcano” package in R, differentially expressed genes as a function of BCAR3 expression were analyzed (Figure 4-7A). A total of 524 protein-coding genes were found to be significantly altered ( $p_{adj} \leq 0.05$ ) with 245 genes downregulated ( $\log_2\text{FoldChange} < 0$ ) and 279 genes upregulated ( $\log_2\text{FoldChange} > 0$ ) as a function of BCAR3 expression (Figure 4-7A; blue colored genes and red colored genes respectively, a  $\log_2\text{FoldChange}$  cutoff of  $\leq -0.5$  and  $\geq 0.5$  was applied for clarity). Gene expression of a subset of significantly altered genes was then measured using RT-PCR to validate the RNASeq data, and some genes were found to be consistent with the RNASeq data (e.g., *TMPRSS11A*) while others were not (e.g., *ENO1B*) (Figure 4-7B). To understand how signaling in normal epithelial cells influences tumorigenesis, human homologs of mouse genes were identified, and 505 genes were found to be significantly

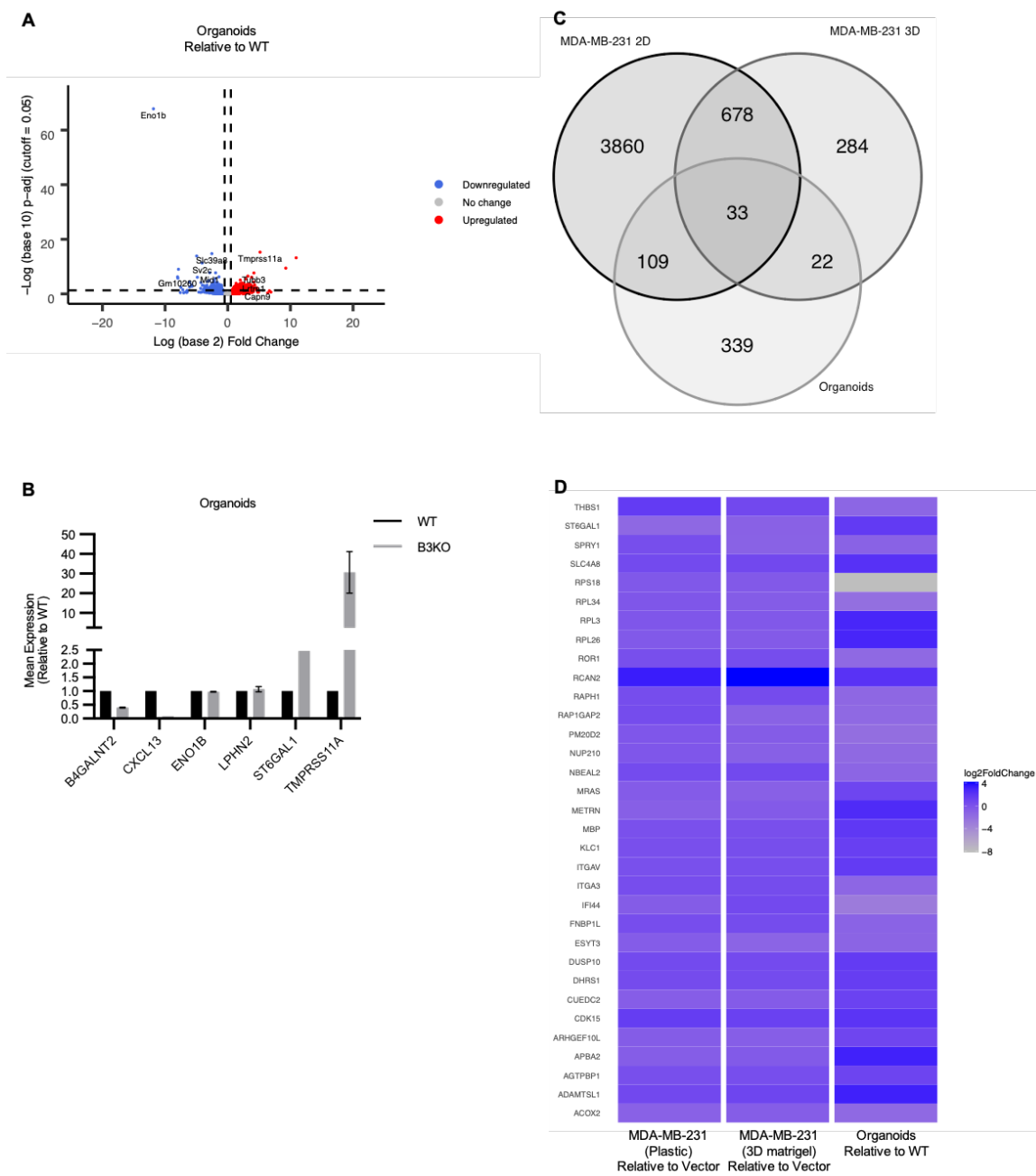


**Figure 4-7. Identification of differentially expressed genes in mouse mammary organoids as a function of BCAR3 expression.**

(A) Protein coding genes obtained from the differential gene expression analysis of epithelial cells derived from BCAR3 KO mouse mammary organoids relative to WT mouse organoids were visualized using the “EnhancedVolcano” package in R. For clarity, genes were marked as downregulated (blue color) if their Log2foldchange was  $< -0.5$ , no change (gray) if Log2foldchange was  $\geq -0.5$  and  $\leq 0.5$ , and upregulated (red color) if Log2foldchange was  $> 0.5$ . Only significantly altered genes ( $p_{adj} \geq 0.05$ ) were colored. (B) Quantitative real-time PCR analysis of B4GALNT2, CXCL13, ENO1B, LPHN2, ST6GAL1, and TMPRSS11A transcript levels in mouse mammary organoids generated from WT mice or BCAR3 KO mice. RT-PCR was conducted with technical duplicates for 1-2 independent experiments. Data shown are from one experiment or from the average  $\pm$  SEM of two biological replicates. (C) Overlap of protein coding genes between TNBC cells and mouse mammary organoids was visualized using the “VennDiagram” package in R. Only genes significantly altered ( $p_{adj} \leq 0.05$ ) were visualized. (D) Gene expression of overlapping genes between the three conditions was analyzed using the “geom\_tile” function in R. Blue color indicates high expression and gray color indicates low expression. Panel B was provided by Ryan Chipman.

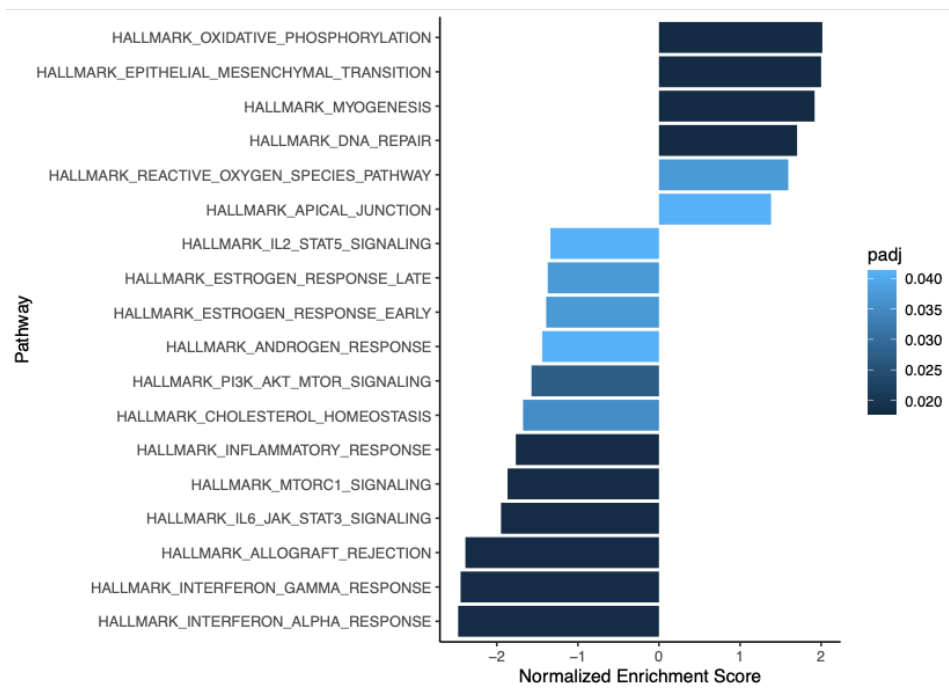
altered ( $\text{padj} \leq 0.05$ ). The “VennDiagram” package in R was used to compare protein-coding genes significantly altered in organoids with BCAR3 knockout with genes altered in TNBC cell lines with reduced BCAR3 expression. This analysis revealed that 33 genes overlapped between all three conditions (Figure 4-7C). Heatmap analysis of these 33 genes showed that a subset of genes that were altered as a function of BCAR3 exhibited transcriptional differences in similar directions (e.g., ACOX2, ESYT3, CDK15, RCAN2) while others were altered in opposing directions (e.g., METRN, ST6GAL1, CUEDC2) or in similar directions but to different extents (e.g., RPS18) (Figure 4-7D). Together, these data suggest that BCAR3 engages some transcriptional programs that are common to all three conditions but that others are unique depending on the culture conditions.

#### **4.4.5 BCAR3-regulated pathways in mouse mammary organoids may drive cell growth**

To identify potential regulatory pathways impacted by BCAR3 in mammary organoids, gene set enrichment analysis was performed using the “fgsea” package in R using the human homologs of differentially expressed genes in organoids with BCAR3 knockout. The top five pathways with significantly elevated enrichment in cells with BCAR3 knockout are pathways involved in the oxidative phosphorylation, epithelial-to-mesenchymal transition, myogenesis, DNA repair, and reactive oxygen species (Figure 4-8A). The top five pathways with significantly reduced

A

Organoids  
Relative to WT



B

JAK-STAT Signaling

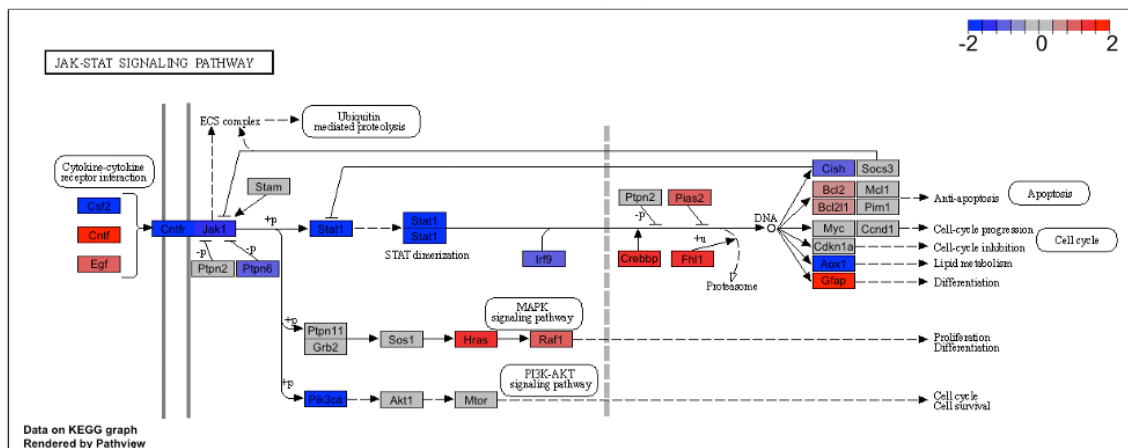


**Figure 4-8. Pathway enrichment in mouse mammary organoids with BCAR3 knockout.** (A) Differentially expressed genes in mouse mammary organoids generated from BCAR3 KO mice relative to organoids generated from WT mice were used for pathway enrichment analysis using the “fgsea” package in R. Enrichment analysis was performed based on the Hallmark gene set using 1000 permutations. Only pathways that were significantly enriched were visualized ( $p_{adj} \leq 0.05$ ). (B) Pathway enrichment analysis using the “pathview” package in R was performed to map the differentially expressed genes described above to the KEGG JAK-STAT signaling pathway.

enrichment are pathways involved in the interferon alpha response, the interferon gamma response, allograft rejection, IL6-JAK-STAT3 signaling, and MTORC1 signaling. As proof of principle, we mapped BCAR3-regulated genes within the KEGG JAK-STAT signaling pathway using the “pathview” package in R. Interestingly, some genes mapping to the JAK-STAT pathway were upregulated while others were downregulated in BCAR3 KO organoids (Figure 4-8B). Of note, JAK1 and STAT1 were highly downregulated consistent with the reduced enrichment of JAK-STAT signaling previously observed. Together, these data support a role for BCAR3 in regulating transcriptional networks in normal mammary glands that enable cell growth during mammary gland branching morphogenesis.

#### **4.5 Discussion**

BCAR3 has been implicated in driving cell growth, migration, and invasion by regulating a variety of processes, including MET receptor signaling and focal adhesion turnover (**Chapter 2** and [125]). Despite extensive data supporting a role for BCAR3 in these cellular functions, however, the transcriptional networks regulated by BCAR3 have never been explored. In this chapter, we used RNA sequencing and computational approaches to identify the differentially expressed genes and enriched pathways regulated by BCAR3 in human TNBC cells and normal mouse mammary epithelial cells. We show that BCAR3 engages pathways involved in cell growth and adhesion in TNBC cells, and that physical and/or molecular elements within the local microenvironment coordinate with BCAR3 in

generating a transcriptional program. The adaptor molecule Cas, which binds to and co-localizes with BCAR3 in focal adhesions [125,126], has mechanosensory functions that contribute to adhesion and motility [205]. It will be interesting to determine whether BCAR3 coordinates with Cas in this process to regulate gene expression in response to mechanical signals from the local environment. Our data show that BCAR3 also engages cell growth pathways in proliferating mammary epithelial cells, and a small subset of genes impacted by BCAR3 depletion in these cells overlap with those in TNBC.

While the data presented in this work provide insight into the transcriptional landscape regulated by BCAR3 in TNBC cells cultured in plastic, 3D matrigel and in organoids, this study is limited by the techniques utilized for analysis. This study focused predominantly on using computational approaches to visualize differentially expressed genes and pathways enriched as a function of BCAR3 expression and additional functional assays are needed to test if any of the changes observed are biologically relevant. In order to determine if the identified pathways contribute to TNBC initiation, growth and progression, biochemical approaches must first be used including validation of gene expression of target genes within pathways of interest using RT-PCR analysis and immunoblot analysis to measure total protein and phosphorylated protein expression. Cell growth, migration, and invasion must also be assessed in response to changes in pathways of interest to determine their role in TNBC tumorigenesis.

Though this study had limitations, our data together, demonstrate the range of pathways regulated by BCAR3 that can be explored to identify new therapeutic

targets. Future studies focused on identifying the transcriptional networks regulated by BCAR3 in both normal and malignant settings will shed light on the deregulated cell growth and survival pathways that drive tumorigenesis. Furthermore, exploring the potential role of BCAR3 in integrating mechanosensory signals from the extracellular environment can contribute to our understanding of the reported risks associated with increased breast tissue density and breast cancer progression [206–208].

## **Chapter 5: Perspectives**

Breast cancer is the leading cancer for newly diagnosed cancers and the second cause of cancer-related deaths among women [1]. As stated in **Chapter 1**, the lifetime likelihood of a woman developing invasive breast cancer is 13%. Compared to the other subsets of breast cancer, triple-negative breast cancer (TNBC) is associated with worse outcomes, affects younger patients, and is more prevalent among African American women [7,76,77]. Currently, the standard-of-care for patients with TNBC is cytotoxic chemotherapy, underscoring the importance of understanding the mechanisms that drive proliferation, migration, and invasion to identify novel therapeutic targets.

The work presented in this thesis focuses on understanding the role of BCAR3 in TNBC growth and progression. BCAR3 is an adaptor molecule that has been implicated in regulating TNBC cell adhesion, migration, and invasion [125]. Together BCAR3 and the adaptor molecule Cas have been shown to regulate Src kinase activity, cell adhesion, invasion, proliferation, and activation of the GTPase Rac1 [125–127,160,161,166]. Using publicly available data obtained from TNBC patients, we showed in **Chapter 2** that BCAR3 mRNA expression strongly correlated with the MET receptor signaling gene set. We also showed that functional interaction between BCAR3 and MET contributed to TNBC cell proliferation and migration. Interestingly, our observations suggest that BCAR3-MET coupling may be mediated through distinct mechanisms depending on the

genetic background of TNBC. This notion is further supported by data presented in **Chapter 3** showing that BCAR3 differentially regulates MET receptor protein expression in basal-like TNBC cells compared to claudin-low cells. Finally, preliminary differential gene expression analysis obtained using RNAseq data from TNBC cultured on plastic or in matrigel as well as mouse mammary gland organoids showed that enrichment of pathways that promote cell growth were reduced under conditions of BCAR3 depletion or knockout. Furthermore, BCAR3-dependent changes in gene expression and pathway enrichment were influenced by the extracellular microenvironment in TNBC. Together, these findings prompt important questions regarding 1) the functional role of BCAR3 in the regulation of receptor tyrosine kinase signaling and aggressive TNBC phenotypes, 2) the role of BCAR3 as a regulator of the early transition to invasive disease, 3) the role of BCAR3 as an integrator of signals from the extracellular matrix (ECM), and 4) BCAR3 as a biomarker and/or therapeutic target for TNBC.

## **5.1 BCAR3-MET dependent regulation of aggressive phenotypes in TNBC**

### **5.1.1 How does BCAR3 regulate MET signaling in claudin-low TNBC?**

The data presented in **Chapter 2** are the first to show that 1) BCAR3 establishes an autocrine signaling loop with the MET ligand, HGF, that promotes cell proliferation and migration in Hs578T cells and that 2) BCAR3 differentially regulates MET signaling depending on the molecular profile of TNBC cells. Despite this evidence, however, the mechanisms by which BCAR3 promotes formation of

autocrine signaling involving MET in Hs578T cells as well as MET activation/phosphorylation in MDA-MB-231 cells are not known.

Numerous reports have shown that adaptors play an important role in receptor tyrosine kinase downstream signaling. Data presented in **Chapter 2** and reports by Cross *et al.* show that TNBC cells with endogenous BCAR3 expression or with BCAR3 knockdown expressing high levels of ectopic BCAR3 exhibit increased cell accumulation, migration, and invasion in 3D matrigel [125]. Recent studies have uncovered a new phospho-tyrosine site (phospho-Tyr117) in BCAR3 that was found not only to be responsible for BCAR3 turnover, but together with the SH2 domain, an important contributor to Cas and Src activation [128]. The kinase responsible for phosphorylation of Tyr117 is currently not known. Since BCAR3 protein levels were impacted by MET-HGF signaling, and BCAR3-MET coupling contributed to cell proliferation and migration (**Chapter 2**), it is interesting to speculate that phosphorylation of Tyr117 may be regulated by MET. This can be tested by measuring Tyr117 phosphorylation following HGF treatment in the presence or absence of the MET inhibitor foretinib. If phosphorylation of this residue is dependent on MET (either directly or indirectly), we would expect it to be increased following stimulation with HGF and reduced with the addition of foretinib. Phosphorylation of Tyr117 on BCAR3 may in turn be required for establishing autocrine signaling in Hs578T cells and/or for MET phosphorylation in MDA-MB-231 and Hs578T cells. If this is the case, we would anticipate that cells with BCAR3 knockdown expressing an ectopic BCAR3 Tyr117 substitution (Tyr-to-Phe) would have the same phenotype as cells with BCAR3 knockdown. Since

this phosphorylation site was also shown to be critical for activation of Cas and Src by BCAR3, it would also be interesting to explore if the interaction between BCAR3 and Cas is important for HGF expression in Hs578T and/or MET phosphorylation in MDA-MB-231 cells and Hs578T cells. To test this, cells with stable BCAR3 knockdown expressing an ectopic BCAR3-Cas binding mutant (L744E/R748E) could be used. If interaction of BCAR3 and Cas is required for the regulation of HGF gene expression in Hs578T cells and/or for MET phosphorylation in MDA-MB-231 cells and Hs578T cells, then we would anticipate that abrogation of this interaction would elicit the same effects observed with BCAR3 knockdown. Together, these studies could help to inform how BCAR3-MET promote the aggressive phenotypes observed in claudin-low TNBC.

### **5.1.2 How does BCAR3 regulate MET expression in basal-like TNBC?**

Regulation of MET signaling by BCAR3 is further supported by data presented in **Chapter 3**. The mechanism by which BCAR3 modulates MET expression is not known but the preliminary evidence suggests the regulation may occur post-transcriptionally. Studies show that the MET receptor is negatively regulated by the E3 ubiquitin-protein ligase Cbl and this regulation requires Grb2 recruitment to the MET receptor, Grb2 interaction with Cbl, and Cbl interaction with a juxtamembrane tyrosine (Tyr1003) residue in the MET receptor [106]. Studies have also shown that Src can regulate Cbl protein stability by phosphorylating Cbl at tyrosine residues, promoting its subsequent ubiquitination and degradation [209]. Since BCAR3 regulates Src through interaction with the adaptor Cas, then

it is reasonable to postulate that Cbl may be regulated by the BCAR3-Cas-Src complex leading to changes in MET protein stability. However, our preliminary observations show that cells with reduced BCAR3 expression exhibit elevated MET protein levels, arguing against Src-mediated degradation of Cbl and MET protein stability in the presence of BCAR3. Instead, BCAR3 may function like Grb2 to promote interaction of Cbl with the MET receptor. Immunoprecipitation can be used to test Cbl binding to MET receptor in cells with vector-control and cells with BCAR3 knockdown. If BCAR3 is required for recruitment of Cbl to the MET receptor, then cells with reduced BCAR3 expression would have reduced binding of Cbl compared to cells with endogenous BCAR3 expression. Together, these studies could help uncover a novel mechanism by which the MET receptor levels are regulated.

### **5.1.3 Does BCAR3-MET coupling serve as a molecular switch of aggressive phenotypes in basal-like TNBC?**

The data presented in **Chapter 3** showed reciprocal modulation of protein expression for MET and BCAR3 in HCC1937, MDA-MB-468, and HCC1187 cells. In contrast, claudin-low cells such as BT549, MDA-MB-436, MDA-MB-231, and Hs578T cells did not exhibit similar reciprocal expression patterns of MET and BCAR3 (Figures 3-7 and 3-8). We hypothesize from these data that BCAR3 may serve as an inhibitor of MET expression to suppress aggressive phenotypes in basal-like TNBC. This would be opposite to what is seen in claudin-low cells, where BCAR3 is pro-oncogenic. To test if BCAR3 expression suppresses

aggressive phenotypes in basal-like cells, cell growth, migration, and invasion must be measured as a function of BCAR3 expression. If BCAR3 suppresses these behaviors, then we would anticipate cells with reduced BCAR3 expression to exhibit enhancement of the phenotypes stated above. If the effects require MET phosphorylation, then we would anticipate that any enhancement observed in cells with reduced BCAR3 expression would be attenuated following MET inhibition with foretinib. Understanding how BCAR3 elicits these differential effects depending on the genetic makeup of the cells is critical when considering the potential effects of targeted therapy as well as mechanisms involved in chemotherapeutic drug resistance.

#### **5.1.4 What are the implications of changes in MET phosphorylation?**

**Chapter 3** showed that cells with reduced BCAR3 expression exhibited increased MET receptor protein expression and phosphorylation. This leads to the question of whether MET catalytic activity is similarly elevated. In our studies, MET phosphorylation was observed at Tyr1234/1235 residues, which are located within the intracellular kinase domain and positively regulate enzymatic activity. Activated MET activates downstream signaling cascades that include Ras/Raf/MAPK, STAT3, FAK, JNK, and AKT [97]. While our studies did not reveal substantial AKT activation, it could be that other downstream targets of MET are activated. If the phosphorylation of MET observed in cells with reduced BCAR3 expression (**Chapter 3**) increases MET activation, then we would anticipate that cells with reduced BCAR3 expression would exhibit elevated phosphorylation of

Ras/Raf/MAPK, STAT3, FAK, and/or JNK and these effects would be abrogated following MET inhibition with foretinib.

The data presented in **Chapter 3** also led us to question how BCAR3 regulates MET phosphorylation. As stated in **Chapter 1**, BCAR3 has been reported to bind to the protein tyrosine phosphatase  $\alpha$  (PTP $\alpha$ ), and this interaction was found to help recruit BCAR3 and Cas to cell adhesions [122]. Studies by Sangwan *et al.*, showed that MET receptor dephosphorylation precedes degradation following HGF stimulation and cells with depletion of the non-receptor protein-tyrosine phosphatases PTP1B or T-cell protein tyrosine phosphatase (TCPTP) exhibited hyper-phosphorylation of the MET receptor after stimulation [107]. Further, these studies showed that phosphorylation at Tyr1234/1235 on MET is required for receptor interaction with PTP1B and TCPTP. To test whether decreased phosphatase activity accounts for the increased phosphorylation of MET on Tyr1234/1235 observed in basal-like cells with depleted for BCAR3, experiments like those described in **Chapter 3** can be performed in the presence or absence of phosphatase inhibitors. If phosphatases are involved, then MET expression should increase with phosphatase inhibition under conditions of endogenous BCAR3 expression and MET expression under conditions of BCAR3 knockdown should not change. It is also possible, that BCAR3 expression facilitates the binding of phosphatases like PTP $\alpha$  to the MET receptor in basal-like cells, preventing MET hyper-phosphorylation. To test this, binding of phosphatases (PTP $\alpha$ , PTPB1, or TCPTP) to the MET receptor can be measured in the previously described cells in the presence or absence of BCAR3 expression

following HGF stimulation. If BCAR3 is required for the binding of the described phosphatases, then we would anticipate reduced phosphatase binding under conditions of reduced BCAR3 expression. Together, these studies could inform if BCAR3 has a role in regulating phosphatases that control MET phosphorylation, activity, and turnover.

## **5.2 Molecular functions of BCAR3 in regulating the transition to invasive breast cancer**

The data presented in **Chapter 2** show that BCAR3 expression is elevated in ductal carcinoma *in situ* (DCIS) and invasive carcinoma compared to normal mammary breast tissue (Figure 2-1A). In light of the pro-invasive phenotype associated with BCAR3, it was somewhat surprising that BCAR3 was found to be elevated to a greater extent in ductal carcinoma *in situ* (DCIS) compared to invasive carcinoma (Figure 2-1A). Based on these and other data showing poor outcomes associated with high BCAR3 expression in patients with TNBC, we hypothesize that BCAR3 may play a role in the transition to invasive disease. The significant heterogeneity in BCAR3 expression within individual tumor samples obtained from breast cancer patients of multiple subtypes provides further support for this hypothesis.

### **5.2.1 What is the role of BCAR3 in early-stage breast cancer?**

Changes in the stroma that surrounds pre-neoplastic lesions have been implicated in the transition of DCIS to IDC and progression of invasive disease

[210,211]. Some of the changes include the accumulation of fibroblasts that can secrete matrix metalloproteinases (MMPs) and various growth factors, as well as accumulation of immune components that can potentiate the activity of tumor-associated fibroblasts. One such growth factor is HGF, which is secreted by fibroblasts and is a strong inducer of cell growth, migration, and invasion in epithelial cells [100–102]. Studies by Jedeszko *et al.*, showed that HGF/MET signaling is important in the transition of DCIS to IDC [212]. Interestingly, the studies in **Chapter 3** showed that basal-like HCC1937 and MD-MB-468 cells have elevated levels of BCAR3 protein expression following long-term HGF treatment (Figures 3-4 and 3-5). It could be that HGF stimulation induces BCAR3 expression as a component of signaling networks that drive cell migration and invasion. This could be tested using co-culture (*in vitro*) and co-injection (*in vivo*) approaches that include basal-like TNBC cells and HGF-secreting mammary fibroblasts; similar experiments have shown that the invasiveness of MCF10.DCIS cells increase under these conditions [212]. If BCAR3 is an important downstream target of MET activation, then an increase in BCAR3 levels would be expected in the presence of HGF-secreting fibroblasts. More importantly, if BCAR3 is required for the transition to invasive disease, then the HGF-secreting fibroblasts would be expected to enhance the invasiveness of the breast cancer cells expressing endogenous BCAR3 but not when BCAR3 is depleted. Since we observed that BCAR3-MET functional coupling is dependent on the genetic profile of the TNBC cell line, it would be interesting to test the full panel of TNBC cells used in **Chapter 3** in these co-culture/co-injection studies to determine whether similar or disparate

responses are observed in these assays depending on the nature of the cells. Together, these studies could help further our understanding of the processes involved in the transition from DCIS to IDC, providing insight into molecular strategies that could be used to prevent this transition from occurring.

### **5.2.2 Can BCAR3 serve as a prognostic tool?**

Breast cancer disease stage/severity is determined based on tumor size, lymph node infiltration, metastasis (TNM), and molecular biomarkers [13]. In addition, tumor histology is used to assess the tumor grade based on characteristics such as cell shape and size, nuclear morphology, mitotic count, and tubule formation [14]. The therapeutic approaches currently in use for treating DCIS are quite limited (see **Chapter 1**) and often resort to invasive procedures even though about 60% of lesions will not progress to invasive cancer [213].

We suggest that BCAR3 may be a valuable prognostic marker to include in breast cancer tumor staging based on its expression patterns, correlation with poor outcomes, and tumor-promoting functions reported in this thesis and elsewhere. Interestingly, elevated phosphorylated (active) MET and total MET protein levels have also been reported to correlate with a poor prognosis in patients with breast cancer [168]. Since the work presented in **Chapters 2 and 3** are strongly suggestive of BCAR3-MET coupling, we hypothesize that DCIS lesions with high BCAR3 expression may help identify patients who could benefit from neoadjuvant MET targeted therapy or HGF blocking antibodies (at least for claudin-low tumors where these molecules appear to function together). This can be tested

preclinically with the use of mouse xenografts. We would propose using MCF10.DCIS cells, which are a cell line that originated from a variant of the MCF10A cell line (MCF10AT) [214]. The original MCF10A cell line is characterized as ER-/PR-/HER2-, basal B (claudin-low) breast cancer [34]. When injected intraductally, MCF10.DCIS cells produce basal-like DCIS lesions that progress to invasive lesions [215]. Of course, it will first be necessary to determine whether these cells show similar BCAR3-dependent effects on MET signaling, proliferation and invasion using the *in vitro* approaches described throughout this thesis. If that is the case, we would then test cells with endogenous, reduced, and ectopically overexpressed BCAR3 for their ability to form DCIS lesions. We could also co-inject HGF-secreting mammary fibroblasts to gain insight into the potential role of BCAR3-MET in DCIS. If BCAR3 is required, then xenografts using MCF10.DCIS cells with reduced BCAR3 expression would exhibit attenuated invasiveness and ectopic BCAR3 overexpression would enhance invasive growth. Further, if BCAR3 is a valuable biomarker for patients with high grade DCIS lesions that may benefit from MET or HGF targeted therapy, then using MET inhibitors or HGF neutralizing antibodies would reduce invasive growth in cells with endogenous or overexpressed BCAR3 expression compared to cells with reduced BCAR3 expression. Together, these studies could increase the therapeutic options for patients with DCIS lesions.

### **5.3 Role of BCAR3 as an integrator of mechanical signals from the tumor microenvironment**

Increased mammographic density is one of the greatest risk factors for developing breast cancer independent of age and sex [206–208]. The extracellular matrix (ECM) is an important component of the tumor microenvironment; it can promote aggressive tumor phenotypes by engaging molecules involved in growth factor and adhesion signaling [134,194,195]. In addition to molecular factors and cellular components of the ECM, changes to the ECM rigidity can significantly alter migration, invasion, proliferation, and transcriptional programs of tumor cells. As mentioned in **Chapter 1**, the adaptor molecule Cas has been reported to serve as a force sensor that enables extracellular mechanical stress to be transduced into cellular signaling [133]. Despite numerous studies reporting that BCAR3 and Cas together are important for migration and invasion, the mechanosensing functions of BCAR3 have never been explored.

#### **5.3.1 Can BCAR3 contribute to the cellular responses to mechanosensory stimuli present in the tumor microenvironment?**

The preliminary data presented in **Chapter 4** show that the BCAR3-dependent changes in gene regulation are impacted by culture conditions, suggesting that BCAR3 may have a role in integrating signals from the ECM. To test whether this is the case, TNBC cell lines with endogenous, depleted, or overexpressed BCAR3 can be used to measure cell growth, migration, and invasion under conditions of increasing matrix rigidity. If BCAR3 integrates signals

from the ECM, then cells with endogenous BCAR3 expression or with stable BCAR3 knockdown expressing ectopic BCAR3 would be expected to exhibit increased cell growth, migration, and invasion as matrix rigidity increased compared to cells with reduced BCAR3 expression. If a phenotype is observed, the next step would be to determine whether BCAR3-Cas interactions are required using cells with stable BCAR3 knockdown engineered to express the Cas binding mutation of BCAR3 (BCAR3 L744E/R748E). Further exploration of the pathways shown in **Chapter 4** to be altered in a BCAR3-dependent manner when cultured only on plastic or only in matrigel could help identify the different engaged by BCAR3.

### **5.3.2 Is BCAR3 a functional regulator of the mammary circadian clock?**

Recently, efforts have been made to understand the role of the mammary circadian clock in breast cancer development. This interest stems from studies reporting that women with 20 years or more of night shift work had a significantly higher risk of breast cancer compared to women with no years of shift work [216]. A study by Yang *et al.*, used circadian time-series microarrays to identify genes rhythmically altered in normal mouse mammary tissues isolated at 4hr intervals for 2 circadian cycles (total 48hrs) [217]. Interestingly, BCAR3 was among the genes found to be altered rhythmically. These investigators showed that genes with functional roles in the circadian clock were important for mammary stem cell function, that molecules involved in cell adhesion and cytoskeletal signals are required for the regulation of the circadian clock, and that the mammary clock is

sensitive to matrix stiffness. While mice with a global knockout of BCAR3 do not show any gross defects in mammary gland development, we found that BCAR3 is required for budding of mammary epithelial cell organoids in response to FGF2 and TGF $\alpha$  (**Chapter 2**). Taken together, these data point to a potential role of BCAR3 in regulation of the mammary circadian clock. It would be interesting to explore this possibility further by testing the expression of circadian genes such as Clock, Bmal1, Per1, Per2, and Cry as a function of BCAR3 expression in mouse mammary organoids harvested at 4hr intervals for 2 circadian cycles (total 48hrs). BCAR3 wild-type and BCAR3 knockout mice expressing the Per2::LUC reporter could be generated and mammary organoids or tissue explants obtained from these mice could be used to measure the amplitude of the circadian rhythm as a function of BCAR3 expression. Together, these studies could help identify the role of BCAR3 in mammary gland biology and could further our understanding of the mechanisms that drive breast cancer initiation.

#### **5.4 Potential role of BCAR3 as a biomarker for targeted therapy and/or a therapeutic target in breast cancer**

Current strategies to identify patient cohorts that could benefit from targeted therapy remain limited. Clinical trials such as the study by Carey *et al.* that showed no benefit to anti-EGFR treatment with cetuximab in combination with carboplatin in TNBC patients with metastatic disease underscore the importance of further subtyping TNBC tumors based on their genetic profiles to improve treatment strategies [90]. The reports mentioned above highlight the involvement of BCAR3

in many aspects of TNBC growth and progression, suggesting that BCAR3 may serve as a valuable biomarker and/or therapeutic target for patients with TNBC.

#### **5.4.1 Can BCAR3 serve as a biomarker to identify breast cancer patients for targeted therapy?**

Because of the prominent role played by phosphoproteins in signaling pathways that regulate cell/tumor growth, survival and invasion, they are conceptually appealing as potential biomarkers. However, various aspects of tissue collection and immunochemical (IHC) staining make these proteins/epitopes challenging to detect [218]. Some of these challenges include phosphorylation stability during surgical processing, tissue ischemia that could occur from excision to processing resulting in altered phospho-proteins, preservation of phosphorylated proteins during processing for immunohistochemistry (IHC), differences in phospho-protein levels observed between tissues that underwent snap-freezing or formalin-fixing, and difficulty in establishing valuable phospho-protein quantification. Given that BCAR3-Cas is a regulator of Src kinase activity and that BCAR3 is readily detected by IHC, BCAR3 could serve as a biomarker to identify patients that may benefit from Src inhibitors. Interestingly, Lehmann *et al.* showed that some of the claudin-low (mesenchymal-like) and basal-like cell lines that have high BCAR3 expression (MDA-MB-231, Hs578T, HCC1937, BT549, and MDA-MB-436) exhibit increased sensitivity to Src inhibition with dasatinib [75].

In addition to Src, our studies using claudin-low TNBC cells suggest that BCAR3 could serve as a biomarker to identify patients who could benefit from MET

receptor inhibitors, MET receptor blocking antibodies, or HGF neutralizing antibodies. *In vitro* drug sensitivity assays measuring cell growth using cell lines engineered to have endogenous BCAR3 (vector-control), stable BCAR3 knockdown, or stable BCAR3 knockdown with ectopic BCAR3 expression can be used to test the sensitivity of cells to the inhibitors mentioned above as a function of BCAR3 expression. If BCAR3 serves as a marker of drug sensitivity, then we would anticipate that cells with endogenous or overexpressed BCAR3 would exhibit increased sensitivity to inhibitors compared to untreated cells. If the molecules function in the same pathway as BCAR3, cells with reduced BCAR3 expression would not be expected to exhibit any augmented effects following drug treatment. On the other hand, based on the observations made in **Chapter 3**, it could be that in the setting of basal-like TNBC BCAR3 may serve as a marker of resistance to MET inhibition. In this case we would anticipate that cells with endogenous or overexpressed BCAR3 would exhibit reduced sensitivity to inhibitors. Together, these *in vitro* assays could provide further rationale for the use of BCAR3 as a biomarker.

#### **5.4.2 Can BCAR3 serve as a therapeutic target?**

The work in this thesis highlights the role of BCAR3 is an important driver of TNBC tumor growth using *in vivo* and *in vitro* techniques. Together the data suggest that BCAR3 may be a therapeutic target for at least a subset of patients with TNBC. Moreover, the fact that a global BCAR3 knock-out does not elicit serious deleterious effects during mouse development other than formation of

spontaneous cataracts suggests that toxicity of BCAR3 inhibition may be minimal [120]. As stated in **Chapter 1**, the SH2 domain of BCAR3 has been reported to bind to EGFR, PTP $\alpha$ , HER3, and LLGL2 while the C-terminus binds to Cas [118,121–123]. These interactions suggest that inhibiting one or more of these protein-protein interactions may be a useful therapeutic strategy. While blocking protein-protein interactions has been historically challenging therapeutically, several approaches have recently been shown to be effective. These include targeting covalent interactions by blocking the amino acid side chains located within the binding site, targeting protein-protein binding “hot-spots”, and targeting molecular fragments within the binding interface [219,220]. To block BCAR3 functions, we would propose starting by blocking the known BCAR3-Cas interaction. Studies by Mace *et al.*, analyzing the crystal structure of BCAR3 found that Cdc25-homology domain located within the C-terminal domain is composed of helices that fold and employ a closed conformation due to hydrophobic interactions, rendering the domain catalytically inactive. Their group also found that the novel SH2-containing protein (NSP) family of adaptor molecules (of which BCAR3 is a member) and Cas have preserved residues within their C-terminal domains that are important for their interaction. The residues on BCAR3 found to be important for BCAR3-Cas binding were Leu744 and Arg748 [118]. Since BCAR3 does not have enzymatic activity, small molecule mimics that bind to these residues could potentially be useful in blocking BCAR3-Cas association and in so doing, prevent activation of downstream signaling. To test the effectiveness of the inhibitor, the previously described proliferation, migration, and invasion *in vitro*

assays could be used. If BCAR3-Cas interactions are required for these behaviors, then we would anticipate a decrease in all three activities following treatment with inhibitor, similar to the effects observed with BCAR3 knockdown. The recent findings that BCAR3 phosphorylation at Tyr117, located near the SH2 domain, is required for BCAR3-dependent activation of Cas reveals an additional potential site to target with inhibitors that would disrupt the BCAR3-Cas interaction, reducing Src activation, proliferation, migration, and invasion. Finally, peptides that block the functionality of the SH2 domain could prove efficacious in inhibiting binding of BCAR3 to the SH2 ligands described above.

BCAR3 could also be targeted using small interfering RNA (siRNA) *in vivo*. Recent advances have improved the specificity, stability, and safety of these molecules for clinical use. For example, modifications such as substitutions to the 2'-OH group, phosphonate modifications, ribose modifications, and base modifications have been shown to reduce immunogenicity, increase longevity and target affinity, and increase stability of siRNA molecules. In addition, advancements in the drug delivery mechanisms for siRNAs have significantly improved with the use of lipids, lipid-like materials, polymers, peptides, among others [221]. Depletion of BCAR3 with targeted siRNA could help 1) reduce tumor growth in patients as we observed in our *in vitro* and *in vivo* studies and/or 2) prevent the development of invasive lesions.

## **5.5 Final conclusions**

The work in this thesis provides insight into the molecular functions of BCAR3 and its role in driving TNBC tumor growth. Novel techniques including epithelial mouse mammary organoids and computational approaches were used to help identify the functional roles of BCAR3 and how this relates to MET receptor signaling. These data open exciting new directions regarding how BCAR3 regulates receptor tyrosine kinase signaling, how BCAR3 is involved in the transition to invasive disease, and whether BCAR3 is involved in integrating signals from the tumor microenvironment, among others. Together, this work expands our understanding of novel functional roles of BCAR3 in TNBC growth and progression and provides avenues for potential clinical applications that could be used to improve the care of patients with TNBC.

## **References**

1. Siegel, R.L., Miller, K.D., Fuchs, H.E., and Jemal, A. (2021) Cancer Statistics, 2021. *CA: A Cancer Journal for Clinicians*, **71** (1), 7–33.
2. Pfeiffer, R.M., Webb-Vargas, Y., Wheeler, W., and Gail, M.H. (2018) Proportion of U.S. Trends in Breast Cancer Incidence Attributable to Long-term Changes in Risk Factor Distributions. *Cancer Epidemiol Biomarkers Prev*, **27** (10), 1214–1222.
3. Tung, N., Lin, N.U., Kidd, J., Allen, B.A., Singh, N., Wenstrup, R.J., Hartman, A.-R., Winer, E.P., and Garber, J.E. (2016) Frequency of Germline Mutations in 25 Cancer Susceptibility Genes in a Sequential Series of Patients With Breast Cancer. *J Clin Oncol*, **34** (13), 1460–1468.
4. Anderson, W.F., Jatoi, I., Tse, J., and Rosenberg, P.S. (2009) Male Breast Cancer: A Population-Based Comparison With Female Breast Cancer. *Journal of Clinical Oncology*.
5. Street, W. Breast Cancer Facts & Figures 2019-2020. 44.
6. Ford, D., Easton, D.F., Stratton, M., Narod, S., Goldgar, D., Devilee, P., Bishop, D.T., Weber, B., Lenoir, G., Chang-Claude, J., Sobol, H., Teare, M.D., Struwing, J., Arason, A., Scherneck, S., Peto, J., Rebbeck, T.R., Tonin, P., Neuhausen, S., Barkardottir, R., Eyfjord, J., Lynch, H., Ponder, B. a. J., Gayther, S.A., Birch, J.M., Lindblom, A., Stoppa-Lyonnet, D., Bignon, Y., Borg, A., Hamann, U., Haites, N., Scott, R.J., Maugard, C.M., Vasen, H., Seitz, S., Cannon-Albright, L.A., Schofield, A., and Zelada-Hedman, M. (1998) Genetic Heterogeneity and Penetrance Analysis of the BRCA1 and BRCA2 Genes in Breast Cancer Families. *The American Journal of Human Genetics*, **62** (3), 676–689.
7. Howlader, N., Cronin, K.A., Kurian, A.W., and Andridge, R. (2018) Differences in Breast Cancer Survival by Molecular Subtypes in the United States. *Cancer Epidemiol Biomarkers Prev*, **27** (6), 619–626.
8. (1930) Cancer Facts & Figures 2021. 72.
9. Bradley, C.J., Given, C.W., and Roberts, C. (2002) Race, Socioeconomic Status, and Breast Cancer Treatment and Survival. *JNCI: Journal of the National Cancer Institute*, **94** (7), 490–496.
10. Joslyn, S.A., and West, M.M. (2000) Racial differences in breast carcinoma survival. *Cancer*, **88** (1), 114–123.

11. Beckmann, M.W., Niederacher, D., Schnürch, H.-G., Gusterson, B.A., and Bender, H.G. (1997) Multistep carcinogenesis of breast cancer and tumour heterogeneity. *J Mol Med*, **75** (6), 429–439.
12. Bombonati, A., and Sgroi, D.C. (2011) The molecular pathology of breast cancer progression. *J Pathol*, **223** (2), 307–317.
13. Giuliano, A.E., Edge, S.B., and Hortobagyi, G.N. (2018) Eighth Edition of the AJCC Cancer Staging Manual: Breast Cancer. *Ann Surg Oncol*, **25** (7), 1783–1785.
14. Rakha, E.A., Reis-Filho, J.S., Baehner, F., Dabbs, D.J., Decker, T., Eusebi, V., Fox, S.B., Ichihara, S., Jacquemier, J., Lakhani, S.R., Palacios, J., Richardson, A.L., Schnitt, S.J., Schmitt, F.C., Tan, P.-H., Tse, G.M., Badve, S., and Ellis, I.O. (2010) Breast cancer prognostic classification in the molecular era: the role of histological grade. *Breast Cancer Res*, **12** (4), 207.
15. Li, C.I., Anderson, B.O., Daling, J.R., and Moe, R.E. (2003) Trends in Incidence Rates of Invasive Lobular and Ductal Breast Carcinoma. *JAMA*, **289** (11), 1421–1424.
16. Chlebowski, R.T., Rohan, T.E., Manson, J.E., Aragaki, A.K., Kaunitz, A., Stefanick, M.L., Simon, M.S., Johnson, K.C., Wactawski-Wende, J., O'Sullivan, M.J., Adams-Campbell, L.L., Nassir, R., Lessin, L.S., and Prentice, R.L. (2015) Breast Cancer After Use of Estrogen Plus Progestin and Estrogen Alone: Analyses of Data From 2 Women's Health Initiative Randomized Clinical Trials. *JAMA Oncology*, **1** (3), 296–305.
17. Kumar, V., and Chambon, P. (1988) The estrogen receptor binds tightly to its responsive element as a ligand-induced homodimer. *Cell*, **55** (1), 145–156.
18. Kuiper, G.G.J.M., Carlsson, B., Grandien, K., Enmark, E., Häggblad, J., Nilsson, S., and Gustafsson, J.-Å. (1997) Comparison of the Ligand Binding Specificity and Transcript Tissue Distribution of Estrogen Receptors  $\alpha$  and  $\beta$ . *Endocrinology*, **138** (3), 863–870.
19. Huang, B., Omoto, Y., Iwase, H., Yamashita, H., Toyama, T., Coombes, R.C., Filipovic, A., Warner, M., and Gustafsson, J.-Å. (2014) Differential expression of estrogen receptor  $\alpha$ ,  $\beta$ 1, and  $\beta$ 2 in lobular and ductal breast cancer. *PNAS*, **111** (5), 1933–1938.
20. Hayashi, S.-I., Eguchi, H., Tanimoto, K., Yoshida, T., Omoto, Y., Inoue, A., Yoshida, N., and Yamaguchi, Y. (2003) The expression and function of estrogen receptor alpha and beta in human breast cancer and its clinical application. *Endocrine-Related Cancer*, **10** (2), 193–202.

21. Lydon, J.P., DeMayo, F.J., Funk, C.R., Mani, S.K., Hughes, A.R., Montgomery, C.A., Shyamala, G., Conneely, O.M., and O'Malley, B.W. (1995) Mice lacking progesterone receptor exhibit pleiotropic reproductive abnormalities. *Genes Dev*, **9** (18), 2266–2278.
22. Aupperlee, M.D., Smith, K.T., Kariagina, A., and Haslam, S.Z. (2005) Progesterone receptor isoforms A and B: temporal and spatial differences in expression during murine mammary gland development. *Endocrinology*, **146** (8), 3577–3588.
23. Mulac-Jericevic, B., Lydon, J.P., DeMayo, F.J., and Conneely, O.M. (2003) Defective mammary gland morphogenesis in mice lacking the progesterone receptor B isoform. *PNAS*, **100** (17), 9744–9749.
24. Mulac-Jericevic, B., Mullinax, R.A., DeMayo, F.J., Lydon, J.P., and Conneely, O.M. (2000) Subgroup of Reproductive Functions of Progesterone Mediated by Progesterone Receptor-B Isoform. *Science*, **289** (5485), 1751–1754.
25. Pollack, J.R., Perou, C.M., Alizadeh, A.A., Eisen, M.B., Pergamenschikov, A., Williams, C.F., Jeffrey, S.S., Botstein, D., and Brown, P.O. (1999) Genome-wide analysis of DNA copy-number changes using cDNA microarrays. *Nat Genet*, **23** (1), 41–46.
26. Pauletti, G., Godolphin, W., Press, M.F., and Slamon, D.J. (1996) Detection and quantitation of HER-2/neu gene amplification in human breast cancer archival material using fluorescence in situ hybridization. *Oncogene*, **13** (1), 63–72.
27. Meric-Bernstam, F., and Hung, M.-C. (2006) Advances in Targeting Human Epidermal Growth Factor Receptor-2 Signaling for Cancer Therapy. *Clin Cancer Res*, **12** (21), 6326–6330.
28. Bose, R., Molina, H., Patterson, A.S., Bitok, J.K., Periaswamy, B., Bader, J.S., Pandey, A., and Cole, P.A. (2006) Phosphoproteomic analysis of Her2/neu signaling and inhibition. *PNAS*, **103** (26), 9773–9778.
29. Tan, M., Yao, J., and Yu, D. (1997) Overexpression of the c-erbB-2 gene enhanced intrinsic metastasis potential in human breast cancer cells without increasing their transformation abilities. *Cancer Res*, **57** (6), 1199–1205.
30. Perou, C.M., Sørlie, T., Eisen, M.B., van de Rijn, M., Jeffrey, S.S., Rees, C.A., Pollack, J.R., Ross, D.T., Johnsen, H., Akslen, L.A., Fluge, Ø., Pergamenschikov, A., Williams, C., Zhu, S.X., Lønning, P.E., Børresen-Dale, A.-L., Brown, P.O., and Botstein, D. (2000) Molecular portraits of human breast tumours. *Nature*, **406** (6797), 747–752.

31. Sørli, T., Perou, C.M., Tibshirani, R., Aas, T., Geisler, S., Johnsen, H., Hastie, T., Eisen, M.B., Rijn, M. van de, Jeffrey, S.S., Thorsen, T., Quist, H., Matese, J.C., Brown, P.O., Botstein, D., Lønning, P.E., and Børresen-Dale, A.-L. (2001) Gene expression patterns of breast carcinomas distinguish tumor subclasses with clinical implications. *PNAS*, **98** (19), 10869–10874.
32. Parker, J.S., Mullins, M., Cheang, M.C.U., Leung, S., Voduc, D., Vickery, T., Davies, S., Fauron, C., He, X., Hu, Z., Quackenbush, J.F., Stijleman, I.J., Palazzo, J., Marron, J. s., Nobel, A.B., Mardis, E., Nielsen, T.O., Ellis, M.J., Perou, C.M., and Bernard, P.S. (2009) Supervised Risk Predictor of Breast Cancer Based on Intrinsic Subtypes. *JCO*, **27** (8), 1160–1167.
33. Prat, A., Parker, J.S., Karginova, O., Fan, C., Livasy, C., Herschkowitz, J.I., He, X., and Perou, C.M. (2010) Phenotypic and molecular characterization of the claudin-low intrinsic subtype of breast cancer. *Breast Cancer Research*, **12** (5), R68.
34. Neve, R.M., Chin, K., Fridlyand, J., Yeh, J., Baehner, F.L., Fevr, T., Clark, L., Bayani, N., Coppe, J.-P., Tong, F., Speed, T., Spellman, P.T., DeVries, S., Lapuk, A., Wang, N.J., Kuo, W.-L., Stilwell, J.L., Pinkel, D., Albertson, D.G., Waldman, F.M., McCormick, F., Dickson, R.B., Johnson, M.D., Lippman, M., Ethier, S., Gazdar, A., and Gray, J.W. (2006) A collection of breast cancer cell lines for the study of functionally distinct cancer subtypes. *Cancer Cell*, **10** (6), 515–527.
35. Polyak, K. (2007) Breast cancer: origins and evolution. *J Clin Invest*, **117** (11), 3155–3163.
36. Fiaschi, M., Rozell, B., Bergström, Å., Toftgård, R., and Kleman, M.I. (2007) Targeted Expression of GLI1 in the Mammary Gland Disrupts Pregnancy-induced Maturation and Causes Lactation Failure. *Journal of Biological Chemistry*, **282** (49), 36090–36101.
37. Jeng, K.-S., Sheen, I.-S., Jeng, W.-J., Yu, M.-C., Hsiao, H.-I., Chang, F.-Y., and Tsai, H.-H. (2013) Activation of the sonic hedgehog signaling pathway occurs in the CD133 positive cells of mouse liver cancer Hepa 1–6 cells. *Oncotargets Ther*, **6**, 1047–1055.
38. Huebner, R.J., and Ewald, A.J. (2014) Cellular foundations of mammary tubulogenesis. *Seminars in Cell & Developmental Biology*, **31**, 124–131.
39. Van Keymeulen, A., Rocha, A.S., Ousset, M., Beck, B., Bouvencourt, G., Rock, J., Sharma, N., Dekoninck, S., and Blanpain, C. (2011) Distinct stem cells contribute to mammary gland development and maintenance. *Nature*, **479** (7372), 189–193.

40. Al-Hajj, M., Wicha, M.S., Benito-Hernandez, A., Morrison, S.J., and Clarke, M.F. (2003) Prospective identification of tumorigenic breast cancer cells. *PNAS*, **100** (7), 3983–3988.
41. Sgroi, D.C. (2010) Preinvasive Breast Cancer. *Annual Review of Pathology: Mechanisms of Disease*, **5** (1), 193–221.
42. Molyneux, G., Geyer, F.C., Magnay, F.-A., McCarthy, A., Kendrick, H., Natrajan, R., MacKay, A., Grigoriadis, A., Tutt, A., Ashworth, A., Reis-Filho, J.S., and Smalley, M.J. (2010) BRCA1 Basal-like Breast Cancers Originate from Luminal Epithelial Progenitors and Not from Basal Stem Cells. *Cell Stem Cell*, **7** (3), 403–417.
43. Kalluri, R., and Weinberg, R.A. (2009) The basics of epithelial-mesenchymal transition. *J Clin Invest*, **119** (6), 1420–1428.
44. Huang, J., Li, H., and Ren, G. (2015) Epithelial-mesenchymal transition and drug resistance in breast cancer (Review). *International Journal of Oncology*, **47** (3), 840–848.
45. Nobes, C.D., and Hall, A. (1999) Rho GTPases Control Polarity, Protrusion, and Adhesion during Cell Movement. *J Cell Biol*, **144** (6), 1235–1244.
46. Weaver, A.M. (2006) Invadopodia: Specialized Cell Structures for Cancer Invasion. *Clin Exp Metastasis*, **23** (2), 97–105.
47. Parsons, J.T., Horwitz, A.R., and Schwartz, M.A. (2010) Cell adhesion: integrating cytoskeletal dynamics and cellular tension. *Nat Rev Mol Cell Biol*, **11** (9), 633–643.
48. McSherry, E.A., Donatello, S., Hopkins, A.M., and McDonnell, S. (2007) Common Molecular Mechanisms of Mammary Gland Development and Breast Cancer: Molecular basis of invasion in breast cancer. *Cell. Mol. Life Sci.*, **64** (24), 3201–3218.
49. Cheung, K.J., and Ewald, A.J. (2014) Illuminating breast cancer invasion: diverse roles for cell–cell interactions. *Current Opinion in Cell Biology*, **30**, 99–111.
50. Maughan, K.L., Lutterbie, M.A., and Ham, P.S. (2010) Treatment of Breast Cancer. *Breast Cancer*, **81** (11), 8.
51. National Comprehensive Cancer Network (2021) Breast Cancer (version8.2021). [https://www.nccn.org/professionals/physician\\_gls/pdf/breast.pdf](https://www.nccn.org/professionals/physician_gls/pdf/breast.pdf).

52. Kharb, R., Haider, K., Neha, K., and Yar, M.S. (2020) Aromatase inhibitors: Role in postmenopausal breast cancer. *Arch Pharm (Weinheim)*, **353** (8), e2000081.
53. Jordan, V.C., Dix, C.J., Rowsby, L., and Prestwich, G. (1977) Studies on the mechanism of action of the nonsteroidal antioestrogen tamoxifen (I.C.I. 46,474) in the rat. *Molecular and Cellular Endocrinology*, **7** (2), 177–192.
54. Osborne, C.K., Wakeling, A., and Nicholson, R.I. (2004) Fulvestrant: an oestrogen receptor antagonist with a novel mechanism of action. *Br J Cancer*, **90** (Suppl 1), S2–S6.
55. Vu, T., and Claret, F.X. (2012) Trastuzumab: updated mechanisms of action and resistance in breast cancer. *Front Oncol*, **2**, 62.
56. Clynes, R.A., Towers, T.L., Presta, L.G., and Ravetch, J.V. (2000) Inhibitory Fc receptors modulate in vivo cytotoxicity against tumor targets. *Nat Med*, **6** (4), 443–446.
57. Klapper, L.N., Waterman, H., Sela, M., and Yarden, Y. (2000) Tumor-inhibitory antibodies to HER-2/ErbB-2 may act by recruiting c-Cbl and enhancing ubiquitination of HER-2. *Cancer Res*, **60** (13), 3384–3388.
58. Miller, K.D., Nogueira, L., Mariotto, A.B., Rowland, J.H., Yabroff, K.R., Alfano, C.M., Jemal, A., Kramer, J.L., and Siegel, R.L. (2019) Cancer treatment and survivorship statistics, 2019. *CA: A Cancer Journal for Clinicians*, **69** (5), 363–385.
59. Choi, Y.J., Li, X., Hydring, P., Sanda, T., Stefano, J., Christie, A.L., Signoretti, S., Look, A.T., Kung, A.L., von Boehmer, H., and Sicinski, P. (2012) The Requirement for Cyclin D Function in Tumor Maintenance. *Cancer Cell*, **22** (4), 438–451.
60. Bartkova, J., Lukas, J., Müller, H., Lützhøt, D., Strauss, M., and Bartek, J. (1994) Cyclin D1 protein expression and function in human breast cancer. *International Journal of Cancer*, **57** (3), 353–361.
61. Yu, Q., Sicinska, E., Geng, Y., Ahnström, M., Zagozdzon, A., Kong, Y., Gardner, H., Kiyokawa, H., Harris, L.N., Stål, O., and Sicinski, P. (2006) Requirement for CDK4 kinase function in breast cancer. *Cancer Cell*, **9** (1), 23–32.
62. Cristofanilli, M., Turner, N.C., Bondarenko, I., Ro, J., Im, S.-A., Masuda, N., Colleoni, M., DeMichele, A., Loi, S., Verma, S., Iwata, H., Harbeck, N., Zhang, K., Theall, K.P., Jiang, Y., Bartlett, C.H., Koehler, M., and Slamon, D. (2016) Fulvestrant plus palbociclib versus fulvestrant plus placebo for treatment of

- hormone-receptor-positive, HER2-negative metastatic breast cancer that progressed on previous endocrine therapy (PALOMA-3): final analysis of the multicentre, double-blind, phase 3 randomised controlled trial. *Lancet Oncol*, **17** (4), 425–439.
63. Baselga, J., Campone, M., Piccart, M., Burris, H.A., Rugo, H.S., Sahmoud, T., Noguchi, S., Gnant, M., Pritchard, K.I., Lebrun, F., Beck, J.T., Ito, Y., Yardley, D., Deleu, I., Perez, A., Bachelot, T., Vittori, L., Xu, Z., Mukhopadhyay, P., Lebowitz, D., and Hortobagyi, G.N. (2012) Everolimus in Postmenopausal Hormone-Receptor-Positive Advanced Breast Cancer. *New England Journal of Medicine*, **366** (6), 520–529.
  64. Mukohara, T. (2015) PI3K mutations in breast cancer: prognostic and therapeutic implications. *Breast Cancer (Dove Med Press)*, **7**, 111–123.
  65. Zhao, J.J., Liu, Z., Wang, L., Shin, E., Loda, M.F., and Roberts, T.M. (2005) The oncogenic properties of mutant p110 $\alpha$  and p110 $\beta$  phosphatidylinositol 3-kinases in human mammary epithelial cells. *PNAS*, **102** (51), 18443–18448.
  66. André, F., Ciruelos, E., Rubovszky, G., Campone, M., Loibl, S., Rugo, H.S., Iwata, H., Conte, P., Mayer, I.A., Kaufman, B., Yamashita, T., Lu, Y.-S., Inoue, K., Takahashi, M., Pápai, Z., Longin, A.-S., Mills, D., Wilke, C., Hirawat, S., Juric, D., and SOLAR-1 Study Group (2019) Alpelisib for PIK3CA-Mutated, Hormone Receptor-Positive Advanced Breast Cancer. *N Engl J Med*, **380** (20), 1929–1940.
  67. Cameron, D., Casey, M., Press, M., Lindquist, D., Pienkowski, T., Romieu, C.G., Chan, S., Jagiello-Gruszfeld, A., Kaufman, B., Crown, J., Chan, A., Campone, M., Viens, P., Davidson, N., Gorbounova, V., Raats, J.I., Skarlos, D., Newstat, B., Roychowdhury, D., Paoletti, P., Oliva, C., Rubin, S., Stein, S., and Geyer, C.E. (2008) A phase III randomized comparison of lapatinib plus capecitabine versus capecitabine alone in women with advanced breast cancer that has progressed on trastuzumab: updated efficacy and biomarker analyses. *Breast Cancer Res Treat*, **112** (3), 533–543.
  68. Murthy, R.K., Loi, S., Okines, A., Paplomata, E., Hamilton, E., Hurvitz, S.A., Lin, N.U., Borges, V., Abramson, V., Anders, C., Bedard, P.L., Oliveira, M., Jakobsen, E., Bachelot, T., Shachar, S.S., Müller, V., Braga, S., Duhoux, F.P., Greil, R., Cameron, D., Carey, L.A., Curigliano, G., Gelmon, K., Hortobagyi, G., Krop, I., Loibl, S., Pegram, M., Slamon, D., Palanca-Wessels, M.C., Walker, L., Feng, W., and Winer, E.P. (2020) Tucatinib, Trastuzumab, and Capecitabine for HER2-Positive Metastatic Breast Cancer. *New England Journal of Medicine*, **382** (7), 597–609.
  69. Chan, A., Delaloge, S., Holmes, F.A., Moy, B., Iwata, H., Harvey, V.J., Robert, N.J., Silovski, T., Gokmen, E., von Minckwitz, G., Ejlertsen, B., Chia,

- S.K.L., Mansi, J., Barrios, C.H., Gnant, M., Buyse, M., Gore, I., Smith, J., Harker, G., Masuda, N., Petrakova, K., Zotano, A.G., Iannotti, N., Rodriguez, G., Tassone, P., Wong, A., Bryce, R., Ye, Y., Yao, B., and Martin, M. (2016) Neratinib after trastuzumab-based adjuvant therapy in patients with HER2-positive breast cancer (ExteNET): a multicentre, randomised, double-blind, placebo-controlled, phase 3 trial. *The Lancet Oncology*, **17** (3), 367–377.
70. von Minckwitz, G., Huang, C.-S., Mano, M.S., Loibl, S., Mamounas, E.P., Untch, M., Wolmark, N., Rastogi, P., Schneeweiss, A., Redondo, A., Fischer, H.H., Jacot, W., Conlin, A.K., Arce-Salinas, C., Wapnir, I.L., Jackisch, C., DiGiovanna, M.P., Fasching, P.A., Crown, J.P., Wülfing, P., Shao, Z., Rota Caremoli, E., Wu, H., Lam, L.H., Tesarowski, D., Smitt, M., Douthwaite, H., Singel, S.M., Geyer, C.E., and KATHERINE Investigators (2019) Trastuzumab Emtansine for Residual Invasive HER2-Positive Breast Cancer. *N Engl J Med*, **380** (7), 617–628.
71. Modi, S., Saura, C., Yamashita, T., Park, Y.H., Kim, S.-B., Tamura, K., Andre, F., Iwata, H., Ito, Y., Tsurutani, J., Sohn, J., Denduluri, N., Perrin, C., Aogi, K., Tokunaga, E., Im, S.-A., Lee, K.S., Hurvitz, S.A., Cortes, J., Lee, C., Chen, S., Zhang, L., Shahidi, J., Yver, A., and Krop, I. (2020) Trastuzumab Deruxtecan in Previously Treated HER2-Positive Breast Cancer. *N Engl J Med*, **382** (7), 610–621.
72. Roy, R., Chun, J., and Powell, S.N. (2012) BRCA1 and BRCA2: important differences with common interests. *Nat Rev Cancer*, **12** (5), 372–372.
73. Konecny, G.E., and Kristeleit, R.S. (2016) PARP inhibitors for BRCA1/2-mutated and sporadic ovarian cancer: current practice and future directions. *Br J Cancer*, **115** (10), 1157–1173.
74. Robson, M., Im, S.-A., Senkus, E., Xu, B., Domchek, S.M., Masuda, N., Delaloge, S., Li, W., Tung, N., Armstrong, A., Wu, W., Goessl, C., Runswick, S., and Conte, P. (2017) Olaparib for Metastatic Breast Cancer in Patients with a Germline BRCA Mutation. *N Engl J Med*, **377** (6), 523–533.
75. Lehmann, B.D., Bauer, J.A., Chen, X., Sanders, M.E., Chakravarthy, A.B., Shyr, Y., and Pietenpol, J.A. (2011) Identification of human triple-negative breast cancer subtypes and preclinical models for selection of targeted therapies. *J Clin Invest*, **121** (7), 2750–2767.
76. Trivers, K.F., Lund, M.J., Porter, P.L., Liff, J.M., Flagg, E.W., Coates, R.J., and Eley, J.W. (2009) The epidemiology of triple-negative breast cancer, including race. *Cancer Causes Control*, **20** (7), 1071–1082.
77. Morris, G.J., Naidu, S., Topham, A.K., Guiles, F., Xu, Y., McCue, P., Schwartz, G.F., Park, P.K., Rosenberg, A.L., Brill, K., and Mitchell, E.P. (2007)

- Differences in breast carcinoma characteristics in newly diagnosed African-American and Caucasian patients: a single-institution compilation compared with the National Cancer Institute's Surveillance, Epidemiology, and End Results database. *Cancer*, **110** (4), 876–884.
78. Livasy, C.A., Karaca, G., Nanda, R., Tretiakova, M.S., Olopade, O.I., Moore, D.T., and Perou, C.M. (2006) Phenotypic evaluation of the basal-like subtype of invasive breast carcinoma. *Mod Pathol*, **19** (2), 264–271.
79. Bareche, Y., Venet, D., Ignatiadis, M., Aftimos, P., Piccart, M., Rothe, F., and Sotiriou, C. (2018) Unravelling triple-negative breast cancer molecular heterogeneity using an integrative multiomic analysis. *Annals of Oncology*, **29** (4), 895–902.
80. Schmid, P., Cortes, J., Pusztai, L., McArthur, H., Kümmel, S., Bergh, J., Denkert, C., Park, Y.H., Hui, R., Harbeck, N., Takahashi, M., Foukakis, T., Fasching, P.A., Cardoso, F., Untch, M., Jia, L., Karantza, V., Zhao, J., Aktan, G., Dent, R., and O'Shaughnessy, J. (2020) Pembrolizumab for Early Triple-Negative Breast Cancer. *New England Journal of Medicine*, **382** (9), 810–821.
81. Moon, S.-J., Govindan, S.V., Cardillo, T.M., D'Souza, C.A., Hansen, H.J., and Goldenberg, D.M. (2008) Antibody conjugates of 7-ethyl-10-hydroxycamptothecin (SN-38) for targeted cancer chemotherapy. *J Med Chem*, **51** (21), 6916–6926.
82. Cardillo, T.M., Govindan, S.V., Sharkey, R.M., Trisal, P., and Goldenberg, D.M. (2011) Humanized Anti-Trop-2 IgG-SN-38 Conjugate for Effective Treatment of Diverse Epithelial Cancers: Preclinical Studies in Human Cancer Xenograft Models and Monkeys. *Clin Cancer Res*, **17** (10), 3157–3169.
83. Bardia, A., Mayer, I.A., Diamond, J.R., Moroosse, R.L., Isakoff, S.J., Starodub, A.N., Shah, N.C., O'Shaughnessy, J., Kalinsky, K., Guarino, M., Abramson, V., Juric, D., Tolaney, S.M., Berlin, J., Messersmith, W.A., Ocean, A.J., Wegener, W.A., Maliakal, P., Sharkey, R.M., Govindan, S.V., Goldenberg, D.M., and Vahdat, L.T. (2017) Efficacy and Safety of Anti-Trop-2 Antibody Drug Conjugate Sacituzumab Govitecan (IMMU-132) in Heavily Pretreated Patients With Metastatic Triple-Negative Breast Cancer. *J Clin Oncol*, **35** (19), 2141–2148.
84. Jhan, J.-R., and Andrechek, E.R. (2017) Triple-negative breast cancer and the potential for targeted therapy. *Pharmacogenomics*, **18** (17), 1595–1609.
85. Wieduwilt, M.J., and Moasser, M.M. (2008) The epidermal growth factor receptor family: biology driving targeted therapeutics. *Cell Mol Life Sci*, **65** (10), 1566–1584.

86. Yarden, Y., and Sliwkowski, M.X. (2001) Untangling the ErbB signalling network. *Nat Rev Mol Cell Biol*, **2** (2), 127–137.
87. Sasaki, T., Hiroki, K., and Yamashita, Y. (2013) The role of epidermal growth factor receptor in cancer metastasis and microenvironment. *Biomed Res Int*, **2013**, 546318.
88. Weernink, P.A.O., and Rijksen, G. (1995) Activation and Translocation of c-Src to the Cytoskeleton by Both Platelet-derived Growth Factor and Epidermal Growth Factor. *Journal of Biological Chemistry*, **270** (5), 2264–2267.
89. Biscardi, J.S., Maa, M.-C., Tice, D.A., Cox, M.E., Leu, T.-H., and Parsons, S.J. (1999) c-Src-mediated Phosphorylation of the Epidermal Growth Factor Receptor on Tyr845 and Tyr1101 Is Associated with Modulation of Receptor Function. *Journal of Biological Chemistry*, **274** (12), 8335–8343.
90. Carey, L.A., Rugo, H.S., Marcom, P.K., Mayer, E.L., Esteva, F.J., Ma, C.X., Liu, M.C., Storniolo, A.M., Rimawi, M.F., Forero-Torres, A., Wolff, A.C., Hobday, T.J., Ivanova, A., Chiu, W.-K., Ferraro, M., Burrows, E., Bernard, P.S., Hoadley, K.A., Perou, C.M., and Winer, E.P. (2012) TBCRC 001: randomized phase II study of cetuximab in combination with carboplatin in stage IV triple-negative breast cancer. *J Clin Oncol*, **30** (21), 2615–2623.
91. Xie, Y., Su, N., Yang, J., Tan, Q., Huang, S., Jin, M., Ni, Z., Zhang, B., Zhang, D., Luo, F., Chen, H., Sun, X., Feng, J.Q., Qi, H., and Chen, L. (2020) FGF/FGFR signaling in health and disease. *Sig Transduct Target Ther*, **5** (1), 1–38.
92. Latko, M., Czyrek, A., Porębska, N., Kucińska, M., Otlewski, J., Zakrzewska, M., and Opaliński, Ł. (2019) Cross-Talk between Fibroblast Growth Factor Receptors and Other Cell Surface Proteins. *Cells*, **8** (5), 455.
93. Theillet, C., Adelaide, J., Louason, G., Bonnet-Dorion, F., Jacquemier, J., Adhane, J., Longy, M., Katsaros, D., Sismondi, P., and Gaudray, P. (1993) FGFR1 and PLAT genes and DNA amplification at 8p12 in breast and ovarian cancers. *Genes Chromosomes Cancer*, **7** (4), 219–226.
94. Turner, N., Pearson, A., Sharpe, R., Lambros, M., Geyer, F., Lopez-Garcia, M.A., Natrajan, R., Marchio, C., Iorns, E., Mackay, A., Gillett, C., Grigoriadis, A., Tutt, A., Reis-Filho, J.S., and Ashworth, A. (2010) FGFR1 amplification drives endocrine therapy resistance and is a therapeutic target in breast cancer. *Cancer Res*, **70** (5), 2085–2094.
95. Cheng, C.L., Thike, A.A., Tan, S.Y.J., Chua, P.J., Bay, B.H., and Tan, P.H. (2015) Expression of FGFR1 is an independent prognostic factor in triple-negative breast cancer. *Breast Cancer Res Treat*, **151** (1), 99–111.

96. Chew, N.J., Nguyen, E.V., Su, S.-P., Novy, K., Chan, H.C., Nguyen, L.K., Luu, J., Simpson, K.J., Lee, R.S., and Daly, R.J. (2020) FGFR3 signaling and function in triple negative breast cancer. *Cell Commun Signal*, **18**, 13.
97. Organ, S.L., and Tsao, M.-S. (2011) An overview of the c-MET signaling pathway. *Ther Adv Med Oncol*, **3** (1 Suppl), S7–S19.
98. Zhu, H., Naujokas, M.A., and Park, M. (1994) Receptor chimeras indicate that the met tyrosine kinase mediates the motility and morphogenic responses of hepatocyte growth/scatter factor. *Cell Growth Differ*, **5** (4), 359–366.
99. Zhang, Y., Xia, M., Jin, K., Wang, S., Wei, H., Fan, C., Wu, Y., Li, X., Li, X., Li, G., Zeng, Z., and Xiong, W. (2018) Function of the c-Met receptor tyrosine kinase in carcinogenesis and associated therapeutic opportunities. *Molecular Cancer*, **17** (1), 45.
100. Stoker, M., Gherardi, E., Perryman, M., and Gray, J. (1987) Scatter factor is a fibroblast-derived modulator of epithelial cell mobility. *Nature*, **327** (6119), 239–242.
101. Nakamura, T., Nawa, K., and Ichihara, A. (1984) Partial purification and characterization of hepatocyte growth factor from serum of hepatectomized rats. *Biochemical and Biophysical Research Communications*, **122** (3), 1450–1459.
102. Nakamura, T., Teramoto, H., and Ichihara, A. (1986) Purification and characterization of a growth factor from rat platelets for mature parenchymal hepatocytes in primary cultures. *PNAS*, **83** (17), 6489–6493.
103. Weidner, K.M., Di Cesare, S., Sachs, M., Brinkmann, V., Behrens, J., and Birchmeier, W. (1996) Interaction between Gab1 and the c-Met receptor tyrosine kinase is responsible for epithelial morphogenesis. *Nature*, **384** (6605), 173–176.
104. Hui, A.Y., Meens, J.A., Schick, C., Organ, S.L., Qiao, H., Tremblay, E.A., Schaeffer, E., Uniyal, S., Chan, B.M.C., and Elliott, B.E. (2009) Src and FAK mediate cell–matrix adhesion-dependent activation of met during transformation of breast epithelial cells. *Journal of Cellular Biochemistry*, **107** (6), 1168–1181.
105. Giordano, S., Corso, S., Conrotto, P., Artigiani, S., Gilestro, G., Barberis, D., Tamagnone, L., and Comoglio, P.M. (2002) The Semaphorin 4D receptor controls invasive growth by coupling with Met. *Nat Cell Biol*, **4** (9), 720–724.
106. Peschard, P., Fournier, T.M., Lamorte, L., Naujokas, M.A., Band, H., Langdon, W.Y., and Park, M. (2001) Mutation of the c-Cbl TKB domain binding

site on the Met receptor tyrosine kinase converts it into a transforming protein. *Mol Cell*, **8** (5), 995–1004.

107. Sangwan, V., Paliouras, G.N., Abella, J.V., Dubé, N., Monast, A., Tremblay, M.L., and Park, M. (2008) Regulation of the Met Receptor-tyrosine Kinase by the Protein-tyrosine Phosphatase 1B and T-cell Phosphatase. *J Biol Chem*, **283** (49), 34374–34383.
108. Goldoni, S., Humphries, A., Nyström, A., Sattar, S., Owens, R.T., McQuillan, D.J., Ireton, K., and Iozzo, R.V. (2009) Decorin is a novel antagonistic ligand of the Met receptor. *J Cell Biol*, **185** (4), 743–754.
109. Zagouri, F., Bago-Horvath, Z., Rössler, F., Brandstetter, A., Bartsch, R., Papadimitriou, C.A., Dimitrakakis, C., Tsigginou, A., Papaspyrou, I., Giannos, A., Dimopoulos, M.-A., and Filipits, M. (2013) High MET expression is an adverse prognostic factor in patients with triple-negative breast cancer. *Br J Cancer*, **108** (5), 1100–1105.
110. Ponzio, M.G., Lesurf, R., Petkiewicz, S., O'Malley, F.P., Pinnaduwege, D., Andrulis, I.L., Bull, S.B., Chughtai, N., Zuo, D., Souleimanova, M., Germain, D., Omeroglu, A., Cardiff, R.D., Hallett, M., and Park, M. (2009) Met induces mammary tumors with diverse histologies and is associated with poor outcome and human basal breast cancer. *Proc Natl Acad Sci U S A*, **106** (31), 12903–12908.
111. Camp, R.L., Rimm, E.B., and Rimm, D.L. (1999) Met expression is associated with poor outcome in patients with axillary lymph node negative breast carcinoma. *Cancer*, **86** (11), 2259–2265.
112. Ghossein, R.A., Dillon, D.A., D'Aquila, T., Rimm, E.B., Fearon, E.R., and Rimm, D.L. (1998) Expression of c-met is a strong independent prognostic factor in breast carcinoma. *Cancer*, **82** (8), 1513–1520.
113. Graveel, C.R., DeGroot, J.D., Su, Y., Koeman, J., Dykema, K., Leung, S., Snider, J., Davies, S.R., Swiatek, P.J., Cottingham, S., Watson, M.A., Ellis, M.J., Sigler, R.E., Furge, K.A., and Woude, G.F.V. (2009) Met induces diverse mammary carcinomas in mice and is associated with human basal breast cancer. *PNAS*, **106** (31), 12909–12914.
114. Ho-Yen, C.M., Jones, J.L., and Kermorgant, S. (2015) The clinical and functional significance of c-Met in breast cancer: a review. *Breast Cancer Res*, **17**, 52.
115. van Agthoven, T., van Agthoven, T.L., Dekker, A., van der Spek, P.J., Vreede, L., and Dorssers, L.C. (1998) Identification of BCAR3 by a random

- search for genes involved in antiestrogen resistance of human breast cancer cells. *EMBO J*, **17** (10), 2799–2808.
116. Lu, Y., Brush, J., and Stewart, T.A. (1999) NSP1 Defines a Novel Family of Adaptor Proteins Linking Integrin and Tyrosine Kinase Receptors to the c-Jun N-terminal Kinase/Stress-activated Protein Kinase Signaling Pathway. *Journal of Biological Chemistry*, **274** (15), 10047–10052.
  117. Garron, M.-L., Arsenieva, D., Zhong, J., Bloom, A.B., Lerner, A., O'Neill, G.M., and Arold, S.T. (2009) Structural insights into the association between BCAR3 and Cas family members, an atypical complex implicated in anti-oestrogen resistance. *J Mol Biol*, **386** (1), 190–203.
  118. Mace, P.D., Wallez, Y., Dobaczewska, M.K., Lee, J.J., Robinson, H., Pasquale, E.B., and Riedl, S.J. (2011) NSP-Cas protein structures reveal a promiscuous interaction module in cell signaling. *Nat Struct Mol Biol*, **18** (12), 1381–1387.
  119. Kondo, T., Nakamori, T., Nagai, H., Takeshita, A., Kusakabe, K.-T., and Okada, T. (2016) A novel spontaneous mutation of BCAR3 results in extrusion cataracts in CF#1 mouse strain. *Mamm Genome*, **27** (9), 451–459.
  120. Near, R.I., Smith, R.S., Toselli, P.A., Freddo, T.F., Bloom, A.B., Vanden Borre, P., Seldin, D.C., and Lerner, A. (2009) Loss of AND-34/BCAR3 expression in mice results in rupture of the adult lens. *Mol Vis*, **15**, 685–699.
  121. Oh, M.-J., van Agthoven, T., Choi, J.-E., Jeong, Y.-J., Chung, Y.-H., Kim, C.-M., and Jhun, B.H. (2008) BCAR3 regulates EGF-induced DNA synthesis in normal human breast MCF-12A cells. *Biochem Biophys Res Commun*, **375** (3), 430–434.
  122. Sun, G., Cheng, S.Y.S., Chen, M., Lim, C.J., and Pallen, C.J. (2012) Protein Tyrosine Phosphatase  $\alpha$  Phosphotyrosyl-789 Binds BCAR3 To Position Cas for Activation at Integrin-Mediated Focal Adhesions. *Mol Cell Biol*, **32** (18), 3776–3789.
  123. Li, C., Wang, S., Xing, Z., Lin, A., Liang, K., Song, J., Hu, Q., Yao, J., Chen, Z., Park, P.K., Hawke, D.H., Zhou, J., Zhou, Y., Zhang, S., Liang, H., Hung, M.-C., Gallick, G.E., Han, L., Lin, C., and Yang, L. (2017) A ROR1-HER3-lncRNA signalling axis modulates the Hippo-YAP pathway to regulate bone metastasis. *Nat Cell Biol*, **19** (2), 106–119.
  124. Cai, D., Iyer, A., Felekis, K.N., Near, R.I., Luo, Z., Chernoff, J., Albanese, C., Pestell, R.G., and Lerner, A. (2003) AND-34/BCAR3, a GDP Exchange Factor Whose Overexpression Confers Antiestrogen Resistance, Activates Rac, PAK1, and the Cyclin D1 Promoter. *Cancer Res*, **63** (20), 6802–6808.

125. Cross, A.M., Wilson, A.L., Guerrero, M.S., Thomas, K.S., Bachir, A.I., Kubow, K.E., Horwitz, A.R., and Bouton, A.H. (2016) Breast cancer antiestrogen resistance 3–p130Cas interactions promote adhesion disassembly and invasion in breast cancer cells. *Oncogene*, **35** (45), 5850–5859.
126. Wilson, A.L., Schrecengost, R.S., Guerrero, M.S., Thomas, K.S., and Bouton, A.H. (2013) Breast Cancer Antiestrogen Resistance 3 (BCAR3) Promotes Cell Motility by Regulating Actin Cytoskeletal and Adhesion Remodeling in Invasive Breast Cancer Cells. *PLOS ONE*, **8** (6), e65678.
127. Riggins, R.B., Quilliam, L.A., and Bouton, A.H. (2003) Synergistic Promotion of c-Src Activation and Cell Migration by Cas and AND-34/BCAR3. *Journal of Biological Chemistry*, **278** (30), 28264–28273.
128. Steenkiste, E.M., Berndt, J.D., Pilling, C., Simpkins, C., and Cooper, J.A. (2021) A Cas-BCAR3 co-regulatory circuit controls lamellipodia dynamics. *eLife*, **10**, e67078.
129. Matsui, H., Harada, I., and Sawada, Y. (2012) Src, p130Cas, and Mechanotransduction in Cancer Cells. *Genes Cancer*, **3** (5–6), 394–401.
130. Sakai, R., Iwamatsu, A., Hirano, N., Ogawa, S., Tanaka, T., Mano, H., Yazaki, Y., and Hirai, H. (1994) A novel signaling molecule, p130, forms stable complexes in vivo with v-Crk and v-Src in a tyrosine phosphorylation-dependent manner. *EMBO J*, **13** (16), 3748–3756.
131. Honda, H., Oda, H., Nakamoto, T., Honda, Z., Sakai, R., Suzuki, T., Saito, T., Nakamura, K., Nakao, K., Ishikawa, T., Katsuki, M., Yazaki, Y., and Hirai, H. (1998) Cardiovascular anomaly, impaired actin bundling and resistance to Src-induced transformation in mice lacking p130Cas. *Nat Genet*, **19** (4), 361–365.
132. Riggins, R.B., Thomas, K.S., Ta, H.Q., Wen, J., Davis, R.J., Schuh, N.R., Donelan, S.S., Owen, K.A., Gibson, M.A., Shupnik, M.A., Silva, C.M., Parsons, S.J., Clarke, R., and Bouton, A.H. (2006) Physical and Functional Interactions between Cas and c-Src Induce Tamoxifen Resistance of Breast Cancer Cells through Pathways Involving Epidermal Growth Factor Receptor and Signal Transducer and Activator of Transcription 5b. *Cancer Res*, **66** (14), 7007–7015.
133. Sawada, Y., Tamada, M., Dubin-Thaler, B.J., Cherniavskaya, O., Sakai, R., Tanaka, S., and Sheetz, M.P. (2006) Force sensing by mechanical extension of the Src family kinase substrate p130Cas. *Cell*, **127** (5), 1015–1026.

134. Yeh, Y.-C., Ling, J.-Y., Chen, W.-C., Lin, H.-H., and Tang, M.-J. (2017) Mechano-transduction of matrix stiffness in regulation of focal adhesion size and number: reciprocal regulation of caveolin-1 and  $\beta$ 1 integrin. *Sci Rep*, **7** (1), 15008.
135. Rous, P. (1910) A TRANSMISSIBLE AVIAN NEOPLASM. (SARCOMA OF THE COMMON FOWL.). *Journal of Experimental Medicine*, **12** (5), 696–705.
136. Wheeler, D.L., Iida, M., and Dunn, E.F. (2009) The role of Src in solid tumors. *Oncologist*, **14** (7), 667–678.
137. Thomas, S.M., and Brugge, J.S. (1997) Cellular Functions Regulated by Src Family Kinases. *Annual Review of Cell and Developmental Biology*, **13** (1), 513–609.
138. Hubbard, S.R. (1999) Src autoinhibition: let us count the ways. *Nat Struct Mol Biol*, **6** (8), 711–714.
139. Burnham, M.R., Bruce-Staskal, P.J., Harte, M.T., Weidow, C.L., Ma, A., Weed, S.A., and Bouton, A.H. (2000) Regulation of c-SRC Activity and Function by the Adapter Protein CAS. *Molecular and Cellular Biology*, **20** (16), 5865–5878.
140. Pellicena, P., and Miller, W.T. (2001) Processive Phosphorylation of p130Cas by Src Depends on SH3-Polyproline Interactions. *Journal of Biological Chemistry*, **276** (30), 28190–28196.
141. Tryfonopoulos, D., Walsh, S., Collins, D.M., Flanagan, L., Quinn, C., Corkery, B., McDermott, E.W., Evoy, D., Pierce, A., O'Donovan, N., Crown, J., and Duffy, M.J. (2011) Src: a potential target for the treatment of triple-negative breast cancer. *Annals of Oncology*, **22** (10), 2234–2240.
142. Qian, X.-L., Zhang, J., Li, P.-Z., Lang, R.-G., Li, W.-D., Sun, H., Liu, F.-F., Guo, X.-J., Gu, F., and Fu, L. (2017) Dasatinib inhibits c-src phosphorylation and prevents the proliferation of Triple-Negative Breast Cancer (TNBC) cells which overexpress Syndecan-Binding Protein (SDCBP). *PLoS One*, **12** (1), e0171169.
143. Kennedy, L.C., and Gadi, V. (2018) Dasatinib in breast cancer: Src-ing for response in all the wrong kinases. *Annals of Translational Medicine*, **0** (0), 60–60.
144. Morris, P.G., Rota, S., Cadoo, K., Zamora, S., Patil, S., D'Andrea, G., Gilewski, T., Bromberg, J., Dang, C., Dickler, M., Modi, S., Seidman, A.D., Sklarin, N., Norton, L., Hudis, C.A., and Fornier, M.N. (2018) Phase II Study of

- Paclitaxel and Dasatinib in Metastatic Breast Cancer. *Clin Breast Cancer*, **18** (5), 387–394.
145. Ma, J., DeFrances, M.C., Zou, C., Johnson, C., Ferrell, R., and Zarnegar, R. (2009) Somatic mutation and functional polymorphism of a novel regulatory element in the HGF gene promoter causes its aberrant expression in human breast cancer. *J. Clin. Invest.*, **119** (3), 478–491.
146. Gonzatti-Haces, M., Seth, A., Park, M., Copeland, T., Oroszlan, S., and Woude, G.F.V. (1988) Characterization of the TPR-MET oncogene p65 and the MET protooncogene p140 protein-tyrosine kinases. *PNAS*, **85** (1), 21–25.
147. Tuck, A.B., Park, M., Sterns, E.E., Boag, A., and Elliott, B.E. (1996) Coexpression of hepatocyte growth factor and receptor (Met) in human breast carcinoma. *Am J Pathol*, **148** (1), 225–232.
148. Yamashita, J., Ogawa, M., Yamashita, S., Nomura, K., Kuramoto, M., Saishoji, T., and Shin, S. (1994) Immunoreactive hepatocyte growth factor is a strong and independent predictor of recurrence and survival in human breast cancer. *Cancer Res*, **54** (7), 1630–1633.
149. Yi, S., and Tsao, M.-S. (2000) Activation of Hepatocyte Growth Factor-Met Autocrine Loop Enhances Tumorigenicity in a Human Lung Adenocarcinoma Cell Line. *Neoplasia*, **2** (3), 226–234.
150. Xie, Q., Liu, K.-D., Hu, M.-Y., and Zhou, K. (2001) SF/HGF-c-Met autocrine and paracrine promote metastasis of hepatocellular carcinoma. *World J Gastroenterol*, **7** (6), 816–820.
151. Camp, J.T., Elloumi, F., Roman-Perez, E., Rein, J., Stewart, D.A., Harrell, J.C., Perou, C.M., and Troester, M.A. (2011) Interactions with Fibroblasts Are Distinct in Basal-Like and Luminal Breast Cancers. *Mol Cancer Res*, **9** (1), 3–13.
152. Niranjan, B., Buluwela, L., Yant, J., Perusinghe, N., Atherton, A., Phippard, D., Dale, T., Gusterson, B., and Kamalati, T. (1995) HGF/SF: a potent cytokine for mammary growth, morphogenesis and development. *Development*, **121** (9), 2897–2908.
153. Shi, Y., and Massagué, J. (2003) Mechanisms of TGF-beta signaling from cell membrane to the nucleus. *Cell*, **113** (6), 685–700.
154. Massagué, J. (1998) TGF- $\beta$  SIGNAL TRANSDUCTION. *Annual Review of Biochemistry*, **67** (1), 753–791.

155. Bierie, B., Stover, D.G., Abel, T.W., Chytil, A., Gorska, A.E., Aakre, M., Forrester, E., Yang, L., Wagner, K.-U., and Moses, H.L. (2008) Transforming Growth Factor- $\beta$  Regulates Mammary Carcinoma Cell Survival and Interaction with the Adjacent Microenvironment. *Cancer Res*, **68** (6), 1809–1819.
156. Massagué, J. (2012) TGF $\beta$  signalling in context. *Nat Rev Mol Cell Biol*, **13** (10), 616–630.
157. Mani, S.A., Guo, W., Liao, M.-J., Eaton, E.N., Ayyanan, A., Zhou, A.Y., Brooks, M., Reinhard, F., Zhang, C.C., Shipitsin, M., Campbell, L.L., Polyak, K., Brisken, C., Yang, J., and Weinberg, R.A. (2008) The epithelial-mesenchymal transition generates cells with properties of stem cells. *Cell*, **133** (4), 704–715.
158. Bierie, B., and Moses, H.L. (2006) Tumour microenvironment: TGF $\beta$ : the molecular Jekyll and Hyde of cancer. *Nat Rev Cancer*, **6** (7), 506–520.
159. Bholra, N.E., Balko, J.M., Dugger, T.C., Kuba, M.G., Sánchez, V., Sanders, M., Stanford, J., Cook, R.S., and Arteaga, C.L. (2013) TGF- $\beta$  inhibition enhances chemotherapy action against triple-negative breast cancer. *J Clin Invest*, **123** (3), 1348–1358.
160. Schuh, N.R., Guerrero, M.S., Schrecengost, R.S., and Bouton, A.H. (2010) BCAR3 regulates Src/p130 Cas association, Src kinase activity, and breast cancer adhesion signaling. *J Biol Chem*, **285** (4), 2309–2317.
161. Makkinje, A., Vanden Borre, P., Near, R.I., Patel, P.S., and Lerner, A. (2012) Breast Cancer Anti-estrogen Resistance 3 (BCAR3) Protein Augments Binding of the c-Src SH3 Domain to Crk-associated Substrate (p130cas). *J Biol Chem*, **287** (33), 27703–27714.
162. Bottaro, D., Rubin, J., Faletto, D., Chan, A., Kmieciak, T., Vande Woude, G., and Aaronson, S. (1991) Identification of the Hepatocyte Growth Factor Receptor as the c-met ProtoOncogene Product. *Science*, **251**, 802–804.
163. Naldini, L., Weidner, K.M., Vigna, E., Gaudino, G., Bardelli, A., Ponzetto, C., Narsimhan, R.P., Hartmann, G., Zarnegar, R., and Michalopoulos, G.K. (1991) Scatter factor and hepatocyte growth factor are indistinguishable ligands for the MET receptor. *EMBO J*, **10** (10), 2867–2878.
164. Weidner, K.M., Sachs, M., and Birchmeier, W. (1993) The Met receptor tyrosine kinase transduces motility, proliferation, and morphogenic signals of scatter factor/hepatocyte growth factor in epithelial cells. *Journal of Cell Biology*, **121** (1), 145–154.

165. Schrecengost, R.S., Riggins, R.B., Thomas, K.S., Guerrero, M.S., and Bouton, A.H. (2007) Breast Cancer Antiestrogen Resistance-3 Expression Regulates Breast Cancer Cell Migration through Promotion of p130Cas Membrane Localization and Membrane Ruffling. *Cancer Res*, **67** (13), 6174–6182.
166. Sakai, R., Iwamatsu, A., Hirano, N., Ogawa, S., Tanaka, T., Nishida, J., Yazaki, Y., and Hirai, H. (1994) Characterization, partial purification, and peptide sequencing of p130, the main phosphoprotein associated with v-Crk oncoprotein. *J Biol Chem*, **269** (52), 32740–32746.
167. Takayama, H., LaRochelle, W.J., Sharp, R., Otsuka, T., Kriebel, P., Anver, M., Aaronson, S.A., and Merlino, G. (1997) Diverse tumorigenesis associated with aberrant development in mice overexpressing hepatocyte growth factor/scatter factor. *Proc Natl Acad Sci U S A*, **94** (2), 701–706.
168. Raghav, K.P., Wang, W., Liu, S., Chavez-MacGregor, M., Meng, X., Hortobagyi, G.N., Mills, G.B., Meric-Bernstam, F., Blumenschein, G.R., and Gonzalez-Angulo, A.M. (2012) cMET and phospho-cMET protein levels in breast cancers and survival outcomes. *Clin Cancer Res*, **18** (8), 2269–2277.
169. Jin, L., Fuchs, A., Schnitt, S.J., Yao, Y., Joseph, A., Lamszus, K., Park, M., Goldberg, I.D., and Rosen, E.M. (1997) Expression of scatter factor and c-met receptor in benign and malignant breast tissue. *Cancer*, **79** (4), 749–760.
170. Dill, E.A., Gru, A.A., Atkins, K.A., Friedman, L.A., Moore, M.E., Bullock, T.N., Cross, J.V., Dillon, P.M., and Mills, A.M. (2017) PD-L1 Expression and Intratumoral Heterogeneity Across Breast Cancer Subtypes and Stages: An Assessment of 245 Primary and 40 Metastatic Tumors. *Am J Surg Pathol*, **41** (3), 334–342.
171. Györfy, B., Lanczky, A., Eklund, A.C., Denkert, C., Budczies, J., Li, Q., and Szallasi, Z. (2010) An online survival analysis tool to rapidly assess the effect of 22,277 genes on breast cancer prognosis using microarray data of 1,809 patients. *Breast Cancer Res Treat*, **123** (3), 725–731.
172. Nguyen-Ngoc, K.-V., Shamir, E.R., Huebner, R.J., Beck, J.N., Cheung, K.J., and Ewald, A.J. (2015) 3D culture assays of murine mammary branching morphogenesis and epithelial invasion. *Methods Mol Biol*, **1189**, 135–162.
173. Hänzelmann, S., Castelo, R., and Guinney, J. (2013) GSVA: gene set variation analysis for microarray and RNA-Seq data. *BMC Bioinformatics*, **14** (1), 7.
174. Jassal, B., Matthews, L., Viteri, G., Gong, C., Lorente, P., Fabregat, A., Sidiropoulos, K., Cook, J., Gillespie, M., Haw, R., Loney, F., May, B., Milacic,

- M., Rothfels, K., Sevilla, C., Shamovsky, V., Shorser, S., Varusai, T., Weiser, J., Wu, G., Stein, L., Hermjakob, H., and D'Eustachio, P. (2020) The reactome pathway knowledgebase. *Nucleic Acids Res*, **48** (D1), D498–D503.
175. Albert, P.S., and Shih, J.H. (2003) Modeling tumor growth with random onset. *Biometrics*, **59** (4), 897–906.
176. Olsson, E., Winter, C., George, A., Chen, Y., Törngren, T., Bendahl, P.-O., Borg, Å., Gruvberger-Saal, S.K., and Saal, L.H. (2015) Mutation Screening of 1,237 Cancer Genes across Six Model Cell Lines of Basal-Like Breast Cancer. *PLOS ONE*, **10** (12), e0144528.
177. Saunus, J.M., Smart, C.E., Kutasovic, J.R., Johnston, R.L., Kalita-de Croft, P., Miranda, M., Rozali, E.N., Vargas, A.C., Reid, L.E., Lorsy, E., Cocciardi, S., Seidens, T., McCart Reed, A.E., Dalley, A.J., Wockner, L.F., Johnson, J., Sarkar, D., Askarian-Amiri, M.E., Simpson, P.T., Khanna, K.K., Chenevix-Trench, G., Al-Ejeh, F., and Lakhani, S.R. (2018) Multidimensional phenotyping of breast cancer cell lines to guide preclinical research. *Breast Cancer Res Treat*, **167** (1), 289–301.
178. Kessenbrock, K., Smith, P., Steenbeek, S.C., Pervolarakis, N., Kumar, R., Minami, Y., Goga, A., Hinck, L., and Werb, Z. (2017) Diverse regulation of mammary epithelial growth and branching morphogenesis through noncanonical Wnt signaling. *PNAS*, **114** (12), 3121–3126.
179. Simian, M., Hirai, Y., Navre, M., Werb, Z., Lochter, A., and Bissell, M.J. (2001) The interplay of matrix metalloproteinases, morphogens and growth factors is necessary for branching of mammary epithelial cells. *Development*, **128** (16), 3117–3131.
180. Ewald, A.J., Brenot, A., Duong, M., Chan, B.S., and Werb, Z. (2008) Collective epithelial migration and cell rearrangements drive mammary branching morphogenesis. *Dev Cell*, **14** (4), 570–581.
181. Simiczyjew, A., Dratkiewicz, E., Van Troys, M., Ampe, C., Styczeń, I., and Nowak, D. (2018) Combination of EGFR Inhibitor Lapatinib and MET Inhibitor Foretinib Inhibits Migration of Triple Negative Breast Cancer Cell Lines. *Cancers (Basel)*, **10** (9), E335.
182. Grotegut, S., von Schweinitz, D., Christofori, G., and Lehenbre, F. (2006) Hepatocyte growth factor induces cell scattering through MAPK/Egr-1-mediated upregulation of Snail. *EMBO J*, **25** (15), 3534–3545.
183. Weidner, K.M., Behrens, J., Vandekerckhove, J., and Birchmeier, W. (1990) Scatter factor: molecular characteristics and effect on the invasiveness of epithelial cells. *J Cell Biol*, **111** (5 Pt 1), 2097–2108.

184. van Agthoven, T., Sieuwerts, A.M., Meijer-van Gelder, M.E., Look, M.P., Smid, M., Veldscholte, J., Sleijfer, S., Foekens, J.A., and Dorssers, L.C.J. (2009) Relevance of breast cancer antiestrogen resistance genes in human breast cancer progression and tamoxifen resistance. *J Clin Oncol*, **27** (4), 542–549.
185. Guo, J., Canaff, L., Rajadurai, C.V., Fils-Aimé, N., Tian, J., Dai, M., Korah, J., Villatoro, M., Park, M., Ali, S., and Lebrun, J.-J. (2014) Breast cancer antiestrogen resistance 3 inhibits transforming growth factor  $\beta$ /Smad signaling and associates with favorable breast cancer disease outcomes. *Breast Cancer Research*, **16** (6), 476.
186. Nielsen, T.O., Hsu, F.D., Jensen, K., Cheang, M., Karaca, G., Hu, Z., Hernandez-Boussard, T., Livasy, C., Cowan, D., Dressler, L., Akslen, L.A., Ragaz, J., Gown, A.M., Gilks, C.B., van de Rijn, M., and Perou, C.M. (2004) Immunohistochemical and clinical characterization of the basal-like subtype of invasive breast carcinoma. *Clin Cancer Res*, **10** (16), 5367–5374.
187. Cheang, M.C.U., Voduc, D., Bajdik, C., Leung, S., McKinney, S., Chia, S.K., Perou, C.M., and Nielsen, T.O. (2008) Basal-like breast cancer defined by five biomarkers has superior prognostic value than triple-negative phenotype. *Clin Cancer Res*, **14** (5), 1368–1376.
188. Navab, R., Liu, J., Seiden-Long, I., Shih, W., Li, M., Bandarchi, B., Chen, Y., Lau, D., Zu, Y.-F., Cescon, D., Zhu, C.Q., Organ, S., Ibrahimov, E., Ohanessian, D., and Tsao, M.-S. (2009) Co-overexpression of Met and hepatocyte growth factor promotes systemic metastasis in NCI-H460 non-small cell lung carcinoma cells. *Neoplasia*, **11** (12), 1292–1300.
189. Charafe-Jauffret, E., Ginestier, C., Monville, F., Finetti, P., Adélaïde, J., Cervera, N., Fekairi, S., Xerri, L., Jacquemier, J., Birnbaum, D., and Bertucci, F. (2006) Gene expression profiling of breast cell lines identifies potential new basal markers. *Oncogene*, **25** (15), 2273–2284.
190. Di-Cicco, A., Petit, V., Chiche, A., Bresson, L., Romagnoli, M., Orian-Rousseau, V., Vivanco, M., dM, Medina, D., Faraldo, M.M., Glukhova, M.A., and Deugnier, M.-A. (2015) Paracrine Met signaling triggers epithelial–mesenchymal transition in mammary luminal progenitors, affecting their fate. *eLife*, **4**, e06104.
191. Schaefer, C.F., Anthony, K., Krupa, S., Buchoff, J., Day, M., Hannay, T., and Buetow, K.H. (2009) PID: the Pathway Interaction Database. *Nucleic Acids Res*, **37** (Database issue), D674-679.

192. Hammond, D.E., Urbé, S., Vande Woude, G.F., and Clague, M.J. (2001) Down-regulation of MET, the receptor for hepatocyte growth factor. *Oncogene*, **20** (22), 2761–2770.
193. Vervoort, V.S., Roselli, S., Oshima, R.G., and Pasquale, E.B. (2007) Splice variants and expression patterns of SHEP1, BCAR3 and NSP1, a gene family involved in integrin and receptor tyrosine kinase signaling. *Gene*, **391** (1–2), 161–170.
194. Paszek, M.J., Zahir, N., Johnson, K.R., Lakins, J.N., Rozenberg, G.I., Gefen, A., Reinhart-King, C.A., Margulies, S.S., Dembo, M., Boettiger, D., Hammer, D.A., and Weaver, V.M. (2005) Tensional homeostasis and the malignant phenotype. *Cancer Cell*, **8** (3), 241–254.
195. Berger, A.J., Renner, C.M., Hale, I., Yang, X., Ponik, S.M., Weisman, P.S., Masters, K.S., and Kreeger, P.K. (2020) Scaffold stiffness influences breast cancer cell invasion via EGFR-linked Mena upregulation and matrix remodeling. *Matrix Biol*, **85–86**, 80–93.
196. Blighe, K., Rana, S., and Lewis, M. (2018) EnhancedVolcano: publication-ready volcano plots with enhanced colouring and labeling. <https://github.com/kevinblighe/EnhancedVolcano>.
197. Chen, H., and Boutros, P.C. (2011) VennDiagram: a package for the generation of highly-customizable Venn and Euler diagrams in R. *BMC Bioinformatics*, **12** (1), 35.
198. Luo, W., and Brouwer, C. (2013) Pathview: an R/Bioconductor package for pathway-based data integration and visualization. *Bioinformatics*, **29** (14), 1830–1831.
199. Kanehisa, M., and Goto, S. (2000) KEGG: Kyoto Encyclopedia of Genes and Genomes. *Nucleic Acids Research*, **28** (1), 27–30.
200. Korotkevich, G., Sukhov, V., Budin, N., Shpak, B., Artyomov, M.N., and Sergushichev, A. (2021) Fast gene set enrichment analysis. *bioRxiv*, 060012.
201. Leight, J.L., Wozniak, M.A., Chen, S., Lynch, M.L., and Chen, C.S. (2012) Matrix rigidity regulates a switch between TGF- $\beta$ 1-induced apoptosis and epithelial-mesenchymal transition. *Mol Biol Cell*, **23** (5), 781–791.
202. Wei, S.C., Fattet, L., Tsai, J.H., Guo, Y., Pai, V.H., Majeski, H.E., Chen, A.C., Sah, R.L., Taylor, S.S., Engler, A.J., and Yang, J. (2015) Matrix stiffness drives epithelial-mesenchymal transition and tumour metastasis through a TWIST1-G3BP2 mechanotransduction pathway. *Nat Cell Biol*, **17** (5), 678–688.

203. Asselin-Labat, M.-L., Sutherland, K.D., Barker, H., Thomas, R., Shackleton, M., Forrest, N.C., Hartley, L., Robb, L., Grosveld, F.G., van der Wees, J., Lindeman, G.J., and Visvader, J.E. (2007) Gata-3 is an essential regulator of mammary-gland morphogenesis and luminal-cell differentiation. *Nat Cell Biol*, **9** (2), 201–209.
204. Miyoshi, K., Shillingford, J.M., Smith, G.H., Grimm, S.L., Wagner, K.-U., Oka, T., Rosen, J.M., Robinson, G.W., and Hennighausen, L. (2001) Signal transducer and activator of transcription (Stat) 5 controls the proliferation and differentiation of mammary alveolar epithelium. *Journal of Cell Biology*, **155** (4), 531–542.
205. Bradbury, P.M., Turner, K., Mitchell, C., Griffin, K.R., Middlemiss, S., Lau, L., Dagg, R., Taran, E., Cooper-White, J., Fabry, B., and O'Neill, G.M. (2017) The focal adhesion targeting domain of p130Cas confers a mechanosensing function. *Journal of Cell Science*, **130** (7), 1263–1273.
206. Li, T., Sun, L., Miller, N., Nicklee, T., Woo, J., Hulse-Smith, L., Tsao, M.-S., Khokha, R., Martin, L., and Boyd, N. (2005) The association of measured breast tissue characteristics with mammographic density and other risk factors for breast cancer. *Cancer Epidemiol Biomarkers Prev*, **14** (2), 343–349.
207. McCormack, V.A., and dos Santos Silva, I. (2006) Breast density and parenchymal patterns as markers of breast cancer risk: a meta-analysis. *Cancer Epidemiol Biomarkers Prev*, **15** (6), 1159–1169.
208. Boyd, N.F., Guo, H., Martin, L.J., Sun, L., Stone, J., Fishell, E., Jong, R.A., Hislop, G., Chiarelli, A., Minkin, S., and Yaffe, M.J. (2007) Mammographic density and the risk and detection of breast cancer. *N Engl J Med*, **356** (3), 227–236.
209. Bao, J., Gur, G., and Yarden, Y. (2003) Src promotes destruction of c-Cbl: Implications for oncogenic synergy between Src and growth factor receptors. *PNAS*, **100** (5), 2438–2443.
210. Bissell, M.J., and Radisky, D. (2001) Putting tumours in context. *Nat Rev Cancer*, **1** (1), 46–54.
211. Orimo, A., and Weinberg, R.A. (2006) Stromal Fibroblasts in Cancer: A Novel Tumor-Promoting Cell Type. *Cell Cycle*, **5** (15), 1597–1601.
212. Jedeszko, C., Victor, B.C., Podgorski, I., and Sloane, B.F. (2009) Fibroblast Hepatocyte Growth Factor Promotes Invasion of Human Mammary Ductal Carcinoma in Situ. *Cancer Res*, **69** (23), 9148–9155.

213. McCormick, B., Winter, K., Hudis, C., Kuerer, H.M., Rakovitch, E., Smith, B.L., Sneige, N., Moughan, J., Shah, A., Germain, I., Hartford, A.C., Rashtian, A., Walker, E.M., Yuen, A., Strom, E.A., Wilcox, J.L., Vallow, L.A., Small, W., Pu, A.T., Kerlin, K., and White, J. (2015) RTOG 9804: A Prospective Randomized Trial for Good-Risk Ductal Carcinoma In Situ Comparing Radiotherapy With Observation. *JCO*, **33** (7), 709–715.
214. Barnabas, N., and Cohen, D. (2013) Phenotypic and Molecular Characterization of MCF10DCIS and SUM Breast Cancer Cell Lines. *Int J Breast Cancer*, **2013**, 872743.
215. Behbod, F., Kittrell, F.S., LaMarca, H., Edwards, D., Kerbawy, S., Heestand, J.C., Young, E., Mukhopadhyay, P., Yeh, H.-W., Allred, D.C., Hu, M., Polyak, K., Rosen, J.M., and Medina, D. (2009) An intraductal human-in-mouse transplantation model mimics the subtypes of ductal carcinoma in situ. *Breast Cancer Research*, **11** (5), R66.
216. Wegrzyn, L.R., Tamimi, R.M., Rosner, B.A., Brown, S.B., Stevens, R.G., Eliassen, A.H., Laden, F., Willett, W.C., Hankinson, S.E., and Schernhammer, E.S. (2017) Rotating Night-Shift Work and the Risk of Breast Cancer in the Nurses' Health Studies. *Am J Epidemiol*, **186** (5), 532–540.
217. Yang, N., Williams, J., Pekovic-Vaughan, V., Wang, P., Olabi, S., McConnell, J., Gossan, N., Hughes, A., Cheung, J., Streuli, C.H., and Meng, Q.-J. (2017) Cellular mechano-environment regulates the mammary circadian clock. *Nat Commun*, **8** (1), 14287.
218. David, K.A., and Juhl, H. (2015) Immunohistochemical Detection of Phosphoproteins and Cancer Pathways, in *Handbook of Practical Immunohistochemistry* (eds.Lin, F., and Prichard, J.), Springer New York, New York, NY, pp. 85–90.
219. Lu, H., Zhou, Q., He, J., Jiang, Z., Peng, C., Tong, R., and Shi, J. (2020) Recent advances in the development of protein–protein interactions modulators: mechanisms and clinical trials. *Sig Transduct Target Ther*, **5** (1), 1–23.
220. Cheng, S.-S., Yang, G.-J., Wang, W., Leung, C.-H., and Ma, D.-L. (2020) The design and development of covalent protein-protein interaction inhibitors for cancer treatment. *Journal of Hematology & Oncology*, **13** (1), 26.
221. Hu, B., Zhong, L., Weng, Y., Peng, L., Huang, Y., Zhao, Y., and Liang, X.-J. (2020) Therapeutic siRNA: state of the art. *Sig Transduct Target Ther*, **5** (1), 1–25.